THESIS

INDUCIBLE PHOTORECEPTOR DEGENERATION MODEL IN GOLDFISH

Submitted by

Dezaray D. Varland

Graduate Degree Program in Cell and Molecular Biology

In partial fulfillment of the requirements

For the Degree of Master of Science

Colorado State University

Fort Collins, Colorado

Summer 2011

Master's Committee:

Advisor: Jozsef Vigh

Juliet Gionfriddo
Douglas Ishii
James Madl
Stuart Tobet

ABSTRACT

INDUCIBLE PHOTORECEPTOR DEGENERATION MODEL IN GOLDFISH

Photoreceptor degenerative diseases are among the leading causes of vision loss and there is presently no known cure. The future success of biological and prosthetic vision rescue approaches following photoreceptor loss remains questionable, due to the morphological and functional changes occurring in the remaining retinal circuitry. In the current study we sought to establish a chemically-induced photoreceptor degenerative model in goldfish, based on the ability of teleost to regenerate their retina following damage. N-methyl-N-nitrosourea (MNU) was chosen to chemically induce the photoreceptor degeneration, because it has been found to be potent, and selective in mammalian studies. We hypothesized that MNU would induce selective and complete photoreceptor loss in the goldfish retina as well as the consequent morphological changes observed in mammalian retinas.

Under anesthesia, fish received a direct, intraocular injection of MNU into the posterior chamber of one eye whereas the contralateral eye served as sham-injected control. The effects of MNU were determined by standard immunohistochemical methods using known, well-established molecular markers of retinal cells.

The MNU induced unilateral, selective, and dose-dependent photoreceptor degeneration: up to ~ 60% of photoreceptors lost the injected eye of the goldfish within 7 days, followed by nearly complete regeneration by ~50 days post-injection. Repeated MNU treatments did not increase the magnitude of degeneration, but delayed the regeneration. Unlike in mammals, MNU did not destroy all of the photoreceptors in fish. The incomplete photoreceptor degeneration together with the quick regeneration may be responsible for preventing the development of chronic morphological and functional consequences. However, the regeneration observed after MNU treatment is promising. Inducing total photoreceptor degeneration in fish retina, possibly by combining MNU with other factors shown to destroy photoreceptors (i.e. strong light) could provide an all-encompassing natural model for studying the potential of stem cell-based vision rescue approaches after photoreceptor loss.

ACKNOWLEDGEMENTS

There are several individuals that I would thank for helping me over the last two years, training me in the essential techniques, providing helpful words and ideas, and continuously providing encouragement and support. First, I would like to thank my advisor Dr. Jozsef Vigh for providing me with the resources and guidance to perform my research. I would like to thank him for all the time and effort he has contributed to helping me meet my research goals and complete my thesis. I would also like to express my gratitude for the continuous support he has shown me, in the pursuit of my future educational and career goals. I would like to thank my committee members: Dr. Juliet Gionfriddo, Dr. Doug Ishii, Dr. James Madl, and Dr. Stuart Tobet for the time, guidance, and valuable information they have offered in helping me complete my thesis. I would like to thank my lab colleagues for all they have done and for providing me with a wonderful work environment. I would like to thank Cheongmin Suh and Lanette Rickborn for assisting me with my research and for allowing me to have the opportunity to serve as a mentor. I would like to thank Shannon Gallagher for time he has spent training me how to do many of the basic techniques I used throughout my thesis. He has also been an invaluable source of ideas and encouragement and a true friend. I would like to thank the Bridge to the Doctorate program for giving me the opportunity to attend graduate school and providing me with a community of peers and friends that have provided continuous advice. I would also like to thank CSU for the CVMBS College

Research Council grant which we received for 2010/2011 that has provided the funding needed to conduct my research. And last, but not least, I need to thank my family and friends for lending a listening ear and for continuously encouraging me to succeed.

TABLE OF CONTENTS

LIST OF TABLES AND FIGURES

TABLES

FIGURES

1. BACKGROUND

1.1 Introduction

Vision loss affects approximately 3.4 million United States citizens over the age of 40. As the number of Americans over this age continues to increase, there appears to be a correlative increase in all age-related diseases including those associated with vision loss (CDC: www.cdc.gov/visionhealth/data/national.htm). Retinal degenerative diseases are among the leading causes of blindness in older people (Gaillard and Sauve, 2007). With the exception of glaucoma (where ganglion cells die due to the compression of their axons), and some forms of vitreoretinal degeneration (affecting the inner retina first), most retinal degenerative diseases are characterized by the progressive loss of photoreceptor cells. For example, age-related macular degeneration (occurrence: 11.5%, ~1.75 million U.S. citizens) (Friedman et al., 2004), characterized by degeneration of photoreceptors in the central neural retina, is the leading cause of blindness in the United States and is on the rise with the ageing population. Retinitis pigmentosa (occurrence: 0.34%, 1 in 3500-4000) (Bunker et al., 1984) is an inherited disorder, caused by gene mutations that results in photoreceptor degeneration and ultimate vision loss (Lamba et al., 2008). Presently, there are no effective treatments available for these blinding diseases; however both biological ("cell-based") and prosthetic approaches for rescue and/or reconstruction of retinal tissue are being investigated.

Although these two approaches are fundamentally different, both are based on the assumption that after the loss of photoreceptors, the remaining retinal neural circuitry remains intact, and is capable of processing the information provided by the reintroduced photoreceptors, regardless of their biological or prosthetic nature.

However, recent research shows that this concept is incorrect. Photoreceptor degenerative diseases, which ultimately result in permanent vision loss in humans as well as in transgenic animal models, are characterized by consequent morphological changes of the remaining retinal tissue, called "remodeling". The "retinal remodeling" theory presented by Marc and Jones (2003) summarizes the process in retina that go well beyond the loss of photoreceptors. In order to understand the functional and structural consequences of photoreceptor degeneration on the rest of the retina, which could affect vision rescue attempts, further studies on both genetic and non-genetic animal models of retinal degeneration must be done.

The teleost fish retina is a traditional model for studying visual information processing (Famiglietti et al., 1977; Kaneko et al., 1981), but even more important model for studying tissue regeneration. It is because in teleost fish, unlike in mammals, retinal neurogenesis continues beyond embryonic development, and proceeds well into adult life. In addition, fish are able to regenerate their functional retina via generation of new retinal neurons following retinal damage (Hitchcock et al., 2004; Johns, 1977; Lyall, 1957). This striking capacity for neuronal regeneration is related to the continued presence of stem cells and their progeny within the mature teleost retina (Otteson and Hitchcock, 2003).

The focus of this research was to determine whether or not chemically-induced photoreceptor degeneration in the goldfish retina would be followed by chronic morphological consequences similar to those observed in human blinding diseases, such as retinitis pigmentosa or macular degeneration, and if the fish retina could regenerate their chemically-destroyed photoreceptors. Together, the current study evaluated if the fish retina can serve as a natural model for cell-based visual function restoration in patients with photoreceptor loss.

The following sections review: (1) the fundamental structure of the vertebrate retina, pointing out specific aspects relevant for this study; (2) the major human photoreceptor degenerative diseases; (3) the existing animal models; and (4) currently explored treatment strategies.

1.2. Vision

Vision is a complex sensory process that allows for the detection of size, color, distance, motion, and orientation of the surrounding environment (Gaillard and Sauve, 2007). The perception of one's surroundings begins when light rays reflect off an object and strike the cornea. The surface of the cornea bends the rays, while the diameter of the pupil controls the quantity of light that pass into the eye. The light rays then pass through the lens, which causes an additional bending of the rays to focus them on the retina at the back of the eye.

Light that strikes the retina, passes through the relatively transparent retinal layers, and is either captured by millions of light-sensing photoreceptors or absorbed by retinal pigment epithelial (RPE) cells sclerad to the photoreceptors. Primary sensory neurons called rod and cone photoreceptors capture the light with photosensitive pigments and

their complex phototransduction mechanisms convert the energy of photons into electrical signals (Sung and Chuang, 2010). The light-evoked electrical signal alters glutamate release from photoreceptors to second order retinal neurons, and with that step the light information is channeled into the neural pathway. The signals travel on seemingly parallel tracks back through the retinal layers (Joselevitch, 2005; Lamba et al., 2008) to the ganglion cells, whose axons transport information to the visual cortex of the brain (Masland, 2001).

1.3. Retina

The retina is an approximately 200 μm thick aggregate of neural tissue which acts as a receiver of incoming light rays and as an image processing center. There are five main classes of neurons that make up the retina: photoreceptors (rods and cones), horizontal cells, bipolar cells, amacrine cells, and ganglion cells (Sung and Chuang, 2010; Wassle, 2004). These highly organized retinal neuron classes reside in 3 well-defined layers in the retina. The outer nuclear layer (ONL) consists of the rod and cone photoreceptor cell bodies. The inner nuclear layer (INL) harbors bipolar cells, horizontal cells and amacrine cells. The ganglion cell layer (GCL) is made up of "displaced" amacrine cells, ganglion cells, and their axons.

The retina also contains supporting cells, which include glial cells and the retinal pigmented epithelial (RPE) cells. RPEs lie against the outer most part of the ONL and encase the photosensitive outer segment of the photoreceptors. It is pigmented and acts as a photon sink that catches all the stray photons not absorbed by the photoreceptors (Sung and Chuang, 2010). RPE cells also play crucial role in recovering bleached photopigments (Strauss, 2005). Müller cells are large "housekeeping" glial cells that span

the entire retina and have several important functions that are vital to the health of the retinal neurons (e.g. migration of progenitor cells, removal of waste) (Lamba et al., 2008).

Retinal cells have been studied for decades and much progress has been made toward understanding their functions and identifying the members of the various cell classes. In some species, only a few cell classes have been completely cataloged (e.g. bipolar cells in mice). However, there is no universal catalog for classifying retinal cells based on either morphology or function across all species.

1.3.1. Photoreceptors

Photoreceptors are millions of tiny, light capturing cells that lie in the outer (sclerad) layers of the retina. The two types are: (1) rods, which are responsible for vision at a low light level and (2) cones, which are responsible for vision at bright light levels and color vision (Wassle, 2004). Structurally, both rods and cones can be divided into 2 parts, the cell bodies and the outer segments (OS). The portion of the photoreceptor cells in which phototransduction takes place is the OS (Sung and Chuang, 2010; Yau and Hardie, 2009). The activation of the transduction pathway by photons leads to hyperpolarization of the photoreceptors and consequent reduction of transmitter (glutamate) release onto second order retinal neurons.

A change in the number of photoreceptors in the fish retina following chemical challenge is in the focus of the present study.

1.3.1.1. Cones

Cone photoreceptors operate in bright light conditions. They contain one of three types of cone photopigments, each with different wavelength-sensitivity: L-cones (red or long-wavelength, λ_{max} = 625 nm), M-cones (green or middle-wavelength, λ_{max} = 530 nm), and S-cones (blue or short wavelength, λ_{max} = 450 nm). Cones also mediate color vision. In darkness, the membrane potential of cones is depolarized and their glutamate release is high. Light produces hyperpolarization, graded with intensity and thereby reduces the glutamate release from the cone's complex synaptic terminal, called the cone pedicle (Wassle, 2004). Glutamate released by cones is sensed by second order retinal neurons, bipolar cells and horizontal cells.

1.3.1.2. Rods

Rods are the predominant, light-sensitive photoreceptor cells that mediate vision in dim light. In humans, rods outnumber cones 20:1, and with the exception of the macula and fovea (which are the areas of central vision), they are distributed throughout the retina. In the mammalian retina, rod signals are processed in a specialized circuitry in which all rods contact to a single type of bipolar cell, the rod bipolar cells (Masland, 2001). These rod bipolar cells do not pass the visual information directly onto ganglion cells, but excite another interneuron, the AII amacrine cell. The AII cells then form synapses with the axon terminals of cone bipolar cells which in turn excite the ganglion cells (Sarthy, 2001). Contrary to mammals, rod distribution in fish is even over the entire retina. In fish, rod signals are processed by Mb (mixed) bipolar cells, which also receive cone input, and connect to ganglion cells directly. Unlike mammals, which lose photoreceptors throughout their lives, the number of photoreceptors in the retina of

goldfish is maintained over the lifetime of the animal (Hitchcock et al., 2004; Johns, 1977; Lyall, 1957). This is due to the continuous regeneration of rods from retinal progenitors located at the ciliary marginal zone (CMZ) and from distal INL progenitor cells, a process which is aided by Müller cells (Raymond and Rivlin, 1987; Sarthy, 2001).

1.3.2. Horizontal cells

Horizontal cells (HCs) are laterally connecting GABAergic interneurons that receive excitatory (glutamatergic) input from photoreceptors. HCs regulate the light signal flow from photoreceptors through feedback inhibition to photoreceptors and feed forward inhibition to bipolar cells. These synaptic interactions enhance sensitivity to illumination and reduce the redundancy of signals transmitted to the bipolar cells (Masland, 2001). HCs also play a fundamental role in mediating the antagonistic center-surround organization of the ganglion cells receptive fields (Trenholm and Baldridge, 2010), a phenomenon thought to be responsible for contrast detection (Masland, 2001).

1.3.3. Bipolar cells

Bipolar cells (BCs) are second-order retinal neurons, responsible for gathering input from photoreceptors and passing it on to ganglion cells. BCs are physiologically classified into two main functional groups (ON-type or OFF-type) based on the polarity of their response to illumination. Illumination of the receptive-field center results in depolarization of ON-type BCs and hyperpolarization of the OFF-type BCs. Thus, when stimulated, ON and OFF type BCs split the visual signals into parallel pathways; one pathway carrying the signal as positive contrast, and the other carrying it as negative contrast information, respectively. The ON-type BCs terminate in the inner part of the

inner plexiform layer (IPL), while OFF-type cells terminate in the outer part of the IPL. Therefore ON and OFF pathways are morphologically separated and remain so until they reach the visual cortex (Suzuki and Kaneko, 1990; Werblin and Dowling, 1969).

The mammalian retina contains 10 types of BCs (Wassle, 2004) whereas at least 15 different morphologically distinct types of BCs have been discovered in the goldfish retina (Ishida et al., 1980; Saito et al., 1985; Suzuki and Kaneko, 1990). Goldfish BCs, besides belonging to either the ON, or OFF-type physiological classes, can be further divided by their input. Mixed input BCs (Mb) receive both rod and cone input and cone-driven BCs receive only cone input. For the purpose of this study, we have chosen the ON-type, Protein Kinase C-α (PKCα) immunopositive, Mb BCs as a marker of appropriate sectioning quality and orientation.

1.3.4. Amacrine cells

Amacrine cells (ACs) are laterally spanning inhibitory interneurons, whose processes are found in the second synaptic layer of the retina, called inner plexiform layer (IPL). A majority of AC bodies are (orthotopically) found in the INL and some AC bodies are found to be displaced into the GCL. These multifunctional cells play a vital role in controlling the synaptic output from BCs onto ganglion cells via inhibitory feedback to BCs (Masland, 2001). ACs also provide (feed forward) inhibition to other ACs and ganglion cells. There are several types of ACs (~ 40 different subtypes) in every species, which are distinguished by the wide variety of neurotransmitters and neuroactive substances that they express, by their distinct synaptic partners, and by the synaptic layer in which they communicate (Masland, 2001). Thus, the ACs are thought be the most diverse class of inhibitory interneurons within the CNS.

In the current study, the dendritic organization of orthotopic or "displaced" ACs, which use acetyl choline as their neurotransmitter, were used to address the structural integrity of the IPL in the fish retina following photoreceptor degeneration.

1.3.5. Ganglion cells

Ganglion cells (GCs) are the final output neurons of the retina. They are responsible for collecting visual information (primary excitatory information from BCs and inhibitory information from ACs), and transmitting it as an electrical signal to different parts of the brain (Wassle and Boycott, 1991). Most GCs are located in the ganglion cell layer (GCL) and have a distinct structure, with a large cell body and prominent dendritic arbors. The historical study of retinal cell morphology, performed by Cajal in 1892, introduced the idea of GC classification based on dendritic morphology, size of the cell body and dendritic tree, and location of the dendritic arbors (Cajal, 1892). Since then, there have been multiple attempts to morphologically classify GCs in different species (Boycott and Wassle, 1974; Polyak, 1941). Based on their light-evoked responses, GCs can be divided into three main classes: "ON" type GCs respond to incremental increases of retinal illumination by increased action potential firing, "OFF" type GCs respond to incremental decreases of illumination with increased action potential firing in the darkness, and ON/OFF type GCs which respond to illumination changes with increase firing at both the beginning and the end of the light stimulus (Schiller, 2010). Accordingly, "ON" type GCs receive excitatory input from ON BCs, OFF GCs from OFF BCs, and ON-OFF GCs from both types of BCs. These classes have been further subdivided based on morphology and function, which can also vary among different animal species.

In the goldfish retina, based on soma size there are 4 different types of GCs, which have been further subdivided into 15 subtypes based on their dendritic stratification patterns (Hitchcock and Easter, 1986). In the human retina, there are at least 18 different morphological types of GCs. In a broad sense, most GCs can be lumped into two types, as described in primates: magnocellular/ parasol/α GCs (M cells) and the parvocellular/ midget/ β GCs (P cells), both of which can also be divided into "ON" and "OFF" subtypes. M cells account for ~ 10% of all GCs. They have large cell bodies and receptive fields, they are sensitive to luminance contrast, and they are primarily concerned with motion detection and analysis of gross features (Kaplan and Shapley, 1986). P cells account for ~ 80% of all GCs. They have smaller cell bodies and receptive fields, a lower luminance contrast, and are primarily concerned with color and fine feature analysis (De Monasterio and Gouras, 1975; Derrington et al., 1984; Wiesel and Hubel, 1966). The remaining, up to 10% of GCs, does not project to the thalamus, but instead to the hypothalamus. They have been identified as members of the non-image forming system: these melanopsin-expressing, intrinsically photosensitive GCs entrain the mammalian circadian clock (Hattar et al., 2002).

One common retinal disease that affects primarily GCs is glaucoma. However, since glaucoma is primarily associated with GC damage the current study did not focus on providing further insight to this disease.

1.3.6. Müller cells

Müller cells (MCs) are one of four distinct types of glial cells and the most predominant (90%) form of retinal glia. These cells function to provide the neuronal retina with support, and they act as housekeeper cells by helping remove excess

neurotransmitter from the extracellular space (Dowling, 1987). MC bodies are located in the INL but their processes span the entire retina, forming basket-like processes, that project from the inner border of the GCL to the distal border of the ONL. The trunk of these cells is interspersed between the other retinal cells and the radial branches stretch throughout retinal layers connecting them to every class of retinal neuron and to the retinal vasculature (Newman and Reichenbach, 1996). The MCs vary in population density and morphology depending on the region of the retina in which they are located. In the central retina, they have longer, finer trunks and a narrower endfoot, and they are higher in density. In the periphery, they have shorter, stout trunks with a wider endfoot, and are less densely populated (Sarthy, 2001). The cytoskeleton of MCs is made up of microfilaments, microtubules, and widely studied intermediate filaments. Glial fibrillary acidic protein (GFAP) and vimentin are the most common MC intermediate filament proteins present in all vertebrates and thus used as molecular markers to immunocytochemically label, identify and study MCs (Sarthy, 2001). Glutamine synthetase (GS), an enzyme expressed in the MCs of all vertebrates, is also a commonly used to molecular marker to label fine MC processes and glial endings (Mack et al., 1998).

In more recent years, MCs have been identified as one source of the newly dividing progenitor cells. In the teleost, retinal regeneration in response damage starts with MC re-differentiation into progenitor cells (Fimbel et al., 2007). In the current study, we examined the MC morphology, which is known to change following photoreceptor degeneration and in response to regeneration (see below).

1.4. Retinal degenerative diseases

In addition to the natural decrease in retinal cell density and visual acuity that occurs with age (Rivolta et al., 2002), disorders that result in the degeneration of the retina have been termed retinal degenerative diseases. Most diseases in this group are considered inherited, genetic diseases, caused by one or more gene mutations. In the human retina, there have already been over a 160 retinal degenerative genes indentified (see RETNET for a list of retinal disease-causing genes and statistics: http://www.sph.uth.tmc.edu/retnet), most of them associated with vision loss due to the death of light-sensitive rod and cone photoreceptors (Rivolta et al., 2002). The two most prevalent disorders among them are age-related macular degeneration and retinitis pigmentosa.

1.4.1. Age-related macular degeneration

Age-related macular degeneration (AMD) is a retinal degenerative disorder associated with ageing that leads to the progressive loss of central vision. This disease affects an estimated 1.8 million Americans over the age of 40 (CDC: http://www.cdc.gov/visionhealth/basic_information/eye_disorders.htm) and is the leading cause of blindness worldwide (Gehrs et al., 2006). Macular degeneration, though the cause is unknown, can occur when mutated genes send faulty messages to the retina that result in the degeneration of RPE cells and the dense population of central photoreceptors (cones), which make up the macula. Due to the responsibility of this region, these mutations often result in a progressive loss of the clear, sharp, central vision (Lamba et al., 2008).

The extent of vision loss depends upon whether the patient has the wet or dry form of AMD. The wet form only occurs in ~ 10% of all AMD cases, and is commonly associated with more severe vision loss. It progresses at a rapid rate and is characterized by the swelling of blood vessels behind the retina, which grow abnormally under the macula and then start to leak fluid and eventually red blood cells. The leakage can lead to scarring and ultimately result in permanent damage to the light-sensitive retinal cells, causing blind spots and central vision loss (Gehrs et al., 2006; Huang et al., 2010). The most common (70-90% of all cases), dry form of AMD progresses at a much slower rate and is often characterized by the thinning of the macula overtime. Blind spots in central vision occur when drusen, yellow deposits or debris from deteriorated tissue, accumulates in or around the macula (Bressler et al., 1988; Gehrs et al., 2006).

1.4.2. Retinitis pigmentosa

Retinitis pigmentosa (RP) is a heterogeneous family of genetically inherited neurodegenerative diseases. These are the most common inherited retinal degenerative diseases, affecting approximately 1 in 4000 people worldwide (Berson, 1993; Bunker et al., 1984). RP results primarily in the loss of the rods and secondarily cone photoreceptors. This is followed by the degeneration of the RPE (Huang et al., 2010). At least 45 different genes have been identified as sites of mutation for this disease alone, which only accounts for ~ 60% of all retinal degeneration patients (~30% unidentified gene defects remain) (Hartong et al., 2006). The most common gene mutations leading to this disorder, are in the rhodopsin gene (RHO) (~25% of dominant RP), the USH2A gene (~20% recessive disease), and the RPGR gene (~70% X-linked RP). Some retinitis pigmentosa patients (20-30%) can also inherit associated non-ocular diseases, the two

most common are Bardet-Biedl syndrome (obesity, hypogenitalism, cognitive impairment, polydactyly, and renal disease) and Usher's syndrome (hearing impairment) (Hartong et al., 2006).

Since the term retinitis pigmentosa encompasses many genetically heterogeneous diseases, the symptoms of this disorder and their severity, as well as, their age of onset can be quite variable. Due to this variability, it has made it nearly impossible to predict a time course for when photoreceptors will degenerate and blindness will result. The classic pattern of blindness for many RP patients begins in adolescence when patients start to develop problems with dark adaptation and experience night blindness. As young adults, the patients will often experience a loss of their peripheral visual field first, followed by the onset of tunnel vision. As the disease progresses toward its final stages, patients will experience a narrowing of the tunnel vision and eventually they will loose central vision entirely (Berson, 1993; Hartong et al., 2006).

1.5. Treating blinding diseases

At this time there are no cures for retinal degenerative diseases, however, there are treatments, drugs, and therapies that can be used to slow their progression. For example, laser surgery can be used to destroy leaky blood vessels in small areas affected with AMD. Wet AMD patients can also undergo photodynamic therapy (PDT). In PDT an intravenous (i.v.) injection of a light activated drug is given. When subsequently exposed to light of the required wavelength the drug destroys new blood vessels. Alternatively, patients can receive monthly eye injections of a drug that blocks the vascular endothelial growth factor (VEGF) that is secreted into the eye and is involved in new blood vessel formation (i.e. anti-VEGF injection therapy) (Ahmadi and Lim, 2008; Miller, 2010).

Patients suffering from Advanced AMD are advised to take a daily dose of the age-related eye disease study (AREDS) formulation to reduce their risk of vision loss. The AREDS formula (vitamin A, vitamin C, vitamin E, and zinc) is an active treatment that protects retinal cells against oxidative stress (Wong et al., 2011). In patients suffering from retinitis pigmentosa, vitamin A (Berson et al., 1993a; Berson et al., 1993b) is prescribed and an omega-3-rich diet is recommended (Berson et al., 2004), in order to increase their time of useful vision.

Several mechanistically diverse approaches to therapy of retinal degeneration are also currently being investigated. These include: (1) gene-specific approaches; (2) nutritional or neuroprotective approaches; (3) prosthetic approaches; and (4) biological "cell-based" approaches.

1.5.1. Gene-specific approach

There are two gene-therapy approaches to the treatment of retinal degeneration. They vary depending upon the type of gene mutation causing the disorder. For dominantly inherited mutations (gain-of-function mutation), the idea is to eliminate the altered amino acid sequence coded by the mutation indirectly, by eliminating the mutant gene. The normal copy of the remaining gene, should then, in theory, code for the functional protein (Hartong et al., 2006). An example of this is the ribozyme-based (catalytic RNA) therapy, which is a mutation-dependent approach that has been used to block the mutant RNA sequence for rhodopsin (pro23his) and slow the progression of photoreceptor degeneration in transgenic mice (LaVail et al., 2000; Lewin et al., 1998; O'Neill et al., 2000). Another example is RNA interference (RNAi)-based therapy, which is a mutation-independent method for posttranslational gene silencing that has been used identify and

silence genes that effect retinal cells (Cashman et al., 2005). For recessively inherited mutation (loss-of-function mutation), the idea is a gene-replacement treatment, in which one could induce the local production of a missing protein, by introducing a normal copy of the gene into the diseased tissue (Hartong et al., 2006). This approach has been successful for the RPE65 gene mutation (mutation associated with Leber congenital amaurosis (LCA)). A subretinal injection of the normal RPE65 gene (which encodes the RPE isomerase required for the production of the 11-cis-retinal photopigment) was able to restore vision in mice and dogs (Acland et al., 2001; Dejneka et al., 2004; Narfstrom et al., 2003; Narfstrom et al., 2005). Similar human trials have also been done on patients with LCA, which resulted in improved navigational testing, visual field, and papillary response (Musarella and MacDonald, 2011).

1.5.2. Nutritional approach

The nutritional approaches are non-specific and as such are used regardless of specific causal mutation. Instead of addressing the genetics, they affect the secondary biochemical pathways that are altered. Small-molecule drugs, such as calcium-channel blockers, and neurotrophic factors have been studied as possible treatments (Hartong et al., 2006). Photoreceptor survival was seen in some animal models of retinal degeneration, treated with neurotrophic factors (Leveillard et al., 2004; Sahel, 2005). However, the small-molecule drug trials on mice and other animals, have failed thus far to confirm any benefits (Frasson et al., 1999).

1.5.3. Prosthetic approach

For over 30 years, the "prosthetic approach" has been aimed toward electrically stimulating the non-retinal components of the visual system in an effort to provide partial restoration of vision to the blind (Dowling, 2009). Early in the development of the technique, visual prostheses were focused on either brain-surface or penetrating electrodes to stimulate the visual cortex (Brindley and Lewin, 1968). Recently, techniques have been focused on retinal stimulation and they fall into two types of retinal prostheses: (1) optoelectronic systems and (2) external power-based multielectrode arrays. However, these approaches have proved to be suboptimal. There are currently more than 20 different groups conducting prosthetic research, but only four groups that have ongoing retinal implantation studies, two of which should have retinal prosthesis systems available for use within the next year (Dowling, 2009).

1.5.3.1. Optoelectronic approaches

Optoelectronic (OE) prostheses convert energy from light into electricity via photodiode arrays. When positioned between the photoreceptor layer and retinal pigment epithelium, these implants provide subretinal stimulation by projecting electrical signals on the remaining retinal neurons (Dowling, 2009). The first two OE systems developed, consisted of the implantation of passive multiphotodiode arrays into the subretinal space (Optobionics Corporation, 1990; Retina Implant, 2003). The later of the two models added additional photodiodes (which could generate electrical power to amplify circuits in the implant) and direct stimulation electrodes, which together elicited phosphenes or light spots. The Retina Implant company was set to release a modified version of this product in 2010 (Zrenner, 2007). A third system developed by Stanford University had a

similar design, in which a multiphotodiode array was implanted into the subretinal or epiretinal space (Asher et al., 2007; Palanker et al., 2005). The OE approach would, theoretically allow for a rescue of vision at any stage in the degeneration process. This particular prosthesis was based on the idea that a correct mathematical model exists that could transform visual signals into physiologically relevant electrical stimulation patterns. The computed electrical information must mimic a normal, functioning retinal circuit in order to be interfaced with the visual pathway. In other words, computer algorithms must be used to process a video stream of images into an electrical signal that the brain can interpret (Asher et al., 2007).

The following is an example of this prosthetic hardware design: Initially a ~ 3 mm chip, covered in photodiodes ($\leq$ 18000 pixels), is implanted into the center of the fovea. A patient then wears specialized goggles, mounted with an LCD screen, to receive images. A video camera is used to capture images and transmit them to a computer. The computer processes the data and the resulting images are displayed on the goggles LCD screen. A pulsed infrared (IR) light illuminates the LCD screen and projects the images through the eye optics onto the implanted chip. Each photodiode that covers the chip converts the projected IR signals into a pulsed biphasic current with a common power supply (inductive coils, lying in the subretinal space). Visual information is then introduced to the damaged retinal tissue, via the chips electrical stimulation. The remaining functional retina should respond normally to the visible light (Asher et al., 2007).

The most recently developed OE system (Imperial College) involves re-engineering retinal ganglion cells and bipolar cells to make them light sensitive (Poher et al., 2008). A

head-mounted gallium nitride LED array could then be used stimulate these new cells to fire action potentials. This system would not require the implantation of a power supply and it would provide the ability to target individual cells and receptive fields (Nikolic, 2007).

1.5.3.2. External power-based approach

The external power-based approach is the alternative to optoelectronic prostheses. Implanted multielectrode arrays and transcutaneous telemetry transfer the data and power by capturing an image and processing the signal externally. These epiretinal multielectrode arrays have demonstrated phosphene perception from local electrical stimulation and thus, there have been several ongoing clinical trials of these devices. These systems appear to be the best for short term use, however, they provide very low spatial resolution (Dowling, 2009).

1.5.4. Biological approach

The cell-based approach is based on the idea of using retinal progenitor cells and stem cells to replace and regenerate damaged retinal tissue, and to improve vision. This idea of "rescue and regeneration" has been studied for many years and to this day still remains a feasible treatment option (Gaillard and Sauve, 2007; Huang et al., 2010).

Early retinal repair strategies date back to the 1940s, when research groups explored the idea of neuronal replacement as a means of restoring retinal function. Retinal transplantation of embryonic rat eyes into the brain was first reported in 1946 (Tansley, 1946). Throughout the 1980s and 1990s, Raymond Lund studied intra-cranial transplantation of fetal rat retina. This was to study axon pathfinding, and in it they

pioneered the early work that showed functional connections between mature nervous system and transplanted neural tissue (Craner et al., 1989; Lamba et al., 2008). In 1959, Royo and Quay performed a direct transplantation of fetal rat retinas into the eye and saw graft survival (Royo and Quay, 1959). During the mid 1980s del Cerro and colleagues began transplanting strips of retinal tissue with attached retinal pigment epithelium (RPE) into the eye and then studied the survival of this graft (Parysek et al., 1985). In 1985, Gouras and colleagues performed the first successful transplantation of cultured human RPE cells in to the subretinal space of a monkey's eye (Gouras et al., 1985). These early studies saw graft survival and cell differentiation, but lacked the migration and integration of these cells into the host retina (Lamba et al., 2008).

In the last 20 years, researchers have focused more on the cell replacement, by transplanting retinal cells and stem cells into the vitreous (between the lens and retina) or into the subretinal space (between the retina and pigment epithelium) (Lamba et al., 2008). Thus far, it has been shown that a direct injection of cells into vitreous of the eye can result in some cell migration into the ONL (Takahashi et al., 1998) and that the subretinal approach can also work (Lu et al., 2002). The more important or perhaps challenging question, that continues to be explored, is what are the potential cell sources for this cell-based replacement approach. The types of cells used to date, include, but are not limited to: retinal pigment epithelial cells (RPE), intact sheets of embryonic retina, dissociated retinal cells, retinal progenitor cells (RPC), neural progenitor cells, embryonic stem cells (ESC), induced pluripotent stem cells (iPS), mesenchymal stem cells (MSC), and bone marrow-derived, very small embryonic-like (VSEL) stem cells (Huang et al., 2010; Lamba et al., 2008). The discussion of all cell types used for this rescue approach

is beyond the scope of this thesis. However, two main sources of retinal cells for replacement have been reported to include: (1) RPE cells and (2) photoreceptor precursors (Huang et al., 2010).

As discussed above, RPE cells have been considered as a source of cell replacement since the 1980s (Gouras et al., 1985; Parysek et al., 1985). In more recent years, RPE cell replacement has been used in human trials in patient suffering from AMD. Some restoration of vision was reported in patients following RPE transplantation (Binder et al., 2004). However, due to surgical complications (fibrosis and rejection) the problems with RPE cell transplantation remain unresolved. In the 1990s, the use of iris pigment epithelial (IPE) cells was also introduced, because of their suitable properties and accessibility. Transplantation of the IPE cells into the subretinal space was found to delay photoreceptor degeneration, but did not improve vision (Rezai et al., 1997).

The transplantation of photoreceptor precursors has also been investigated, which involves the introduction of healthy retinal cells into the degenerated retina of the host eye. This approach would, theoretically, slow the progression of the disease and/or replace the damaged retinal cells. Cell survival, cell differentiation, and some synapse formation between the transplanted cells and the host retina has been shown to occur for both embryonic dissociated cells and retinal sheets that were injected subretinally in rodent models, but no improvement of vision was observed (Radtke et al., 2008). Researchers hypothesized that the inability of the implanted cells to form functional connections was responsible the failure of vision restoration. These connection problems were attributed to the formation of a glial scar ("glial seal", discussed further in section 1.6) and the neural remodeling of inner retinal circuitry, characteristics which accompany

most forms of retinal degenerative diseases. These are the likely causes for a decrease in synaptic receptivity of the damaged retinal neurons to the newly introduced cells (Huang et al., 2010; Marc et al., 2003).

The overall goal of the current study was to test the fish retina as a natural model system, where the cell-based rescue approach might be tested at different stages of remodeling, following photoreceptor loss.

1.6. The retinal remodeling theory

Photoreceptor degenerative diseases can be placed into three broad categories, rod-degenerative, mixed rod/cone degenerative and debris-associated degeneration. These forms can vary by the primary genetic or environmental insult (Jones et al., 2005). However, all forms appear to have a common sequence. Degeneration begins in the retinal pigmented epithelium or in rod photoreceptors, which initiates photoreceptor loss. This is followed by continuous cell death, which results in the rewiring/ remodeling of surviving neural retina. Since corruption of this magnitude was known to evoke remodeling and atrophy in deafferented central nervous system (CNS), it was hypothesized by Marc and Jones (2003) that photoreceptor degeneration would result in a similar remodeling of the retina.

The idea of neuronal remodeling is, therefore, not a new, retina specific concept. It had been widely documented in field learning/memory (Doubell and Stewart, 1993; Gao et al., 1998; Vanreempts et al., 1992) and epilepsy (Koyama et al., 2004; Pollard et al., 1994; Represa and Benari, 1992), and in 1974, Kolb and Gouras first noted indications of altered retinal circuitry following retinal degeneration (Kolb and Gouras, 1974). Still, for nearly twenty years, the idea of retinal remodeling was not recognized. Limited by time,

cost investment, and visualization tools, the early retinal remodeling studies were focused on neural retinal survival and the early stages of photoreceptor loss. Researchers focused on working with models that could produce rapid photoreceptor loss rather than keeping animal models around long enough to fully understand the progression of these diseases. Simple cell counts were preformed on the early stages of photoreceptor loss, but specific changes occurring to the surviving neuronal retina were not documented (Jones and Marc, 2005), until photoreceptor degeneration studies revealed neurite sprouting and abnormal changes in the inner retina (Jones et al., 2005; Machida et al., 2000). Marc and Jones set out to confirm their theory of retinal remodeling by documenting the stages of degeneration and the specific changes that occur within the surviving retinal cells. They used computational molecular phenotyping (CMP) (Marc and Jones, 2002) and overlay electron microscopy (Marc and Liu, 2000) to screen human and animal models of retinal degeneration. CMP allowed them to quantitatively track the fate of all major retinal cell groups throughout the disease process and across different animal models (Marc and Cameron, 2001; Marc and Jones, 2002; 2003). They began by using aged human retina from RP patients and then moved on to animal models, which allowed them to determine if all retinal degenerations trigger the same remodeling. Using several disease models, from various species, they were able to demonstrate that most of these retinal degenerative models accurately reflect human diseases. From the CMP theme maps, they were able to reconstruct the three phases of retinal remodeling in the animal and determine that almost all retinal degenerations result in remodeling (Jones and Marc, 2005).

Phase 1: Photoreceptor stress: Retinal degeneration causes photoreceptors to become stressed. Rods begin to shorten, RPE cells become altered and uncouple, photoreceptor synaptic terminals are depleted, and neurite extensions extend down past their normal BC and HC target into the GCL. The depletion of normal synaptic signaling then triggers a cascade of new rewiring events. BCs retract their dendrites and switch their synaptic targets and HCs extend their processes into the IPL (Jones and Marc, 2005). MCs begin to hypertrophy (Jones et al., 2003a).

Phase 2: Photoreceptor death: Microglia remove retinal debris from the initial trigger of photoreceptor stress, while trophic effects ultimately result in the death of most photoreceptors. Once photoreceptors are depleted and MCs hypertrophy is significant, the distal processes of MCs form a "glial seal," almost completely sealing-off the neural retina from the surviving RPE and choroid (Jones and Marc, 2005).

Phase 3: Neuronal remodeling: BC corruption, due to the loss of dendritic synapses, contributes to further disruption and leaves surviving cells vulnerable to cell death. As the retina thins and neurons die, MCs hypertrophy and migrate, partially filling the empty space of the ONL. This provides a pathway for neuronal migration and causes distortion the INL and ONL laminations. RPE cells and choroidal vessels can also migrate into retina through the gaps in the "glial seal" and cause displacement of INL cells. ACs use the glial processes to migrate into the GCL. The surviving AC, BC and GC neurite extensions form tangled microneuromas that can merge with the existing IPL and OPL and result several new synapses. The overall result was the reorganization or rewiring of the inner retinal circuitry (Jones and Marc, 2005).

Marc and Jones (2005) also modeled the signal processing by microneuromas, a model derived from a serial section reconstruction of excitatory and inhibitory components. In a normal retinal circuit BCs contribute a brief impulse of depolarizing current to yield a small-signal GC voltage response. This brief impulse response occurs due to nested AC feedback (Marc and Liu, 2000), which truncates the BC output. In a microneuroma, the modeled BC output is a resonant "ringing", much like in epileptic seizures. This oscillatory response would occur due to the formation of new, reverberatory, serial excitatory (BC to BC) synapses and its interaction with the persistent inhibitory feedback from ACs (Jones and Marc, 2005).

Current physiological studies have added further understanding to the remodeling and functional changes that occur in the degeneration-induced retina. Using the *rd-1/rd-1* mouse, Margolis and colleagues (2008) have found that spontaneous rhythmic synaptic activity, which is thought to originate from a negative feedback loop between ACs and BCs, drives both ON and OFF GCs to fire at a fundamental "beating" frequency of ~10 Hz (Margolis and Detwiler, 2011; Margolis et al., 2008). In addition, neurochemical remodeling of glutamate receptors on BCs and ACs during the early stages of retinal degeneration (Chua et al., 2009) may also contribute to the already hypothesized oscillating membrane potential of GCs (Margolis and Detwiler, 2011). Overall, the rhythmic activity of GC output in the remodeled retina does agree with the Jones and Marc (2005) hypothesis of a "ringing" output of BCs, but the exact mechanisms involved remains unclear.

Retinal remodeling could interfere with the success of photoreceptor rescue. If the retinal circuitry is corrupt, the newly introduced photoreceptors would have to make

proper connections with the remaining retinal neurons and trigger a rearrangement of the downstream retinal circuitry in order to process visual signals properly.

1.7. Animal models for retinal degeneration

There are various types of photoreceptor degenerative diseases that are responsible for impairing vision and eventually leading to blindness. Regardless of the inherited genetic cause, a major characteristic of these chronic diseases is photoreceptor loss, resulting in the significant reorganization of the inner retinal circuitry over time (Marc and Jones, 2003). Several animal models have been investigated in order to better understand the various forms of the retinal degenerative diseases.

1.7.1. Hereditary animal models

One of the first documented hereditary models for retinal defects was a mouse strain (*r* mouse) that lacked rod photoreceptors (Keeler, 1924). Almost 20 years later, an identical mouse strain (*rd* mouse) was discovered (extinct *r* mice are believed to have been rediscovered as *rd* mice) and later became the primary model for studying human autosomal recessive retinitis pigmentosa (Bruckner, 1951). The number of retinal disease genes that have been identified has since increased exponentially (Rivolta et al., 2002). As a consequence, numerous genetically engineered mouse models carrying those genetic defects have been developed. A detailed review of these models far exceeds the scope of this thesis; however, it is important to note here that many of the existing "cell-based" therapeutic approaches investigate the possibility of preventing or slowing down photoreceptor degeneration in these transgenic mouse, or zebrafish lines (Jones et al., 2003b; Strettoi et al., 2003; Strettoi et al., 2002).

1.7.2. Inducible, acute animal models of retinal degeneration

Previous studies have also identified several inducible, acute models for inducing photoreceptor stress/damage in the vertebrate retina, such as: (1) exposure to strong light (Noell et al., 1966); (2) increased intraocular pressure (Seidehamel and Dungan, 1974) ; (3) modified diet (Scott et al., 1964); and (4) intraperitoneal or intraocular injections of chemical agents (Alkemade, 1968; Bellhorn et al., 1973; Kiuchi et al., 2002; Lee and Valentine, 1990; Matsumura et al., 1986). It is important to note that although the primary target in which retinal degeneration occurs in humans and in these inducible animal models differ, the result of photoreceptor cell death remains the same (Nambu et al., 1997).

1.7.2.1. N-methyl-N-nitrosourea (MNU) triggered retinal degeneration

MNU is a direct acting DNA alkylating agent and is a known carcinogen, teratogen, and mutagen in a variety of laboratory animal tissues (Nakajima et al., 1996; Yoshizawa et al., 1999). Previous studies have shown that this alkylating agent selectively destroys retinal photoreceptors. MNU induces degeneration by reacting with the 7-position of guanine in the DNA base molecules, yielding the 7-methyldeoxyguanosine (7-medGua) adduct (Ogino et al., 1993; Yoshizawa et al., 1999). Immunohistochemical labeling of the 7-medGua revealed selective 7-medGua DNA adduct formation in the photoreceptor nuclei (Ogino et al., 1993). If the damage from these adducts is severe enough and not repaired, it will result in the up-regulation of the Bax protein (which induces cell death), and the down-regulation of the Bcl-2 protein (which is known to prevent apoptosis). The consequence is the activation of the caspase 3, 6, and 8 proteins, which ultimately results in apoptotic cell death (Ogino et al., 1993; Tominaga et al., 1997; Tsubura et al., 2003;

Yoshizawa et al., 1999). Several methods (TUNEL, electron microscopy, and DNA fragmentation) have confirmed that MNU induces selective photoreceptor loss in a variety of animal species by this process (Yoshizawa et al., 1999).

A single intraperitoneal (i.p.) or intravenous (i.v.) injection of MNU, induced selective and progressive photoreceptor degeneration in the retina of rat (Nakajima et al., 1996; Yoshizawa et al., 1999), mouse (Nagar et al., 2009; Nambu et al., 1997; Yuge et al., 1996), hamsters (Herrold, 1967); (Taomoto et al., 1998), rabbits (Ogino et al., 1993), and non-human primates (Tsubura, 1998).

In the mouse, the long term retinal effects of MNU-triggered photoreceptor degeneration showed a striking similarity to the chronic morphological consequences that have been identified in humans with blinding photoreceptor degenerative diseases (Nagar et al., 2009).

1.7.2.2. Establishing photoreceptor degeneration model in goldfish

Retinal growth in teleost fish is a gradual and continuous process that takes place throughout the life of the animal. New retinal neurons and glial cells are continuously added from the small zone of mitotically active cells known as the ciliary marginal zone (CMZ). These new neurons can differentiate and become incorporated into the retinal circuitry (Lamba et al., 2008; Reh, 1987). In the central retina, rod photoreceptors arise from rod progenitor cells, which migrate along MC processes to reach the ONL (Hitchcock et al., 2004). These rod progenitor cells are generated from a population of slowly dividing MCs located in the INL, that act as retinal stem cells (Bernardos et al., 2007). When damage occurs to the fish retina, the normally mitotically quiescent MCs rapidly re-enter the cell cycle and re-differentiate into the progenitor-like cells needed to

regenerate the damaged area of retina (Lamba et al., 2008). Depending upon the cause of the retinal damage, the regeneration can lead to almost full morphological and functional recovery in 28 days (Vihtelic and Hyde, 2000). Due to its appealing characteristics and strong regenerative capabilities, the current study is focused on exploring the goldfish retina as new model of retinal degeneration.

In order to establish a new model, first we needed to find a way to physically or chemically-induce photoreceptor degeneration by: (1) eliminating photoreceptors selectively and more or less evenly across the retina and (2) do this in a way that would allow the fish to survive long enough for circuitry remodeling to occur. For this study, we chose to chemically-induce photoreceptor degeneration in the goldfish retina using the carcinogenic drug MNU. This drug has been shown to cause acute photoreceptor cell death in mammals (Nakajima et al., 1996; Tsubura, 1998; Yuge et al., 1996), in a dose-dependent manner (mice, rat, monkey), and its selectivity suggests that it could be used to induce local and unilateral photoreceptor degeneration.

2. STATEMENT OF HYPOTHESIS

Presently, there is no cure for human retinal photoreceptor degenerative diseases. Experimental success with biological rescue approaches using transgenic mouse models is restricted to the very early stages of these diseases: the progression of diseases can be slowed, or even limited vision can be transiently regained. The potential use of biological, cell-based rescue approaches in treating late chronic stages of photoreceptor degeneration remains questionable due to the morphological and functional changes of the remaining retinal circuitry. Previously, N-methyl-N-nitrosourea (MNU) has been shown to cause photoreceptor loss in various mammalian retinas. Importantly, MNU also triggered all of the well-characterized structural changes (degeneration, glial seal formation, remodeling) which are associated with inherited human photoreceptor degenerative diseases. Unlike the mammalian retinas, fish retina regenerates after damage. Thus, MNU treatment of the goldfish retina, considering its unique capability to regenerate photoreceptors, could provide a new model for studying stem cell-based vision rescue approaches after photoreceptor loss.

The overall hypothesis of this study was that MNU induces photoreceptor loss in the goldfish retina and consequently triggers similar chronic morphological changes to those observed in mammalian retinas.

In order to test whether or not the MNU-treated goldfish retina can serve as a natural model for stem cell-based vision rescue strategies after photoreceptor degeneration, the following hypotheses were examined experimentally:

(1) A unilateral, intraocular injection of MNU into the eye will induce local, unilateral photoreceptor degeneration and allow for survival of the goldfish.

(2) MNU will induce complete photoreceptor cell loss in the goldfish retina as seen in previous mammalian models.

(3) Chronic morphological consequences of photoreceptor degeneration (i.e. glial seal formation, remodeling), as seen in humans, will follow MNU-triggered photoreceptor loss in the goldfish retina.

(4) Following MNU treatment, the goldfish retina remains capable of regenerating photoreceptors.

3. MATERIALS AND METHODS

3.1. Animals

Adult, 3-5" (~3-4 years old) and 8-9" (~6-8 years old) goldfish (Carassius auratus), weighing 30-100g were obtained from Alpine Koi & HomeScapes, Fort Collins, CO. Fish were maintained between 19- 21ºC in 50 gallon tanks, filled with tap water circulating through a filter system, and then placed into 10 gallon tanks (3 fish/tank) by treatment group. Fish were fed once daily and kept on a 12 hour light: 12 hour dark schedule, throughout the project, with lights turned on at 10:00 AM. Animals were handled in compliance with Colorado State University Institutional Animal Care and Use Committee; in accordance to our CSU IACUC protocol 09-1419A.

3.2. Chemicals

Unless otherwise stated, all salts and chemicals were obtained from Sigma (St. Louis, MO). The fish Ringer's solution contained 119 mM NaCl, 12 mM HEPES, 3.25 mM $MgCl_2$, 0.25 mM $CaCl_2$, 2.5 mM KCl, and 12 mM glucose, pH 7.4 (set with NaOH), osmolarity ~260 mosm. Upon arrival, N-Methyl-N-nitrosourea (MNU) was prepared immediately by dissolving the powder in 7 mL of 100% Dimethyl Sulfoxide (DMSO) (vehicle), protected from light, and stored in 25 µl aliquots at -20º C until use. MNU is sensitive to humidity and light, its half-life ranges from 125 hours at pH 4 to approximately 2 minutes at pH 9 (Report on Carcinogens, Eleventh Edition, U.S. DHHS, viewed at: http://ntp.niehs.nih.gov/ntp/roc/eleventh/profiles/s132nitr.pdf). The half-life

time of intravenously applied MNU in rat is approximately 15 minutes post injection (Swann, 1968). Thus, precautions were taken to minimize light exposure during injections. The MNU stocks were removed from the -20º C freezer, vortexed lightly, and each aliquot was used within 45 minutes.

3.3. Surgical procedures/ drug administration

Goldfish were deeply anesthetized by placing them into a solution of MS-222 (100 mg/L tricaine methane sulfonate, Sigma, St. Louis, MO), immediately before injections (Braisted and Raymond, 1993). Deep anesthesia in fish is characterized by the loss of posture, loss of reflexes, and cessation of opercular movement (Summerfelt, 1990). Following MS-222 anesthesia, a 10 µl Hamilton syringe fitted with a 26-gauge needle was used to intraocularly inject 4 µl or 6 µl of MNU (14% w/v (stock) MNU in DMSO or 7% w/v in DMSO) into the posterior chamber of the one eye. The contralateral eye in each fish served as a sham-injected control (4 µl or 6 µl of 100% DMSO). For "DMSO control" experiments, fish received an intraocular injection of 4 µl of 100% DMSO into one eye, and 4 µl of fish Ringer's solution into the contralateral eye. The appropriate injection volume (4-6 µl) was determined from an estimated ocular volume and previous fish studies, involving goldfish of approximately the same size (~ 5 inches long fish, (Yazulla and Studholme, 1997). The appropriate concentration of MNU was calculated from the mammalian dose (60 mg/kg), in which rodents received an intraperitoneal (i.p.) injection of MNU (Nagar et al., 2009; Wan et al., 2006). The saturated MNU solution contains 1 g MNU in 7 ml DMSO, thus a 4 µl bolus of the stock would contain 0.56 mg MNU. Based on the i.p. used, efficient mammalian dose of 60 mg/kg, intraocular injection of 4 µl saturated MNU (stock) solution would translate into and effective dose

for 8.3 grams of body weight. A goldfish eye weights about 0.2 g. Thus, 4 µl of the stock solution contained roughly 40 times the mammalian dose, considering that the eyes are somewhat isolated from systemic circulation. Injections were repeated a second time on 13 fish, at 14 days post initial injection. After all injections, fish were placed back into the MS-222 water for a couple of minutes and then returned to 10 gallon filtered and oxygenated tanks for the rest of the experiments, until euthanasia.

3.4. Tissue preparation

Retinal tissue was harvested after euthanasia by overdose of MS-222 (100 mg/l). Fish were kept in the water containing MS-222 for 10 minutes after the cessation of opercular movement and then were decapitated. After decapitation, the brain and spinal cord were immediately pithed. This method of euthanasia is in full agreement with the guidelines for fish published by the AVMA Panel on Euthanasia (2007). Fish treated with a single dose of MNU were euthanized at 1, 3, 5, 7, 10, 14, 21, 28, 35, 42, and 49 days post-injection (dpi). Double-injected fish received a second treatment 14 days after the first injection and were euthanized at 7 (21), 14 (28), 21 (35) days post second injection (days post first injection). “DMSO control” fish were euthanized at 7 dpi. After euthanasia, the eyes were enucleated and processed for cryosectioning. The whole eye was puncture fixed at room temperature for 15 minutes in freshly prepared 4% paraformaldehyde in 0.1M phosphate buffered saline (PBS; pH 7.4, osmolarity: ~260 mosm). The eyes were bisected in the coronal plane, separating the anterior and posterior chambers, and the lens was removed. Eyecups were then placed in digestive enzyme (18 mg/ml Hyaluronidase in 0.1 M PBS) for 5 minutes, to break down dense vitreous humor. Eyecups were rinsed, post-fixed in 4% paraformaldehyde in 0.1M PBS for 5 minutes,

washed 3 times with 0.1M PBS for 15 minutes per wash, and then cryoprotected by keeping overnight in 30% sucrose solution at 4°C. The eyecups were embedded in Tissue- Tek* O.C.T Compound (Sakura* Finetek, VWR International), frozen at -80°C for ~20 minutes, and cryostat (HM500; Microm) sectioned into 20 µm thick vertical sections. Sections taken in the middle portion of the eyecups (i.e. just outside the optic nerve, but within ~2000 µm) were mounted on Superfrost/Plus glass slides (VWR International), air dried for at least 10 minutes at room temperature, and stored at -20ºC until use.

3.5. Immunohistochemsitry

Standard procedures (Gallagher et al., 2010) were used and all steps were performed at room temperature. Retinal sections were rehydrated by washing 3 times in 0.1M PBS, for 7 minutes per wash, outlined with a Pap Pen (Electron Microscopy Sciences, Hatfield, PA), and then incubated in blocking solution (0.3% Triton X-100 v/v, 0.1% sodium azide w/v, and 1% bovine serum albumin (BSA) w/v in 0.1M PBS) for 1 hour. Retinal sections were incubated overnight with primary antibodies (listed in Table 1) diluted in blocking solution. Primary antibodies used were goat anti-choline acetyltransferase (ChAT) (1:100, Millipore, Billerica, MA), mouse anti-glial fibrillary acidic protein (GFAP) (GA5, 1:500, Cell Signaling, Danvers, MA), rabbit anti-glial fibrillary acidic protein (GFAP) (1:1000, DAKO, Glostrup, Denmark), mouse anti-glutamine synthetase (clone GS-6, 1:500, Chemicon, Temecula, CA), rabbit anti-proliferating cell nuclear antigen (PCNA) (FL-261, 1:100, Santa Cruz Biotechnology, Santa Cruz, CA), mouse anti-PKCα (clone MC5, 1:500, Biomol/ Assay Design/ Enzo Life Sciences, Plymouth Meeting, PA), rabbit anti-PRKCA (PKCα-type recombinant protein) (1:500, Sigma), and mouse anti-vimentin

(clone V9, 1:500, Sigma). Retinal sections were washed with 0.1M PBS, 3 times at 15 minutes per wash, and then incubated in the appropriate secondary antibodies (Table 2) for 2 hours. The secondary antibodies used were Alexa Fluor 488 and 546 (1:400, Invitrogen, Carlsbad, CA), Fluorescein polyclonal chicken anti-mouse (1:400, Rockland, Gilbertsville, PA), and Cy3 polyclonal donkey anti-rabbit (1:400, Millipore). Cell nuclei were labeled with the cyanine monomer TO-PRO®-3 (1:5000, Molecular Probes), applied concurrently with secondary antibodies. Retinas received 3 final washes in 0.1M PBS, at 15 minute per wash, slides were cover-mounted by glass slides in Vestrashield (Vector Laboratories, Burlingame, CA), and observed with a scanning laser confocal microscope (Zeiss LSM 510 Meta).

Table 1. Primary Antibodies

Primary Antibody	Antiserum	Dilution	Source	Catalog #	Description
Choline acetyltransferase (ChAT)	Goat, Polyclonal	1:100	Millipore	AB144P	Cholinergic amacrine cell marker
Glial fibrillary acidic protein (GFAP)	Rabbit, Polyclonal	1:1000	DAKO	Z0334	Muller cell marker
Glial fibrillary acidic protein (GFAP)	Mouse, Polyclonal	1:500	Cell Signaling	3670	Muller cell marker
Glutamine synthetase (GS)	Mouse, Monoclonal	1:500	Chemicon/ Millipore	MAB302	Muller cell marker
Protein Kinase C alpha (PKCα)	Mouse, Monoclonal	1:500	Biomol/ Assay Design	SA-143/ KAM-PK020	Bipolar cell marker
Protein Kinase C alpha (PKCα)	Rabbit, Polyclonal	1:500	Sigma	HPA006563	Bipolar cell marker
Vimentin (VIM)	Mouse, Monoclonal IgG1	1:500	Sigma	V6630	Muller cell marker

Table 2. Secondary Antibodies

Antigen	Host Animal	Excitation	Emission	Fluorophore	Source	Catalog #
Goat IgG	Donkey, Polyclonal	495	519	Alexa Fluor 488	Invitrogen	A11055
Rabbit IgG	Donkey, Polyclonal	495	519	Alexa Fluor 488	Invitrogen	A21206
Rabbit IgG	Donkey, Polyclonal	550	570	Cy3	Millipore	AP182C
Rabbit IgG	Goat, Polyclonal	495	519	Alexa Fluor 488	Invitrogen	A11008
Mouse IgG	Chicken, Polyclonal	495	528	Fluorescein	Rockland	610-9202
Mouse IgG	Donkey, Polyclonal	556	573	Alexa Fluor 546	Invitrogen	A10036
TO-PRO®-3		642	661	Cyanine Monomer	Molecular Probes	T3605

3.5.1. Antibodies

Choline Acetyltransferase (ChAT): The affinity purified polyclonal anti-ChAT antibody was generated in goat, using human placental enzyme. Its specificity was established via immunoblot, recognizing a single band of 68-70 kDa, for rat, mouse, macaque monkey, guinea pig, chicken, opossum, avian and human. In retina, this antibody selectively labels a subtype of amacrine cell (AC) that also internalizes radioactive acetylchoine (Masland and Mills, 1979; Voigt, 1986). Immunocytochemical techniques have demonstrated that this anti-ChAT antibody labels the soma of cholinergic neurons in the INL and GCL of the inner retina of goldfish, and neurite bands in laminae 2 and 4 of the IPL (Tumosa et al., 1984).

Glial Fibrillary Acidic Protein (GFAP), rabbit: The polyclonal anti-GFAP antibody was purified in an immunoglobulin fraction of rabbit antiserum, produced by immunizing rabbit with native GFAP isolated from bovine spinal cord. Immunoreactivity of this antibody has been shown to cross-react with the GFAP in cat, dog, mouse, rat, and sheep. The sequence homology is 90-95% between species. In several animals, including the goldfish (Bignami, 1984; Jones and Schechter, 1987), GFAP has been shown to label astrocytes and retinal Müller cells (MCs). Nagar et al (2009) confirmed that this antibody specifically labels MCs in the mouse retina and a single ~ 50 kDa band in Western blot, which correlated with the manufacturer's specifications. In our hands, double label experiments with mouse anti-vimentin and rabbit anti-GFAP resulted in perfect overlap in MCs. The results confirmed that fish GFAP expression level in every MC of the goldfish retina is high enough to use GFAP as a molecular marker even in control retinas (Bignami, 1984).

Glial Fibrillary Acidic Protein (GFAP), mouse: The polyclonal anti-GFAP antibody was produced by immunizing mice with native GFAP purified from pig spinal cord. According to the manufacturer's report, western blot analysis of extracts from mouse and rat brain recognize a single band of 50-55 kDa. Immunohistochemical experiments have shown that this antibody will label astrocytes of mouse brain. In order to confirm that this antibody would label the MCs of the goldfish retina, a co-labeling experiment was performed between the mouse anti-GFAP and rabbit anti-GFAP, which resulted in prefect overlap between the labeling of the two antibodies.

Glutamine Synthetase (GS): The monoclonal anti-GS antibody (clone GS-6) is a mouse IgG2a isotype purified from sheep brain. Western blot analysis of supernatants from rat brain, spinal cord, liver, and kidney with this antibody showed a band of ~ 42 kDa (Serbedzija et al., 2009) similar to the 45 kDa band seen in the manufacturer's Western blot analysis of rat brain. The GS antibody is a known marker of astrocytes and oligodendrocytes in the rat brain (Serbedzija et al., 2009) and it has been shown to primarily immunolabel the fine processes and glial endings of MCs in fish, including goldfish (Mack, 2007; Strettoi et al., 2002).

Proliferating Cell Nuclear Antigen (PCNA): The polyclonal anti-PCNA (FL-261) antibody was generated in the rabbit, raised against the entire human PCNA gene (261 amino acids). Western blot analysis using this antibody has shown, in multiple species, including zebrafish, appropriate banding for PCNA between 34 and 36 kDa (Manufacture's Report). In the teleost, including goldfish, PCNA immunolabeling has been used to identify cell proliferation during retinal regeneration (Hitchcock and Raymond, 1992; Negishi and Shinagawa, 1993; Vihtelic and Hyde, 2000).

Protein Kinase C alpha (PKCα) mouse: The affinity purified monoclonal anti-PKCα antibody (clone MC5) was generated in mouse, using bovine brain PKCα. Western blot analysis of chick and rat brain with this antibody showed a single band of 80kDa in size (Vanderzee et al., 1995). This correlates with the manufacturer's Western blot analysis indicating reactive specificity in humans, mouse, rat, bovine, canine, fish (rainbow trout), guinea pig, monkey, pig, rabbit, and sheep PKCα, detected by a single band of ~80kDa. This antibody does not detect other PKC isoforms; it is specific for PKCα, in the V3 region. In the rat and human retina, Gong and colleagues (2006) used this antibody to immunolabel rod bipolar cells (BCs). This is consistent with the observation that PCKα (clone MC5) is a rod BC marker (Wassle et al., 1991). In the goldfish retina, the monoclonal anti-PKCα antibody has been shown to selectively label Mb (ON-type) BCs (Suzuki and Kaneko, 1990; Vaquero et al., 1997; Yazulla and Studholme, 1998).

Protein Kinase C alpha (PRKCA/PKCα) rabbit: The affinity isolated polyclonal anti-PRKCA antibody was produced in rabbit by Prestige Antibodies® Powered by Atlas Antibodies, developed and validated by the Human Proteome Resource project (www.proteinatlas.org). Using the recombinant protein fragment, CVINVPSLCGMDHT EKRGRIYLKAEVADEKLHVTVRDAKNLIPMDPNGLSDPYVKLKLIPDPKNESKQ KTKTIRST, in human PKCα, the antibody was tested by immunohistochemistry, protein array, and Western blotting against hundreds of normal and diseased human tissues. Because this antibody was fairly new, its specificity in goldfish was questionable. Therefore, co-labeling experiments were performed between the well characterized mouse and rabbit anti-PKCα antibodies. The results confirmed that the rabbit anti-

PRKCA antibody is specific to PKCα and labels Mb BCs of the goldfish retina, perfectly overlapping with the mouse anti-PKCα antibody labeling.

Vimentin (VIM): The monoclonal anti-vimentin, clone V9, is a mouse IgG1 isotype derived from the hybridoma produced by the fusion of mouse myeloma cells and splenocytes from an immunized mouse. Its specificity has been confirmed in horse, monkey, bovine, rabbit, canine, gerbil, feline, hamster, human, pig, chicken, and rat. The anti-VIM antibody can be used for labeling cultured mammalian cells and tumors (Zhang et al., 2009), and for localizing vimentin in fibroblasts, endothelial cells, lymphoid tissue, and melanocytes, in normal and pathological tissues of mesenchymal origin (Bohn et al., 1992). VIM is an intermediate filament protein of MCs and it is present in the teleost neural retina (Liepe et al., 1994). It has been shown to have a strong immunoreactivity in the main radial process and endfeet of the MCs (Mack et al., 1998).

TO-PRO®-3: The monomeric cyanine nucleic acid stain, TO-PRO-3, allows for ultrasensitive detection of double-stranded nucleic acids. It is an exclusively detectable far-red fluorescent, excited around 633 nm. It has demonstrated highly specific and stable nuclear labeling on sectioned tissue (Suzuki et al., 1997), and thus may be used as an alternative to the short wavelength nuclear stain DAPI (Bink et al., 2001). TO-PRO®-3 has been used to label lateral cells in living zebrafish, specifically labeling hair cell nuclei (Santos et al., 2006).

3.5.2. Confocal laser microscopy

Fluorescent imaging of the OCT-embedded sections was performed with a Ziess LSM-510 confocal microscope (Carl Ziess, Oberkochen, Germany) equipped with lasers and the appropriate combination of emission filters. An argon laser (Ar 488) was used to

trigger green fluorescence and two helium/neon lasers (HeNe 543 and HeNe 633) were used to evoke red and far-red fluorescence of the fluorophores used in this study (see Table 2 above). On double labeled sections, sequential scans were performed at the different wavelengths to avoid cross talk between channels. All images were taken with a 40x, oil immersion objective. Single optical plane images were used unless otherwise noted. If it was necessary, Z-stack images were taken at 2 µm intervals then composite images were generated by overlapping the middle portion of the Z-stacks, ~10- 12 µm in thickness. Such images were used, for example, to reconstruct entire cross sections of eyecups in order to determine possible local differences in the thickness of retinal layers (see below). Ziess LSM Image Examiner software (Carl Zeiss, Oberkochen, Germany) was used to view the images and crop to the areas of interest. When necessary, image brightness and contrast was uniformly adjusted for the entire digital image in Photoshop CS3 and CS4 (Adobe 10.1).

3.5.3. Eyecup reconstruction

For morphological analysis of an entire goldfish retina, previously discussed methods were used for immunolabeling (TO-PRO®-3 and PKCα). Vertical cross-sections of eyecups were imaged entirely, via confocal microscopy, as Z-stack images of consecutive optical planes (~40 images). Adjacent, unitary frames (consisting Z-stack images) were taken from one side of the eyecup to the other in a consecutive manner; the initial image was taken at the most peripheral location. Ziess LSM Image Examiner software was used to scroll between the Z-stack images needed for gathering measurements and to mark a representative, 175 µm long area of retina per image.

Photoshop CS3 and CS4 (Adobe 10.1) was used to reduce the image size for reconstruction and to adjust the brightness and contrast of the images.

Adjacent unitary, 40x frames with identifiable, overlapping edge regions were aligned to reconstruct the entire eyecup using Microsoft® Office Power Point® 2003 version (Boudard et al., 2010). Figure 1 demonstrates a control eyecup reconstruction, which was used for evaluating the overall retinal structure and for determining corresponding regions of the eyecups. Each image was used to determine three measurements: (1) ONL soma count (within the 175µm long white bracket), (2) ONL width (3 measurements per image, yellow lines), and (3) bipolar cell (BC) length (light blue line) (Fig. 1, inset).

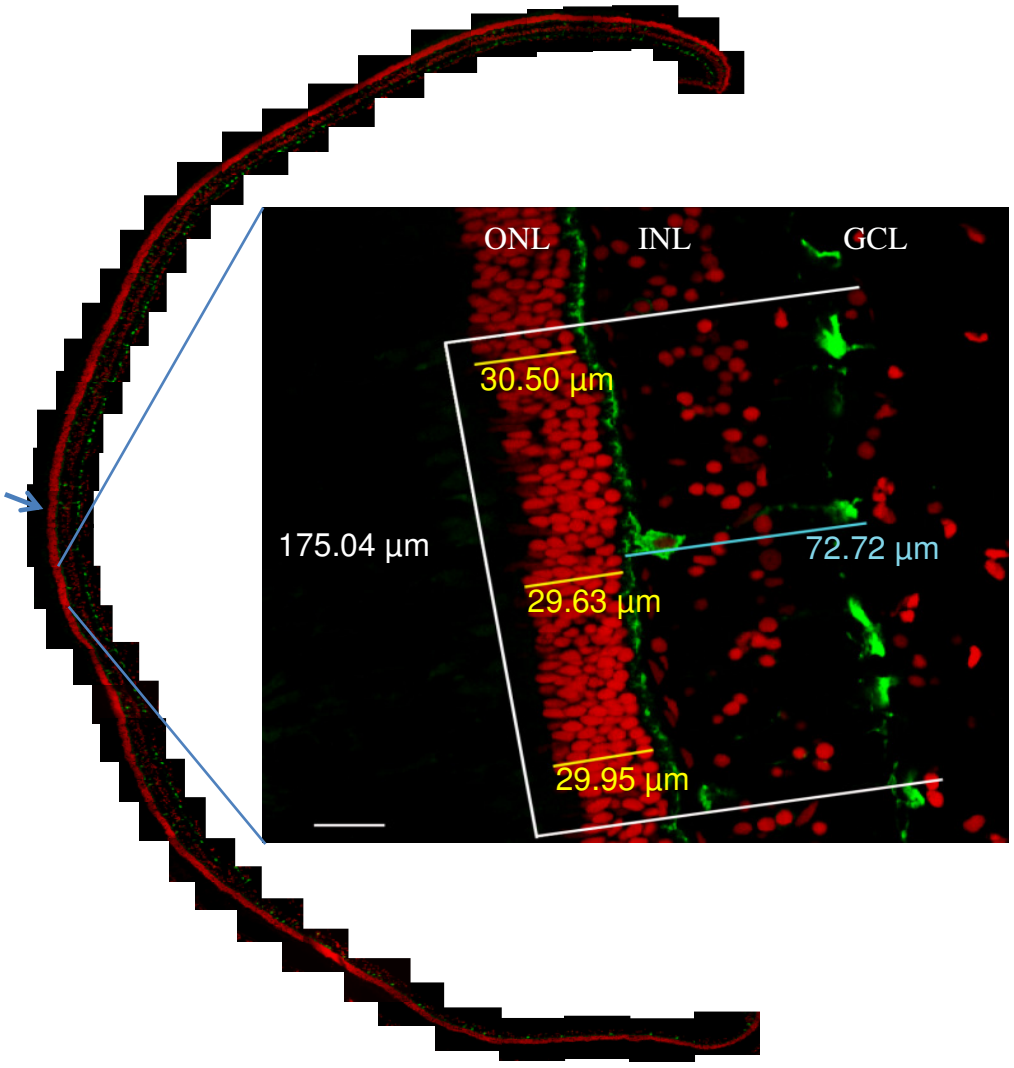

Fig. 1. Reconstructed image of the retina in an entire vertical cross-section of the eye. Immunohistochemical labeling shows the overall morphology of retinal layers in the goldfish retina. All somas were labeled with the nuclear dye TO-PRO®-3 (red). Mb bipolar cells are labeled with anti-PKCα antibodies (green). The entire cross section was reconstructed with adjacent images taken at 40x magnification. Region of the optic nerve head is shown with a blue arrow. (**Insert**) Representative unitary image taken at 40x magnification, demonstrates measurements acquired for morphological analysis. A 175 µm long area of retina (white bracket) was used for each image to count somas of ONL and to acquire ONL width (yellow lines) and Mb bipolar cell (light blue lines) length measurements. Scale bar: 20 µm.

3.5.4. Validating the plane of sectioning

The length and morphology of Mb BCs, labeled with PKCα antibody (Yazulla and Studholme, 1998), were used to judge the appropriate perpendicularity of the sectioning. To determine the average BC length from reconstructed control retinas, all positively labeled Mb BCs (PKCα), which could be identified as a full cell within a single slice of the Z-stack image, were measured. The length was measured from the most distal dendritic, outer plexiform layer (OPL) process, to the most proximal point of the axon terminal in the inner plexiform layer (IPL). Only BCs with a rather linear axon were considered to have an appropriate Mb BC morphology. If the length of labeled Mb BCs from the dendritic layer in the outer plexiform layer (OPL) to the axon terminal in the inner plexiform layer (IPL) were either longer or shorter than the average length of these cells (65 $\pm$ 10 µm, (Yazulla and Studholme, 1998)), sections were excluded from further analysis. A mismatch in the BC length indicated that the sectioning plane was not perpendicular.

3.6. Data analysis

3.6.1. Morphometrical analysis

TO-PRO®-3- labeled somas in the ONL and INL, were manually counted using a handheld tally counter on the best quality, single optical plane image chosen from a Z-stack. The area of interest was either a 175 µm, or 100 µm long area (Braisted and Raymond, 1993) of the 40x image of the vertically cross-sectioned retina (Fig. 1, inset, white brackets). All soma counts were done twice per image to ensure consistency and minimize errors. In every section, two separate 100 µm wide areas were counted and

averaged. Two separate sections were used per animal (Fimbel et al., 2007). To determine the average ONL width for each image, three measurements were taken. Width measurements were done by measuring the TO-PRO®-3- labeled somas from the outer most edge of the ONL (closest to the photoreceptor outer segments) to the inner most edge of the ONL (closest to the outer plexiform layer (OPL)). The three measurements were averaged for each image, identifying the uniformity of the ONL layer across the entire eyecup. Variation between animals was compared as discussed above.
All BC length measurements from both of the entire reconstructed control retinas were averaged.

3.6.2. Statistical analysis of morphometrical data

SigmaPlot 11.0 software extended with a statistical package and Microsoft Excel (2003) were used to statistically analyze all data. When comparing independent variables (i.e. data from multiple groups of animals), a Two or Three Way Analysis of Variance (ANOVA) test was performed. When appropriate, the Holm-Sidak method was used, because the test is more powerful than the Turkey and Bonferroni tests for multiple comparisons. For analyzing dependent samples (i.e. the experimental data obtained in a self-controlled experiments), a two-tailed, paired-Student's t test was used (Microsoft Excel, 2003). For all data analysis the P-values of ≤ 0.05 was considered significant. Cumulative quantitative data are presented as averages $\pm$ SEM.

3.6.3. Analysis of colocalization for molecular markers

Quantitative estimation of colocalization between known immunohistochemical markers was performed using Image J software (NIH, Bethesda, MD, USA). The JACoP

plug-in was used to calculate the Pearson's coefficient (Bolte and Cordelieres, 2006) using Costes' approach. Pearson's coefficient provides an analysis of pixel intensity and location in a duel-channel image with values ranging from -1 to 1 (-1: negative correlation; 0: no correlation; 1: complete correlation) (Gonzalez, 1987; Liu et al., 2010; Manders et al., 1992). Costes' approach performs two things: 1) it sets an automatic threshold level for both channels, eliminating inconsistent or irreproducible results, and 2) it provides a statistical analysis of true colocalization through evaluation of randomized images (Bolte and Cordelieres, 2006; Costes et al., 2004). To evaluate colocalization, single optical plane confocal images of the control goldfish retina were used.

4. RESULTS

4.1. Morphology of the control goldfish retina

To determine the overall morphology of the retinal layers in goldfish retina, immunohistochemical experiments were performed with the nuclear dye, TO-PRO®-3, and a PKCα antibody on vertically cryosectioned retinas. Mb bipolar cells (BC), labeled with PKCα (Yazulla and Studholme, 1998), provided the means of determining retinal stretching and deformations, and were used to judge the appropriate perpendicularity of the sectioning (see Methods for details). Retinal morphometric analysis was performed on the entire vertical cross-section of the eyecup. Reconstructed images were built from adjacent Z-stack images, taken at 40x magnification, using Microsoft® Office Power Point® 2003 version. A 40x image depicts an approximately 200 µm long area of the full retina cross-section, out of which the best 175 µm long area was analyzed quantitatively as a unit. Focusing on the ONL (see Methods, Fig. 1, inset), somas were counted in the outer nuclear layer (ONL) and three measurements of the ONL width were recorded and averaged, for each image.

This simple, but systematic morphometric analysis of the ONL was performed in order to (1) set the design of consequent experiments by providing information on the variation of these ONL parameters within and across control retinas and (2) to provide a base for determining possible chemically-induced morphological changes of the ONL in future experiments.

In Figure 2, values resulted by the above described morphometric analysis of two eyecups (Fish 1and Fish 2, respectively) were plotted.

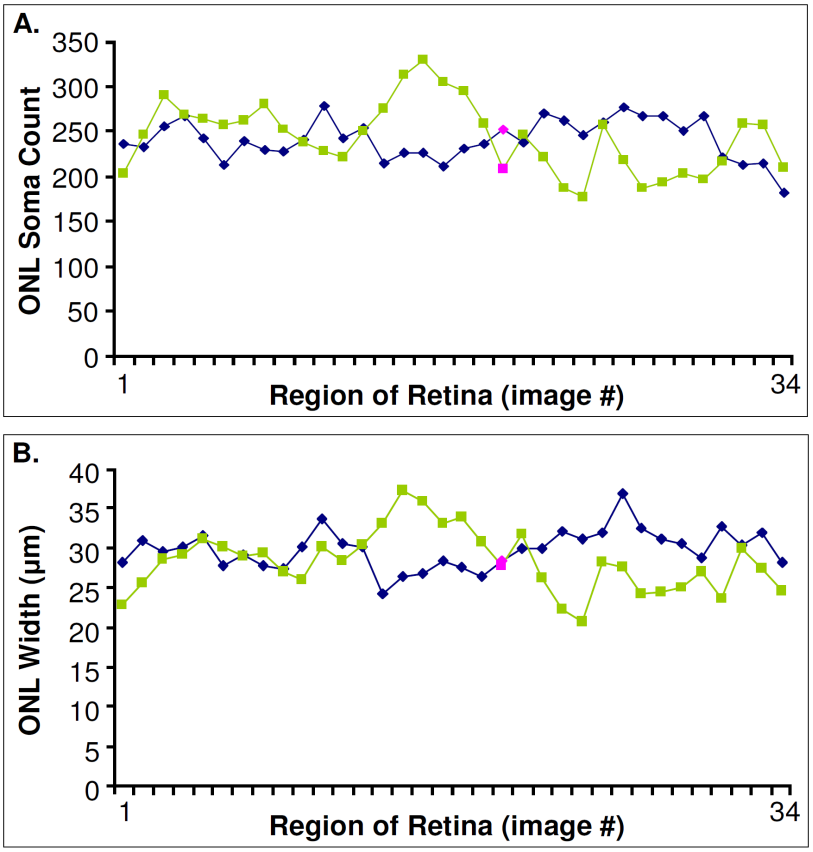

Fig. 2. Morphometric analysis of the ONL of two control goldfish retinas. Vertical cross-sections of the retinas were imaged with a 40x objective, covering ~200 µm long area/image. Full retinal cross-sections across the entire eyecups were reconstructed from slightly overlapping images of adjacent regions. Pink points represent the central region adjacent to the optic nerve head. Diagrams of the ONL soma counts (**A**) and ONL width (**B**) demonstrate that these parameters of the ONL are similar across animals (**Fish 1** and **Fish 2**).

The plotted lines show that the measured ONL parameters, ONL soma count and ONL width (Fig.2A and 2B, respectively) are approximately uniform across the entire eyecup. The most peripheral portions were thinner and contained fewer somas (Otteson and Hitchcock, 2003). The average soma count was similar between fish (Fish 1: 240$\pm$16; Fish 2: 242$\pm$27; n=34 sections for each), as was the ONL width (Fish 1: 29.8$\pm$1.7 µm; Fish 2: 28.3$\pm$2.7 µm; n=34x3 measurements for each, respectively). Statistical analysis by means of Two Way Analysis of Variance (Holm-Sidak method, see Methods for details) tests were performed on both the ONL soma count and the ONL width data. The tests confirmed that there were no statistically significant differences among the regions

of retina for a given fish (ONL soma count: p=0.981; ONL width: p=0.995). In other words, the measured parameters of the ONL "within" each retina were homogenous. Moreover, neither of the two morphometrical parameters analyzed were significantly different between the two retinas analyzed here (ONL soma count: p=0.782; ONL width: p=0.116) (see Appendix 1 for details).

In summary, the absolute numbers of morphometrical data describing the ONL of control retinas appeared very similar between individual fish. In addition, the ONL in the goldfish retina appears to be uniform in thickness and soma numbers across the entire vertically cross-sectioned retina, except for the most peripheral regions. It should be noted, that the size of the fish used for these experiments were similar. Together this data suggests that the retina, of similarly sized fish, is relatively uniform "within" and between animals.

4.2. Effects of DMSO injections on the morphology of the goldfish retina

N-Methyl-N-nitrosourea (MNU), our choice of chemical agent to induce photoreceptor degeneration, is insoluble in water. Therefore, for intraocular delivery, MNU has to be dissolved in dimethyl sulfoxide (DMSO). Although DMSO is considered to be a relatively safe solvent for in vivo administration of several water-insoluble substances (Santos et al., 2003), intravitreal DMSO injections reportedly caused toxic effects in the rabbit retina (Silverman, 1983). Therefore, we first determined if intraocular DMSO administration alone caused photoreceptor damage in fish. Following the previously-described counting methods, data was obtained from DMSO-injected eyes (4µl DMSO injected eyes into one eye, n=3) at 7 days post-injection (dpi) and was

compared to the data obtained from control retinas (no injection, n=2, same as on Fig. 2A). The results are plotted in Figure 3.

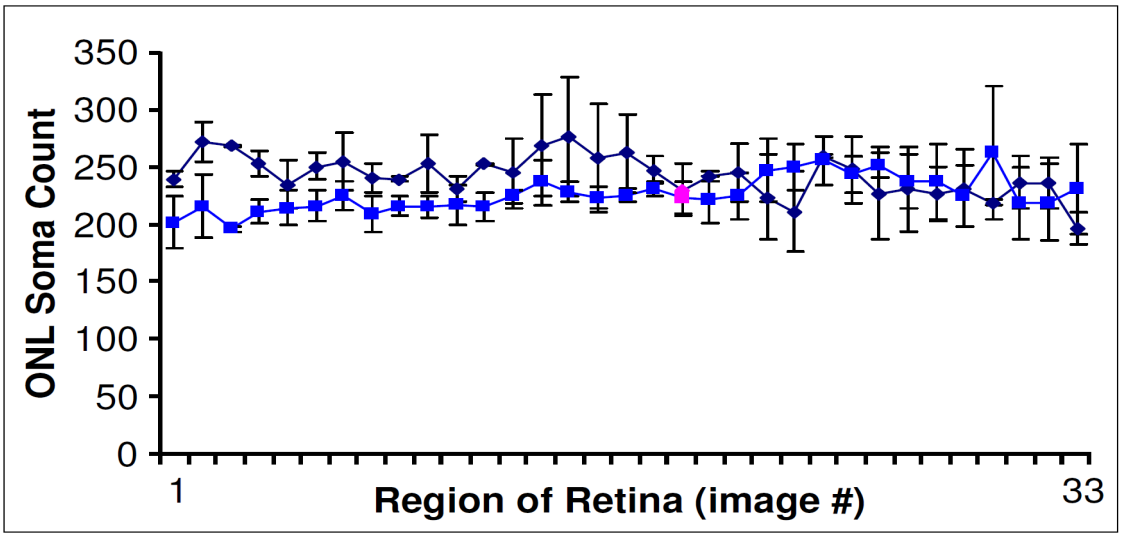

Fig. 3. Morphometric analysis of control versus DMSO injected eyes at 7 dpi. Data obtained from **control** (no injection, n=2) and **DMSO** (4 µl, n=3) injected eyes is aligned by corresponding eccentricity. ONL soma counts were obtained from a 175 µm long area of retina per image, across an entire vertical cross-section of eyecups. Data is presented as average ± sem. Pink points represent the regions adjacent to the optic nerve head. The difference between control and DMSO-treated retinas were significantly different (Two Way ANOVA, p= 0.007).

Based on the averaged ONL soma counts, intraocular DMSO application does appear to cause a small reduction of photoreceptor numbers (i.e. Fig. 3, Regions 1-12). Indeed, a Two Way Analysis of Variance (Holm-Sidak method) test confirmed that the difference in ONL soma counts between the control (averaging 242±4.6/area, n=2x34) and DMSO-treated retinas (averaging 226±3.8/area, n=3x34) was significant (p= 0.007). There was no significant difference in ONL soma counts (p= 1.000) across the regions of individual retinas from DMSO-injected eyes. Statistical comparison of ONL width data (not shown) between the control and DMSO-treated retinas resulted in no significant difference (p= 0.097) (Appendix 2).

These findings suggested that an intraocular injection of 4 µl DMSO caused some damage to the outer retina and reduced the number of photoreceptors in a uniform manner across the entire retina. Due to the low number of fish used in this experiment and the variation between the two measured parameters, these results had to be treated with caution. This data also suggested that the ONL soma counts provide a more sensitive test for measuring photoreceptor numbers than averaged ONL width measurements.

4.3. Morphology of the MNU-treated retina

The ability of MNU to induce photoreceptor degeneration in the fish retina was tested by administering a direct intraocular injection of MNU (4 µl of 14% w/v in DMSO) unilaterally, along with a concurrent direct DMSO (4 µl, "sham") injection into the contralateral eye. MNU has never been used in fish, so a pilot study (n=3) was performed to alleviate any concerns about the possible side effects of the drug. The fish were carefully monitored over the course of the experiments, but no behavioral signs of MNU-induced extended pain were noted. Following the time course of MNU effects on photoreceptors seen in mice (Nagar et al., 2009; Nambu et al., 1997; Yuge et al., 1996), fish were euthanized and retinal tissue was harvested and processed at 7 dpi. Representative images of retina, obtained from an MNU-treated and the contralateral (sham) eye from the same animal, are presented in Figure 4.

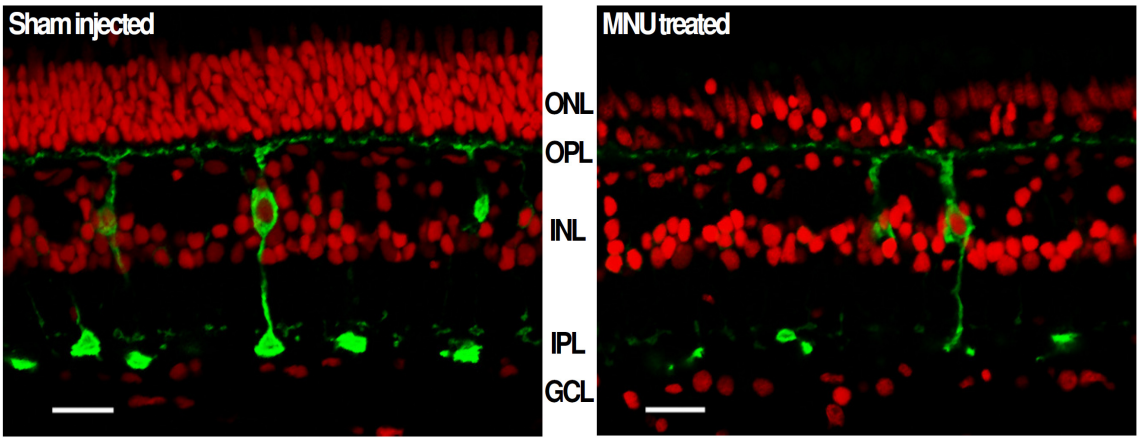

Fig. 4. Qualitative comparison of sham-injected (DMSO) versus MNU-treated goldfish retinal sections at 7 dpi. Representative images (40x magnification) were taken from areas of corresponding eccentricity from reconstructed retinas of the same fish. Somas were labeled with the nuclear dye TO-PRO®-3 (1:5000, red) and Mb bipolar cells were labeled with the PKCα antibody (1:500, green). The decrease in ONL somas demonstrates photoreceptor cell loss following MNU (14% w/v in DMSO) injection. Scale bar: 20 µm.

The overall layered retinal structure was preserved in the MNU-treated eye. Nonetheless, the ONL layer of the retina harvested from the MNU-treated eye appeared much thinner than that of the sham-injected control. This clearly indicated a decrease in the number of photoreceptors, whose somas make up the ONL (Fig. 4).

In order to determine whether or not the intraocular MNU injection affected photoreceptors evenly across the retina, the entire vertical cross-section of both MNU-treated and contralateral, sham-injected eyecups were reconstructed for 3 fish and their morphometric parameters (see methods, Fig. 1) were compared. The average ONL soma count and ONL width data obtained by such measurements are plotted on Figure 5.

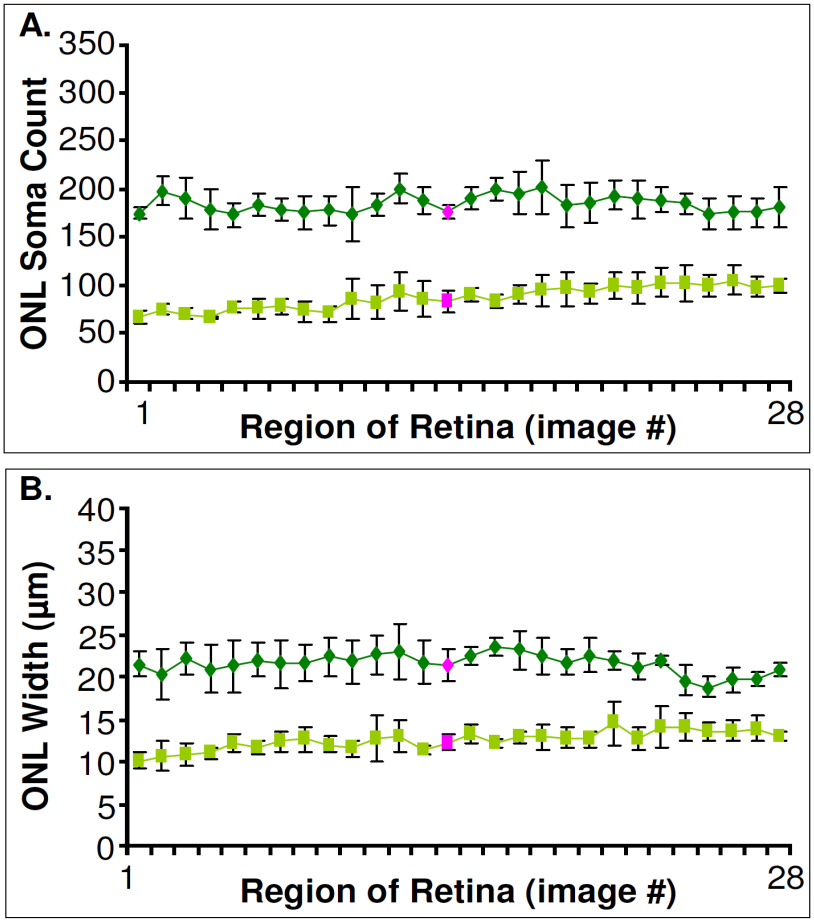

Fig. 5. Morphometric analysis of three MNU-treated goldfish retinas at 7dpi. The animals received a single intraocular injection of 4 µl of **MNU** (14% w/v) into the left eye and 4 µl of DMSO (**sham**) into the contralateral right eye. All ONL soma counts and width measurements were taken from a 175 µm long area of retina per image, across the entire eye cup. Data is presented as average ± sem (n=3). Pink points represent the region adjacent to the optic nerve. The diagrams show that MNU treatment reduced both the number of somas in the ONL soma count (**A**) and the ONL width (**B**). The MNU-induced photoreceptor loss was significant ($p<0.001$) and uniform across the retina.

MNU application reduced both of the measured ONL parameters across the entire retina (Fig. 5). Two Way Analysis of Variance (Holm-Sidak) tests confirmed that when compared to the sham-injected retinas, ONL parameters of MNU-treated retinas were significantly different both in terms of a decrease photoreceptor soma number ($p<0.001$) and a decrease in ONL width ($p<0.001$). The analysis did not detect a significant difference ($p= 0.958$) in the ONL soma numbers and ONL width ($p= 0.998$) across the regions of MNU-treated retina, indicating that MNU treatment induced uniform photoreceptor loss (Appendix 3).

In order to determine whether MNU induced photoreceptor degeneration locally, the average "unitary" ONL soma count (i.e. for a 175 µm long section/image) of three

DMSO ("DMSO sham") retinas, obtained from animals that received an MNU treatment in the contralateral eye, were compared to three DMSO-treated retinas ("DMSO control") obtained from animals whose contralateral eye was injected with fish Ringer's solution (183±10, n=3x32 vs. 227±15, n=3x32, respectively). The average ONL soma counts are plotted in Figure 6.

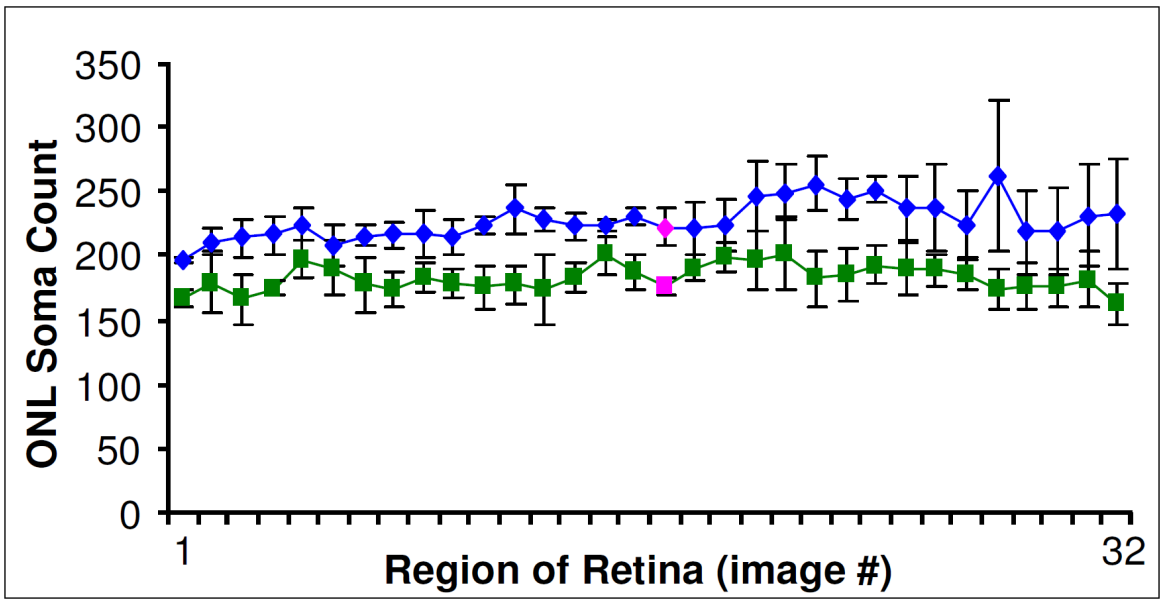

Fig. 6. Morphometric analysis of "DMSO control" versus "DMSO sham" injected eyes at 7 dpi. Data obtained from **DMSO control** (4 µl, n=3) and **DMSO sham** injected eyes (4 µl, n=3) is aligned by corresponding regions of retina. ONL soma counts were obtained from a 175 µm long area of retina per image, across an entire vertical cross-section of eyecups. Data is presented as average ± sem. Pink points represent the regions adjacent to the optic nerve head. ONL soma numbers of the DMSO sham-injected retinas were significantly lower than that of the DMSO control retinas at 7 dpi (Two Way ANOVA, $p<0.001$).

The plotted line graph shows that the average number of ONL somas in the "DMSO sham" retinas were less than that of the "DMSO control" retinas in almost every region analyzed (Fig. 6). A Two Way Analysis of Variance (Holm-Sidak) test confirmed that the difference was significant ($p<0.001$) (Appendix 4). This result suggested that a unilateral, intraocular MNU injection induced photoreceptor degeneration primarily locally, in the MNU-treated eye in 7 days. However, the MNU effect was not restricted to the treated

eye. A slight decrease (~15 %) in the number of photoreceptors in the contralateral eye was also noted, which was more than one could expect from DMSO itself (Fig.6). These results were not unexpected: intraperitoneal administration of MNU has been shown to cause photoreceptor degeneration in a variety of species (Herrold, 1967; Nakajima et al., 1996; Ogino et al., 1993; Tsubura, 1998; Yuge et al., 1996), indicating that MNU or its active metabolites can get into the eye by crossing the blood/ retina barrier. Therefore, it is not surprising that intraocularly applied MNU might leak out and exerts effects on other parts of the body, including the contralateral eye. These concerns notwithstanding, the pilot experiments confirmed that our experimental design was correct and applicable. Even if some photoreceptor loss occurred in the contralateral eye, the unilateral, intraocular MNU injection did not blind the fish on both eyes, so they could feed, and thus survive. Therefore, we tested further whether or not the MNU-induced photoreceptor degeneration in fish could be used to model human photoreceptor degenerative diseases.

4.4. MNU-induced cell death is photoreceptors specific

The results presented so far confirmed that (1) the main morphological parameters of the ONL (thickness and soma density/numbers) in the goldfish retina are uniform across the central portion of the fish retina, and (2) intraocular MNU application could induce significant photoreceptor degeneration by 7 dpi in a uniform manner across the retina of the injected eye (Fig. 5). These findings also demonstrated that morphometric analysis of the central retina provides representative data which are valid for all retinal areas, especially if the effects of intraocular MNU injections are evaluated in a self-controlled manner (e.g. comparing the qualitative parameters to those obtained from the corresponding retinal area of sham treated, contralateral eye to reduce individual

differences across fish). Thus, the study from this point on was focused on the central region of retina, ~2000 µm on either side of the optic nerve head (see methods, Fig. 1, ~10 images in both directions from blue arrow).

The next question we asked was whether or not the intraocular MNU application triggered cell death that was specific to photoreceptors, as it was found to be the case in mouse after i.p. MNU application (Nagar et al., 2009; Yuge et al., 1996). In order to determine that the initial MNU dose (14% w/v) yielded a reproducible retinal damage response, 6 more fish were intraocularly injected with the initial MNU dose (14% w/v). Tissue was harvested and processed, following the protocols applied previously (Methods). Immunohistochemical labeling was used to evaluate the 100 µm sections of retina for MNU-induced photoreceptor damage (Fig. 7).

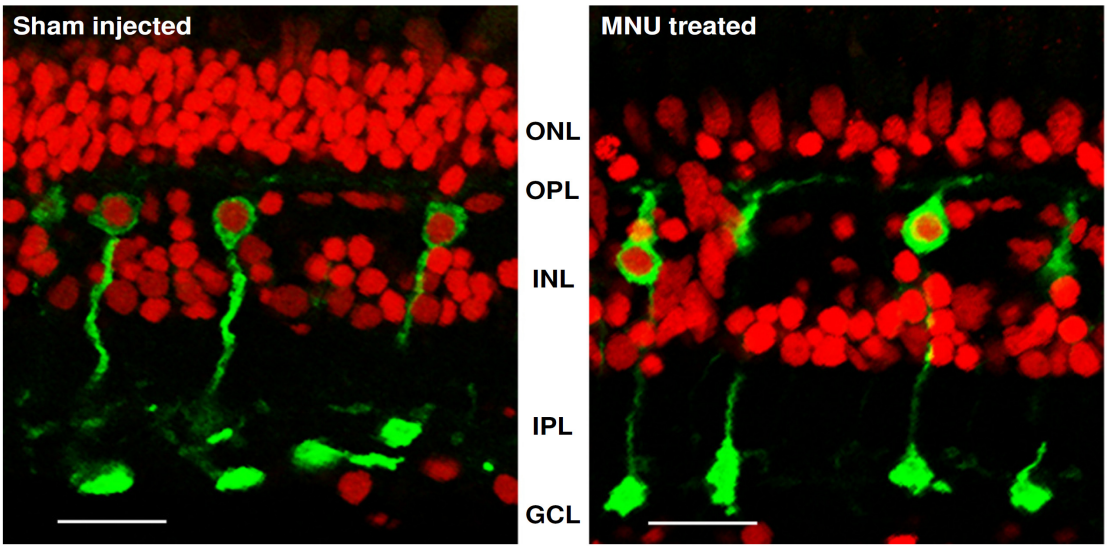

Fig. 7. Representative images for quantitative analysis of sham-injected versus MNU-treated goldfish retinal sections at 7 dpi. Representative images (40x magnification) were taken from corresponding areas of retina for the same fish. Somas labeled with the nuclear dye TO-PRO®-3 (1:5000, red) and Mb bipolar cells labeled with the PKCα antibody (1:500, green). Scale bar: 20 µm.

Cumulative data is presented in Figure 8.

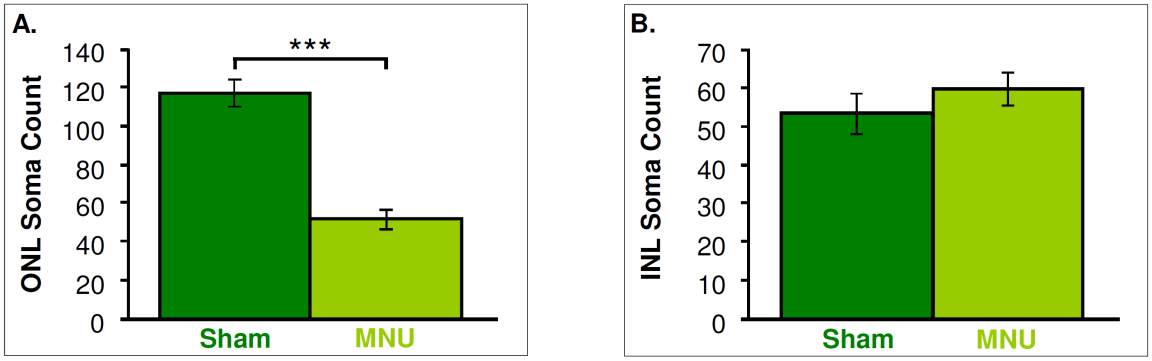

Fig. 8. Summary diagram of MNU-induced photoreceptor cell loss at 7 dpi. Diagrams represent the decrease in average (n=9) ONL (A) soma counts following MNU treatment at 7 days post single intraocular injection of 4 µl of 14% MNU (MNU) versus 4 µl of DMSO (Sham). No significant loss was seen in the INL (B) soma counts. Data is presented as average ± sem. ***: p<0.00005, paired-Student's t test.

Soma counts of the ONL and INL were collected and averaged for 7 day post MNU-injected fish (n=9). Paired-Student's t tests were performed to compare the dependent samples, soma count numbers between the MNU-treated and sham-injected contralateral retinas of the same animals. The analysis confirmed that a single, direct intraocular injection of MNU (14% w/v) caused significant (two-tailed, p<0.00005) photoreceptor degeneration in the MNU-treated eye, by 7 dpi (Fig. 8A). No significant differences were seen in the INL layer (two-tailed, p=0.37) between treatment groups (sham vs. MNU, Fig. 8B). This data was in agreement with the results of our pilot study and strengthened the claim that an intraocular injection of MNU can induce photoreceptor degeneration in the in the treated eye within 7 days.

4.5. MNU-induced photoreceptor degeneration in both left and right eyes

Photochemical stress models demonstrate that chemicals, triggered by light (e.g. Rose Bengal), can lead to retinal cell death (Eichenbaum et al., 2009). Since MNU is a light-sensitive chemical, we wanted to ensure that the observed photoreceptor degeneration in MNU-injected eyes was not associated with photochemical stress

triggered by accidental, uneven illumination of our fish tanks. To do this 4 fish received a direct intraocular injection of 4 µl of MNU (14% w/v) into the right eye, along with a sham injection of 4 µl of DMSO into the contralateral (left) eye. Fish were kept in the same tanks under the exact same light cycle and illumination as before. The tissue was harvested and processed at 7 dpi, following the protocols discussed above. The ONL and INL soma counts were compared between the MNU-treated and sham-injected eyes, obtained from the same fish in a pair-wise manner via paired-Student's t test. The data confirmed that the ONL soma count was significantly (two-tailed $p<0.0008$) reduced for the MNU-treated eye, when compared to its sham-injected control (Fig. 9). The INL was not affected by MNU treatment (data not shown).

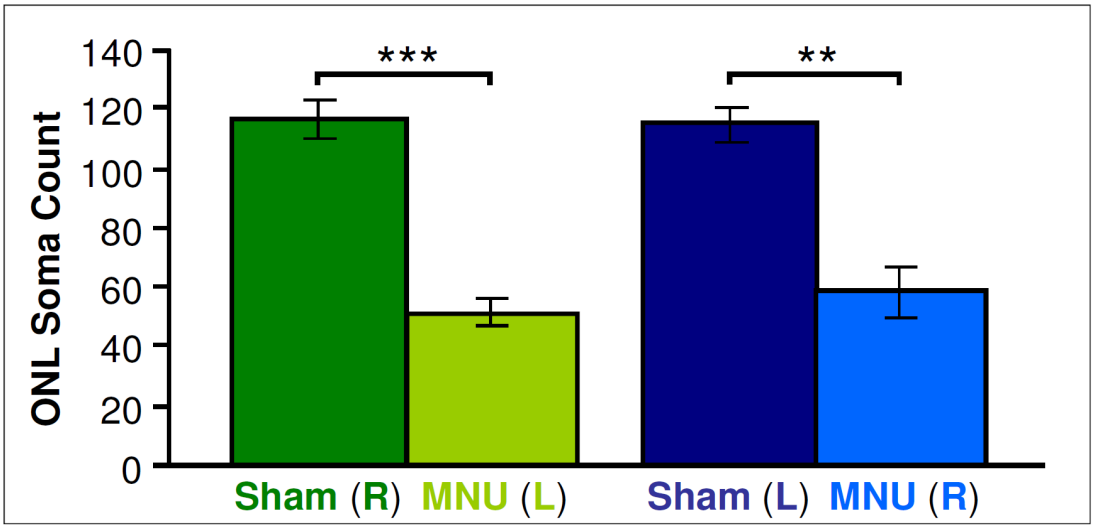

Fig. 9. Ocular laterality comparison of MNU-induced photoreceptor cell loss. Comparison of left (L) (n=4) versus right (R) (n=9) eye injections of 4 µl of MNU (14% w/v in DMSO) and 4 µl of sham (DMSO). Data is presented as average ± sem. Diagram represents a decrease in ONL soma counts, at 7 dpi, between the MNU and sham-injected eyes. ***: $p<0.00005$, **: $p<0.0008$, paired-Student's t test. No significant difference was detected between two sides (L vs. R) for the same treatment: sham versus sham or MNU versus MNU, respectively (Two Way ANOVA, $p=0.531$).

To determine the ocular laterality of the injection or systemic absorption of MNU affected by photoreceptor loss, a Two Way Analysis of Variance (Holm-Sidak method) test was performed for multiple comparisons of independent samples to compare the

treatments (sham and MNU) between the right and left eye MNU injections. The analysis confirmed that the extent of photoreceptor loss was independent of which eye received the MNU treatment. There was no significant difference ($p=0.531$) seen when comparing either of the treatments (sham or MNU) between the right and left eyes (Appendix 5).

4.6. MNU-induced selective, dose dependent photoreceptor degeneration

In order to determine the lowest concentration of MNU that would induce photoreceptor loss, a simple dilution experiment was performed using the calculated MNU stock (14% w/v) and half of its concentration (7% w/v). Fish received a single direct intraocular injection of either 14% or 7% MNU, as discussed above, and then at 7 dpi the tissue was harvested and processed for morphometrical evaluation. Vertical cross-sections of retina were labeled using the nuclear dye TO-PRO®-3 and antibodies against PKCα, and the soma counts of the sham and MNU-treated eyes were compared at both the ONL and INL layers. The data was first evaluated separately by the dose (between sham and MNU-treated eyes for each dose), using paired Student's t test for the dependent samples, to look for effects of the MNU treatment. Significant photoreceptor cell loss was found in the ONL (two-tailed, $p<0.00005$) by one week following a single intraocular injection of 4µl of MNU (14% w/v): about 60% of the photoreceptors were eliminated compared to sham injected eyes (n=9). The reduced dose of MNU (4µl of 7% w/v solution per eye) caused a smaller (~30%), but significant (two-tailed $p<0.002$) reduction in the number of photoreceptors (n=5) within the same one week period (Fig. 10A). It should be noted that, due to the ability of MNU to cause damage in the corresponding, sham-injected eye, percentages of photoreceptor loss may be greater if

compared to control retinas. The number of cells in the INL of the treated eyes appeared to be unaffected by MNU (Fig. 10B).

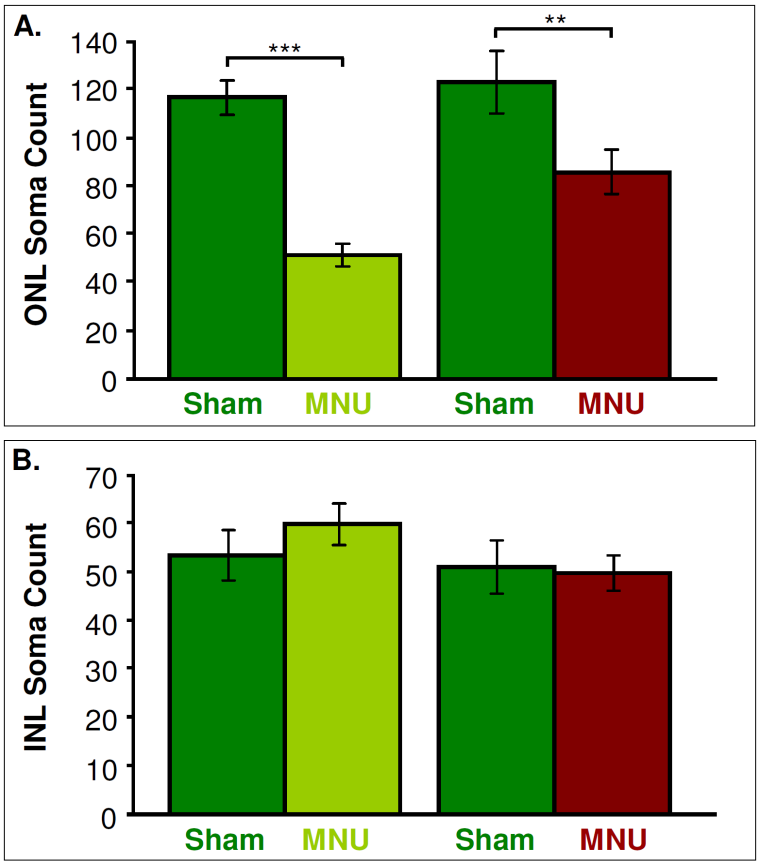

Fig. 10. Dose experiment: 14% versus 7% MNU treatment at 7 dpi. Data demonstrates the MNU induced photoreceptor loss following a single direct intraocular injection of 4 µl of **14%** MNU stock or 4 µl of **7%** MNU half concentration. The diagrams summarize the ONL (**A**) and INL (**B**) soma counts of the **14%** (n=9) and **7%** (n=5) MNU-treated eyes versus their **sham**-injected control. (**A**) Significant photoreceptor loss was seen in both the **14%** and **7%** MNU-treated eye, when compared to the sham. (**B**) INL was not significantly affected. Data is presented as average ±sem. ***: $p<0.00005$, **: $p<0.002$, paired-Student's t test.

Two Way Analysis of Variance (Holm-Sidak method) test was performed to compare photoreceptor loss between doses. The results indicated that ONL soma counts of the MNU-treated groups (14% and 7% MNU doses) were significantly different ($p=0.007$) (Appendix 6). In concert with previous MNU studies performed in mammals (Herrold, 1967; Nakajima et al., 1996), MNU caused specific and dose-dependent photoreceptor degeneration in fish. Based on the fact that photoreceptor loss was greater with the 14% than with the 7% MNU dose (Fig. 10A), it was decided that the study would continue with the stronger 14% MNU dose.

4.7. Age does not contribute to MNU effects

One of the known risk factors associated to retinal degenerative diseases is advanced age. Some hereditary disorders begin relatively suddenly at a specific age, while for others photoreceptor degeneration is marked by the progressive deterioration of the retina over time (Parapuram et al., 2010). To determine whether age is a contributing factor to the MNU-induced retinal degeneration in the goldfish, we considered studies to test the intraocular MNU effects on older goldfish. However, it is very difficult to determine the exact age of a commercially available goldfish without an expert analysis of scales, which we could not perform. Alternatively, size can be used as an indicator of age. The larger goldfish is normally older. However, growth is not linear and depends –at least– on two factors we could not track: (1) food resources during the lifetime of the fish, and (2) the size of the pond (tank) where the fish were raised.

Despite these concerns, an experiment was performed on two of the largest goldfish we could obtain. These were 8-10 inches long, which is approximately the maximum size goldfish can reach. Note that the standard size of goldfish in all other experiments was 3-5 inches (see Methods). These larger fish had a larger eye volume, so the injection volumes were scaled accordingly, 6 µl of MNU (14% w/v) was injected into the left eye, and 6 µl of DMSO served as sham into the contralateral right eye. Following the previously discussed protocols, at 7 dpi the processed tissue was immunohistochemically labeled and compared by ONL soma count for treatment (sham or MNU) and age of the animal (Fig. 11). Throughout this study, the larger fish were referred to as “Old” fish, while all standard sized fish were referred to as “Young” fish.

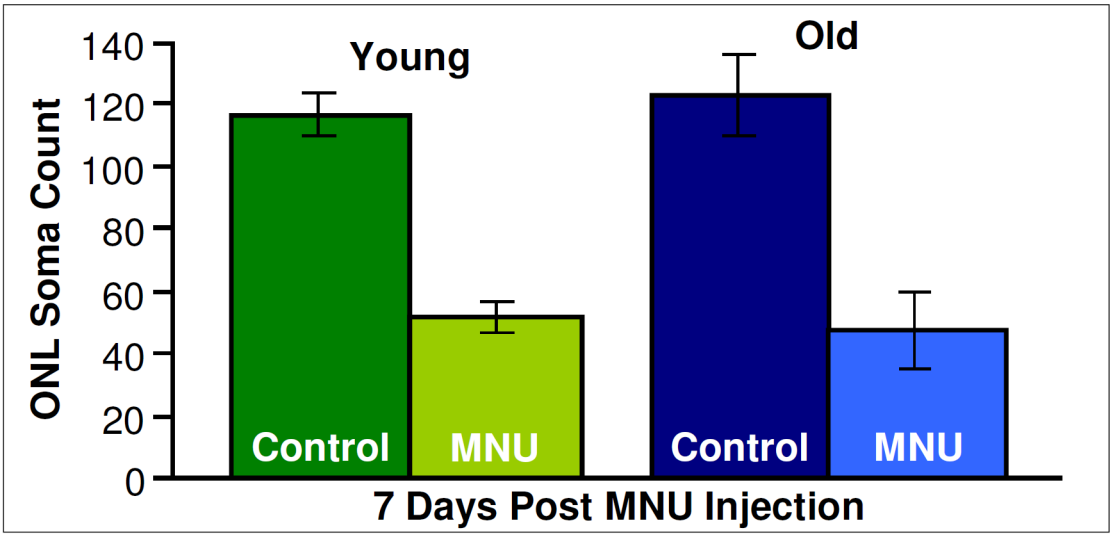

Fig. 11. Comparative study of MNU-induced photoreceptor cell loss in young versus old goldfish retina at 7 dpi. Summary diagrams represent ONL soma counts of MNU-treated young goldfish (**MNU**) versus sham-injected contralateral (**C**) eyes (n=9) and MNU-treated old goldfish (**MNU**) versus sham-injected contralateral (**C**) eyes (n=2). Data is presented as average ± sem.

It was concluded that MNU (14% w/v) could induce photoreceptor degeneration in the older fish; however, it did not seem to be more extensive than the effect in younger animals (Fig. 11). Thus, the MNU-triggered photoreceptor loss appeared fairly uniform between the different age groups. Only a more systematic study (i.e. larger sample size) could rule out age completely as a contributing factor. Nevertheless, the results of these pilot experiments did not justify the notion of focusing the rest of our investigations to older goldfish.

4.8. Time course of MNU-triggered photoreceptor death in fish

In rat and mouse retinas there is evidence of photoreceptor disruption by 1 day post i.p. MNU injection (Yoshizawa et al., 1999; Yuge et al., 1996). In several studies, widespread photoreceptor death was seen after 3 days, and the entire ONL was nearly gone within 7 dpi (Yoshizawa et al., 1999; Yuge et al., 1996). In order to determine the time course of photoreceptor degeneration in the goldfish, following a single intraocular

injection of 4µl of 14% w/v MNU, fish were sacrificed at 0, 1, 3, 5, 7, 10, 14, 21, 28, 35, 42, and 49 dpi. Representative images of retinal cross-sections are presented in Figure 12.

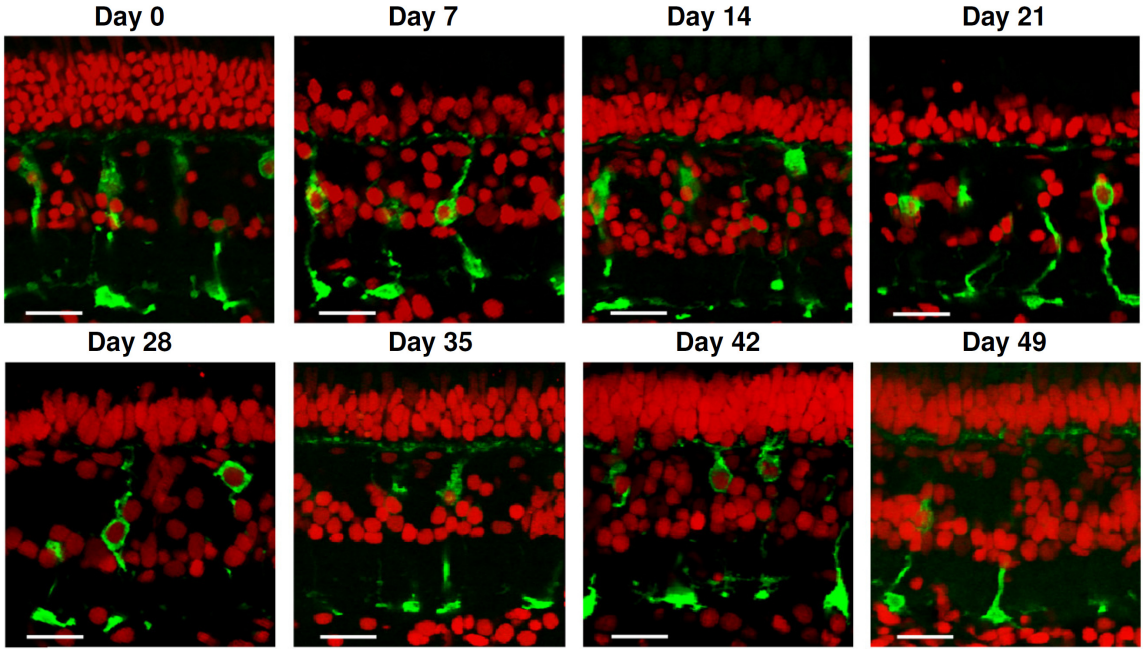

Fig. 12. Time course of morphological changes in the retina following a single MNU injection. Fish were euthanized and retinas were processed on the days post MNU application as shown above the images. Somas labeled with the nuclear dye TO-PRO®-3 (1:5000, red) and Mb bipolar cells labeled with the PKCα antibody (1:500, green). Scale bar: 20 µm.

Population data on the time course of MNU effect is plotted in Figure13. The number of TO-PRO®-3 nuclear stain labeled somas did not change in the sham-injected retinas throughout the time course of the experiment. In the MNU-treated eye, marked (~50%) loss of photoreceptor was first observed in the ONL 5 dpi, (Fig. 13A, **: $p=0.001$, n=5, Two way ANOVA). The goldfish photoreceptor loss was nearly maximal by 7 days (***: $p<0.001$, n=9): approximately 60% of the photoreceptors was destroyed. The number of photoreceptor somas in the ONL remained at the same level through 21 dpi (***: $p<0.001$, n=5).

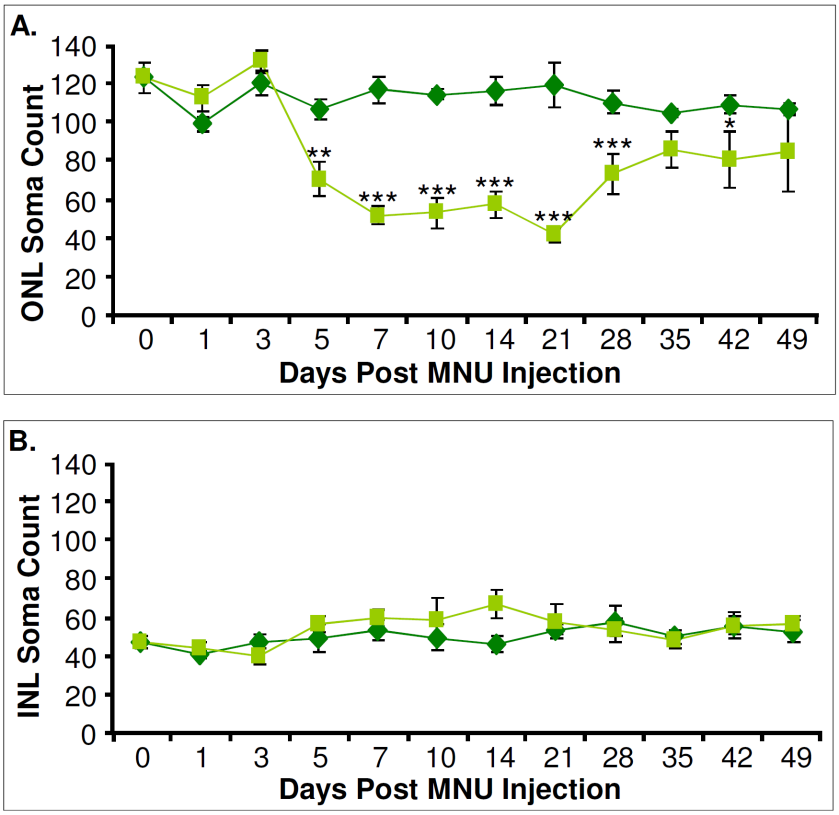

Fig. 13. Time course of MNU-induced retinal degeneration following a single intraocular injection. Line graphs plot soma counts in the ONL (**A**) and INL (**B**) for 14% MNU-treated (**MNU**) versus sham-injected (**Sham**) eyes. Data is presented as average ± sem. (n=4-9, for details see corresponding text in Results).

*: p<0.02, **: p=0.001, ***: p<0.001, Two Way ANOVA, Holm-Sidak method.

By 28 dpi the number of photoreceptor started to increase compared the period 7-21 dpi, but remained still significantly less then than the corresponding numbers in the sham-injected retinas (***: p<0.001, n=7). Only at 42 dpi, out of the last three time points (35 dpi, 42 dpi and 49 dpi), were there significantly fewer photoreceptor somas found in the ONL when compared to the sham numbers (*: p=0.018, n=5). The number of cells in the INL did not change significantly over the time course of the experiments in either eye (p=0.538) (Fig. 13B) (Appendix 7).

These data demonstrated that, although a single dose (4 µl, 14% w/v) of intraocular MNU treatment could induce selective photoreceptor degeneration in the fish retina, it did not lead to complete photoreceptor loss. In summary, the maximal MNU effect was ~ 60% loss (as compared to the contralateral sham-injected control) and it was reached by 7dpi. The photoreceptor number remained unchanged until about 21 dpi, and then started

to increase. The increase in the photoreceptor number between 21- 28 dpi suggested that retinal regeneration had started. By approximately 50 dpi the photoreceptor numbers were not significantly different from those in control or sham-treated retinas.

4.9. A second dose of MNU extended the degenerated state

A single dose of MNU (4 µl, 14% w/v) induced substantial photoreceptor degeneration, but it was not complete. Considering that lower dose (4 µl, 7% w/v) appeared to be less effective (Fig.9), we sought an experiment using a higher MNU dose. However, 14% w/v is the most concentrated MNU solution one can make, based on the solubility of MNU. In addition, the injection volume cannot be elevated above 4 µl. This has been calibrated for the size of goldfish used in the current set of experiments (Yazulla and Studholme, 1997). In pilot trials, increasing the volume caused an obvious leak of the drug solution out of the eye at the injection site during the end phase of injection. Thus, despite an increased injection volume, the actual amount of MNU delivered into the eye was probably not increased. Therefore, in order to increase the dose of delivered MNU we decided to give a second MNU injection of the same dose (4 µl, 14% w/v) to the same eye 14 days after the initial MNU injection. Likewise, the contralateral eye received a second sham treatment at the same time. Fish were euthanized at 7 (21), 14 (28), and 21 (35) days post second injection (initial dpi), and retinas were processed and analyzed as previously described. For demonstration purposes, the data representing time course of the double MNU-injection induced degeneration was plotted (Fig. 14) along with the data obtained from a single dose experiments (same as on Fig. 13).

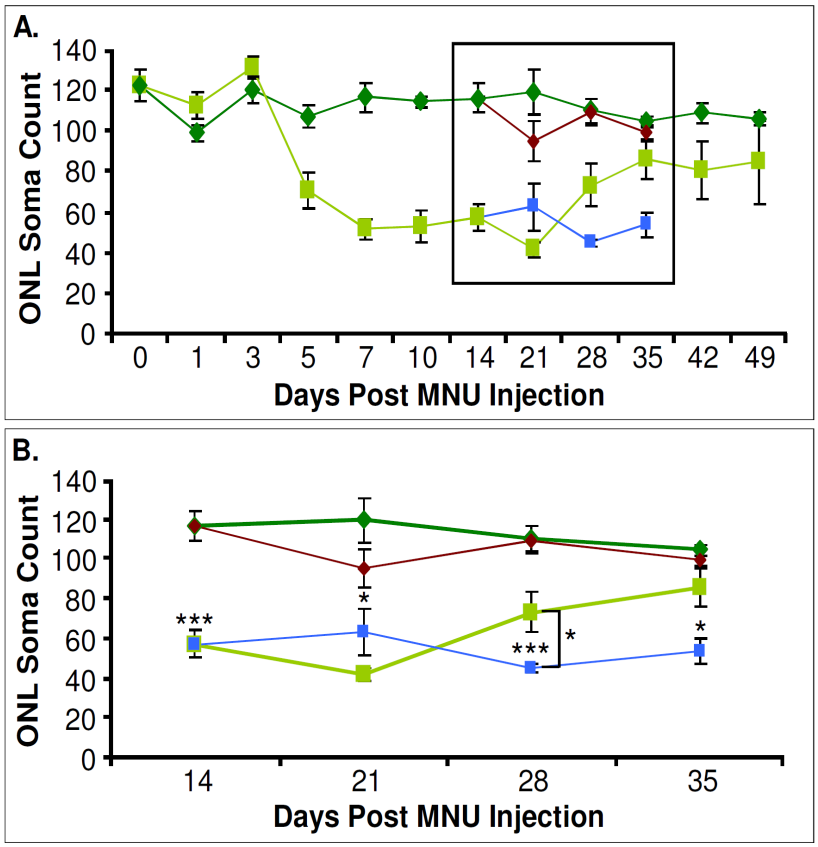

Fig. 14. Time course diagram demonstrating the effects of a second dose of MNU on photoreceptor degeneration. (**A**) Line graph indicates the ONL soma counts following the 14% MNU treatment (single dose of **MNU**, double dose of **MNU**) versus the sham-injected (**Sham** single, **Sham** double) eyes. (**B**) Expanded view of the double injected time points. Data is presented as average ± sem. All time points represent at least an n=5 fish per group except for day 49 (n=4) and day 35 double injected (n=2). (*: p<0.02, ***: p<0.001, Two Way ANOVA, Holm-Sidak method.

We expected the second MNU injection to exert its maximal effect on the same time scale as the first one (about 7dpi). However, the second intraocular MNU injection had serious consequences in the eye. These included inflammation, yellowish coloration of the lens, white coloration of the cornea, and often times led to the complete destruction of the entire retina and pigment epithelium. Morphological analysis of the ONL was possible only on a limited number of double injected eyes. When analysis was possible, however, we found no additional loss of photoreceptors at 7 (21), 14 (28), and 21 (35) days post second injection (initial dpi). The average number of somas/unitary area in the ONL on these days were 62±11, (n=5); 44±2, (n=6) and 53±5 (n=2). These numbers represent about 40% of the corresponding control values. Thus, we could not reach complete photoreceptor degeneration with the second MNU injection.

When Two Way Analysis of Variance (Holm-Sidak method) tests were used to analyze the data, it was determined that there was a significant photoreceptor loss, when compared to the control, at day 21 ($p=0.010$), day 28 ($p<0.001$), and day 35 ($p=0.019$) (Appendix 8). From these data, it was concluded that the second dose of MNU (14% w/v) did not induce further degeneration of the ONL, but instead extended the period of retinal degeneration (~60% photoreceptor loss at 35 day post initial injection) compared to that caused by a single injection (Fig. 14). The number of cells in the INL remained unaffected by the second MNU injection (data not shown). It should also be noted that the previously-mentioned inflammation and irritation to the retina following the second dose of MNU prevented further investigation of these particular retinas at later time points. Based on these results, it was concluded that a double injection of MNU could maintain degeneration for an extended period of time, but does not lead to more complete, specific photoreceptor degeneration.

4.10. Retinal regeneration following MNU treatment

Unlike mammals, the teleost retina is known to exhibit persistent neurogenesis throughout its life due to two stem cell populations (Hitchcock et al., 2004). Nearly all retinal cell types arise from the stem cell population located at the ciliary marginal zone (CMZ), which is continuously added to the periphery of the retina as the animal grows. The other stem cell population, responsible for producing rod precursor cells in the ONL, arises from Müller cells (MCs) in INL (Fimbel et al., 2007; Johns, 1977; Thummel et al., 2008). Decades of research has demonstrated that injury or damage to the teleost retina (via high light exposure, puncture, or toxic injection) stimulates a rapid response to regenerate the damaged retinal neurons (Braisted et al., 1994; Fimbel et al., 2007;

Hitchcock et al., 1992; Raymond et al., 1988). One such response is the proliferation of MCs. MCs have been shown to reenter the cell cycle and produce the appropriate progenitor cells needed to replace the damaged retinal cells (Braisted et al., 1994; Fimbel et al., 2007; Vihtelic et al., 2006a; Yurco and Cameron, 2005). This rapid response was demonstrated in the zebrafish following a single intravitreal injection of ouabain, a drug that induces rapid cell death in all nuclear layers of the retina. Regeneration reportedly started within 1 day post intravitreal ouabain injection (Fimbel et al., 2007). In our goldfish study, we saw an increase in the ONL soma numbers between 21- 28 dpi (Fig. 13), which would suggest that retinal regeneration had started. In order to identify whether regeneration was responsible for the increase of soma numbers in the ONL following MNU treatment, immunohistochemical labeling of newly dividing cells was performed using an antibody for proliferating cell nuclear antigen (PCNA). PCNA has been used to detect regeneration in several teleost retinas (Cid et al., 2002; Vihtelic and Hyde, 2000). Vertical cross-sections of a control and MNU-treated retina, harvested at 14 dpi, were labeled with the nuclear dye, TO-PRO®-3, and progenitor cell marker, anti-PCNA antibody, to identify a regeneration response following the MNU-induced photoreceptor damage (Fig. 15).

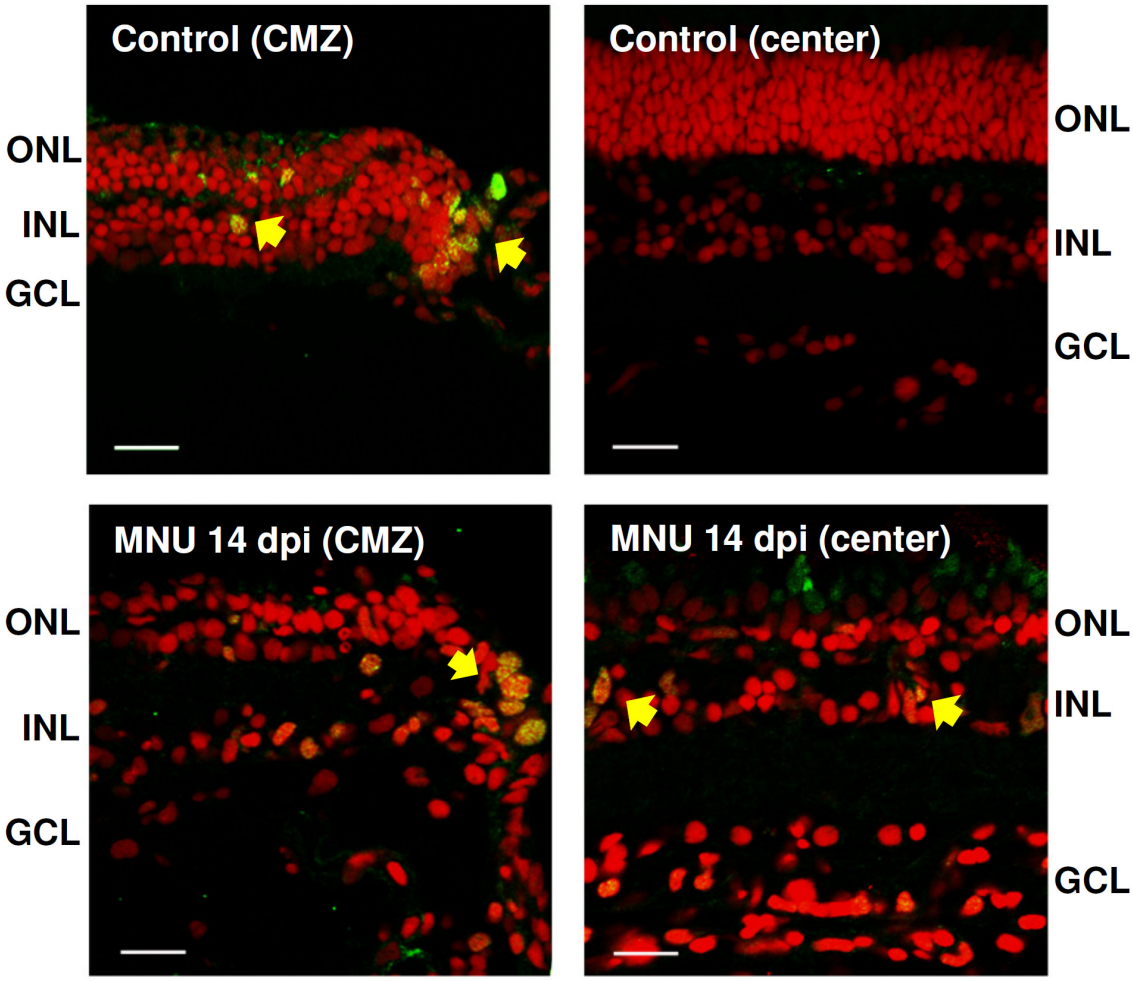

Fig. 15. Immunohistochemical analysis of newly dividing cells in the goldfish retina. Vertical cross-sections of a control (no injection) (**top**) and 14 day post MNU-injected retina (**bottom**) were double labeled with the nuclear dye, TO-PRO®-3 (1:5000, red) and the progenitor cell marker, proliferating cell nuclear antigen antibody (1:100, green, PCNA). The low power (40x) view of the control retina demonstrates the presence of PCNA+ cells primarily in the ciliary marginal zone (CMZ), representing the continuously dividing precursor cells. PCNA+ cells in the 14 days post MNU-treated retina were located in the ONL and INL, suggesting cell proliferation and migration. Arrows mark PCNA+ cells. Scale bar: 20 µm.

Previous immunohistochemical analysis of fish retinas has demonstrated that normal retinal growth is mediated by the CMZ, where PCNA labeling was found (Johns, 1977; Marcus et al., 1999; Vihtelic and Hyde, 2000). Our data is in agreement with those findings. PCNA immunolabeling was found primarily in the CMZ (Fig. 15, top left) of the control retina and there was minimal labeling observed across the central retina (Fig.

15, top right). For the damaged (14 dpi MNU-treated) retina, PCNA immunolabeled cells were also observed in the CMZ (Fig. 15, bottom left). However, unlike the control retina, additional PCNA+ cells were found in both the ONL and INL layers across the central retina (Fig. 15, bottom right). The morphologies of the PCNA+ cells appeared to be different from each other and depended upon their location in the retinal layers. Similar to what has been reported on the shape of the PCNA+ cells in regenerating teleost retina, PCNA+ cells in the ONL layer appeared to have a round and compact morphology, whereas cells in the INL they were spindle-shaped and organized in clusters (Vihtelic and Hyde, 2000). Together these observations suggest that (1) MNU treatment induces a retinal regeneration response in the goldfish retina at 14 dpi and (2) this regeneration response is strong enough to recover the ONL soma numbers by ~50 dpi.

4.11. MNU did not cause Müller cell hypertrophy

Müller cells, which stretch radially from the GCL to the OPL, are involved in several important functions that are vital to the health of retinal neurons: migration of progenitor cells, removal of waste, balance of glutamate and K^+ in the extracellular space (Lamba et al., 2008). In vertebrates, the MCs are known to react to retinal damage and stress by increasing expression of the intermediate filament protein, glial fibrillary acidic protein (GFAP), and undergoing reactive gliosis (Bringmann et al., 2006; Fimbel et al., 2007). One of the chronic consequences of photoreceptor degeneration is a marked extension of processes and hypertrophy of MCs into the empty space of the ONL and the formation of a “glial seal” or “glial scar”. Nagar and colleagues (2009) found in the mouse retina that the MNU-induced photoreceptor loss triggered glial activation. The activation was characterized by enhanced GFAP expression and promoted the growth and extension of

the MCs. The end result was the formation of a "glial seal" (stage 2 of the retinal remodeling theory, see Background, section 1.6) which covered the entire retina by 28 days post MNU i.p. injection (Nagar et al., 2009).

In order to demonstrate that MNU-induced photoreceptor degeneration in fish triggers chronic consequences similar to those seen in mammals, it was important to identify whether a "glial seal" formation occurs in the goldfish retina following MNU treatment. A reliable MC marker for the goldfish retina had to first be determined. Thus, an immunohistochemical analysis was performed with known MC markers: GFAP (Mack et al., 1998; Nagar et al., 2009), vimentin (VIM) (Drager, 1983; Vaughan and Lasater, 1990), and glutamine synthetase (GS) (Mack et al., 1998; Riepe, 1978), on vertical cross-sections of control goldfish retina (Fig.16).

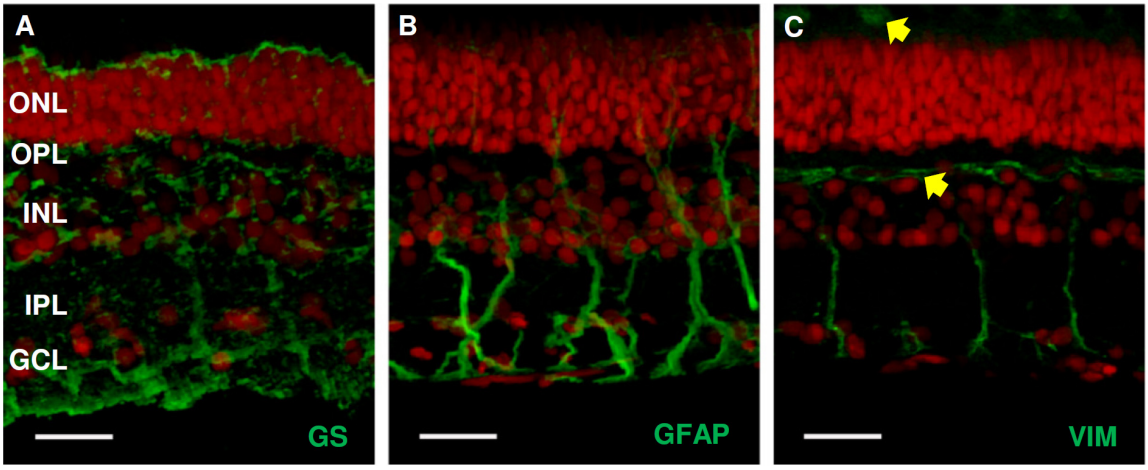

Fig. 16. Immunohistochemical analysis of Müller cell markers in control goldfish retina. Vertical cross-sections of control retinas were double labeled with the nuclear dye, TO-PRO®-3 (1:5000, red), and Müller cell markers (green) mouse anti-glutamine synthetase (1:500, **GS**, A), mouse anti-glial fibrillary acidic protein (1:500, **GFAP**, B), and mouse anti-vimentin (1:500, **VIM**, C). The low power (40x) view the control retina demonstrates that all three antibodies can label Müller cells in the goldfish retina. GFAP appears to provide the clearest Müller cell labeling. VIM also weakly labeled a band in the OPL (horizontal cells) and some photoreceptor outer segments (arrows). Scale bar: 20 µm.

Our results confirmed that all three antibodies labeled MCs in the goldfish retina (Fig. 16). The anti-GS immunolabeling in the goldfish retina was extensive, but did not

well-define the outlines of MCs and their processes, and thus, did not allow for discrimination of individual MCs. However, an advantage of this immunostaining was that it clearly labeled the outer border of the ONL and marked the proximal extent of MCs (Fig.16A). The anti-GFAP and anti-VIM antibodies (Fig. 16 B and C, respectively) provided less extensive immunolabeling, but both made the individual MCs distinguishable.

GS antibody was ruled out for future use. The anti-GFAP antibody appeared to label the MCs better than the anti-VIM antibody, delineating thicker processes and more complete structures. The GFAP immunolabeling marked MC processes throughout the retina, including in the outer retina, whereas the anti-VIM antibody immunolabeled processes primarily in the inner retina. Even in the inner retina, the VIM+ labeling was less intense than that produced by the antibody labeling for GFAP. Labeling with the anti-VIM antibody also produced an immunopositive band in the OPL with some weak labeling occurring in the photoreceptor outer segments (Fig. 16C, arrow). This was consistent with previous studies showing VIM+ OPL labeling as putative horizontal cell (HC) process (Vaughan and Lasater, 1990).

Based on these results, GFAP immunolabeling seemed to be the best choice to detect possible changes in the MC morphology following MNU-induced photoreceptor loss. As mentioned above, GFAP is thought to be an inducible protein in that its quantity increases with retinal damage (Sarthy, 2001). Consequently, one could argue that GFAP immunolabeling in the control retinas was restricted to a subpopulation of (active) MCs. This hypothesis had to be tested before the GFAP immunolabeling was used as a MC marker for comparative studies between MNU-treated and sham-injected goldfish retinas.

We predicted that VIM immunolabeling should mark all MCs because VIM is a structural protein in these cells (Sarthy, 2001). Taking into account that to our anti-VIM antibody also labeled HCs in the goldfish retina (Fig. 16), double immunolabeling studies were performed with anti-VIM and anti-GFAP antibodies to determine whether or not they were labeling the same MC populations. A representative image of the colabeling experiment is shown in Figure 17.

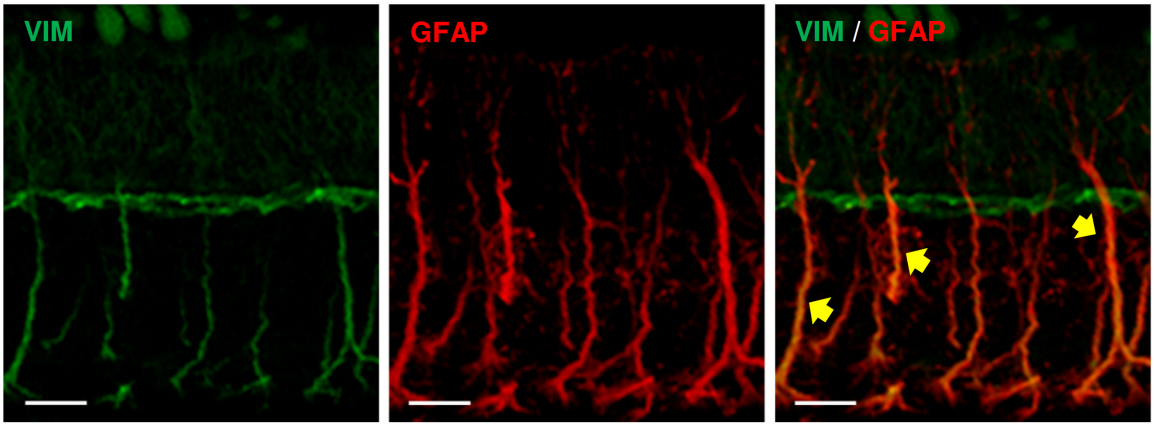

Fig. 17. Colabeling study with the Müller cell markers GFAP and Vimentin in control goldfish retina. Vertical cross-sections of a control (no injection) retina were double immunolabeled with the Müller cell markers: mouse anti-vimentin antibody (1:500, **VIM**, green) and rabbit anti-glial fibrillary acidic protein antibody (1:1000, **GFAP**, red). Low power (40x) view the control retina demonstrates that both the VIM and GFAP antibodies can label Müller cells in the goldfish retina, and there is colabeling between these antibodies (arrows), especially in the inner retina. Scale bar: 20 µm.

Colocalization between the two antibodies (anti-VIM and anti-GFAP) was assessed using a correlation analysis which determines the Pearson's coefficient (PC). PC describes the spatial correlation of pixels in dual-colored images and gives it a value ranging from -1 to 1 (Gonzalez, 1987; Liu et al., 2010; Manders et al., 1992). A negative correlation between the red and green pixels is defined by values < 0; no correlation is designated by a value equal to zero; positive correlation is defined by values > 0, with 1 equaling complete correlation (Bolte and Cordelieres, 2006). In this study we chose to calculate the PC by using Costes' approach (Costes et al., 2004), which is best suited for

images with background noise, as this approach automatically determines the threshold for both green and red intensities, thereby minimizing human error. Additionally, this approach elevates the possibility of colocalization do to chance, by providing a statistical comparison between the actual PC value of the image and a PC value calculated for the same image after randomizing red and green values associated with the pixels (Bolte and Cordelieres, 2006). For a given image, the true colocalization of red and green labeling occurs when the PC for the red and green pixels of the image is significantly higher (probability of colocalization, p-value > 95%) than the PC calculated for randomized red and green pixels of the same image (Costes et al., 2004).

Costes' approach was used to analyze a representative single optical plane image from the projected image shown in Figure 17. The PC calculated was 0.526 with a P-value equal to 100% (see Appendix 9 for details). This PC shows a significant positive correlation between VIM and GFAP immunolabeling and its value indicates only partial colocalization. This index is consistent with what would be expected, based on the restricted VIM immunolabeling to the inner retinal MC processes and the additional immunolabeling of VIM+ HCs and photoreceptor outer segments. In conclusion, this analysis suggested that we did get true colocalization between the VIM and GFAP immunolabeling in the goldfish control retina.

After establishing GFAP as a specific MC marker, which labeled not just the subpopulation of active MCs, but all MCs in the control goldfish retina, immunohistochemical analysis of the MNU-treated retinas were performed. Here we focused on the evaluation of morphological changes in MCs at multiple time points (0, 7 dpi, and 49 dpi). The anti-VIM antibody was used as an additional control in this

colabeling study to further evaluate any MNU treatment-specific MC changes. Furthermore, we maintained a clear sense of retinal layer orientation and photoreceptor damage by using the nuclear dye TO-PRO®-3. Figure 18 (bottom) summarizes the MC densities seen in the control (no injection), 7 dpi, and 49 dpi MNU-treated retinas.

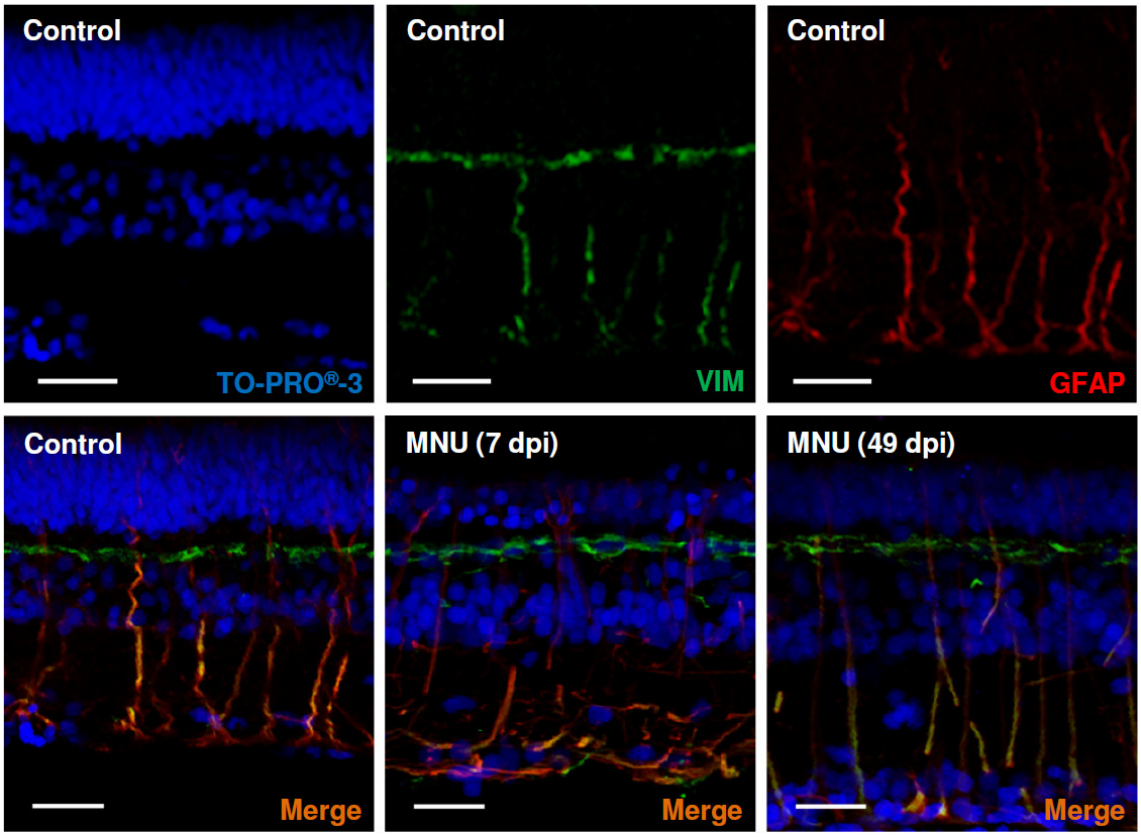

Fig. 18. Immunohistochemical analysis of Müller cell morphology over the time course of the study. Vertical cross-sections of retina were triple labeled with the nuclear dye, TO-PRO®-3 (1:5000, **TO-PRO®-3**, blue) and the Müller cell markers, mouse anti-vimentin antibody (1:500, **VIM**, green) and rabbit anti-glial fibrillary acidic protein antibody (1:1000, **GFAP**, red). (**Top**) A control retina demonstrating the level and location of immunohistochemical labeling for each antibody. (**Bottom**) The merged images for the control (no injection), 7 days post MNU-injected (7 dpi), and 49 days post MNU-injected (49 dpi) demonstrate that both Müller cell markers can be identified throughout the degeneration (7 dpi) and regeneration (49 dpi) process. The MNU-treatment did not appear to affect the Müller cell density over the time course of the study. Müller cells did not form a "glial seal". Scale bar: 20 µm.

In this portion of the study we did not quantify the intensity of GFAP immunolabeling. However, the qualitative data clearly demonstrates that over the time course of our experiments MC hypertrophy and "glial seal" formation did not occur in the

MNU-treated goldfish retina. The GFAP and VIM antibodies did colabel the MC processes, but the colocalization appeared to be restricted to the inner retina.

4.12. MNU did not trigger the remodeling of amacrine cell processes in the IPL

According to Jones and Marc (2005), the third stage of the "retinal remodeling theory" is marked by extension of neurites, entanglement of inner plexiform layer (IPL), and the rewiring or remodeling of inner retinal cell circuitry. To identify whether inner retinal remodeling/rewiring occurs and to further confirm that MNU-induced selective photoreceptor degeneration in the goldfish, an inner retinal cell marker had to be established. In the mouse retina, antibodies directed against choline acetyl transferase (ChAT) have been shown to selectively label cholinergic amacrine cells (ACs) within the INL and GCL (i.e. orthotopic and displaced subtypes), with labeled processes forming two straight bands across the IPL (Haverkamp and Wassle, 2000). We hypothesized that if extensive remodeling of the AC processes takes place in the inner retina (Jones and Marc, 2005), then these bands should lose their laminated appearance. In order to test that, we first performed immunohistochemical studies to confirm that the ChAT antibody provides appropriate, two-band labeling in the goldfish retina as it was described in mouse (not shown), which it did. Retinas from MNU-treated eyes were then immunolabeled with anti-ChAT antibody, as were control eyes, to compare labeling patterns and identifying inner retinal deformities (Fig. 19). The nuclear dye, TO-PRO®-3, was used to label retinal somas for orientation purposes.

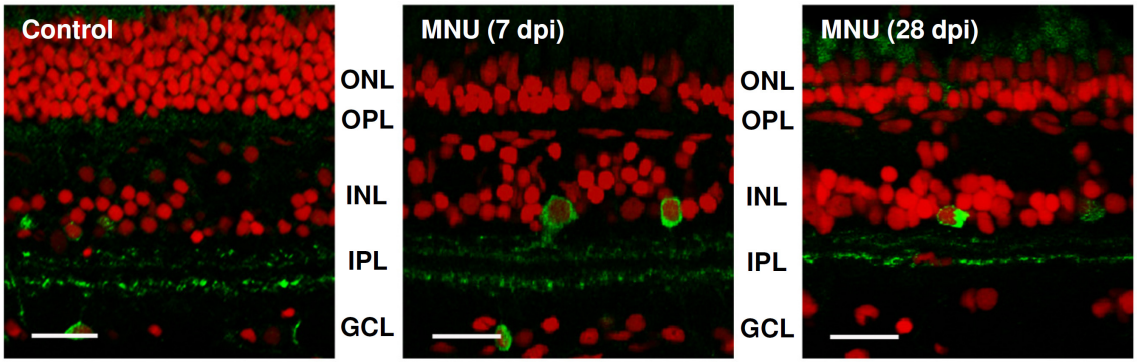

Fig. 19. Representative low power (40x) view of the INL morphology in control versus MNU-treated retinal sections at 7 and 28 dpi. Cholinergic amacrine cells labeled with anti-Choline acetyl transferase antibody (1:100, ChAT, green) and all somas labeled with the nuclear dye TO-PRO®-3 (1:5000, red). Scale bar: 20 µm.

In a control goldfish retina, the anti-ChAT antibody labeled cholinergic ACs somas in both the INL and the GCL, and two distinct IPL bands, similar to the mouse references. Labeling patterns did not change for MNU-treated eyes at 7 or 28 dpi. From the immunohistochemical labeling results we concluded that MNU does not cause any visible changes to the inner retinal ACs and MNU had no inner retinal effects by 7 or 28 dpi (Fig. 19). However, since the anti-ChAT antibody clearly provided laminated band labeling in the IPL of the goldfish retina, it may be used at later time points to identify morphological changes to the retina at later stages of the remodeling theory.

5. DISCUSSION

The goal of this thesis project was to establish a chemically-induced, acute photoreceptor degeneration model in goldfish, using the drug MNU, and to evaluate it for its appropriateness in examining the chronic morphological consequences of photoreceptor degeneration, seen in human diseases (Marc and Jones, 2003). Furthermore, such a model system could then be used to study functional changes associated with the reorganization of the retinal circuitry after photoreceptor loss. It is essential to perform functional studies before attempting vision restoration techniques in human patients. The teleost fish seems to be a promising model for these functional studies because they are known to regenerate their retina following retinal damage (Hitchcock et al., 2004; Johns, 1977; Lyall, 1957). The capacity for this neuronal regeneration is due to the life long presence of stem cells in the ciliary marginal zone along with Müller cells (MCs) capable of re-differentiating within the mature fish retina (Otteson and Hitchcock, 2003). Assuming that the regenerative capabilities of the goldfish retina would be preserved throughout the degeneration and remodeling stages, the goldfish retina could provide an excellent natural model system for studying the steps of the stem cell-based rescue approach following blinding photoreceptor loss.

5.1. Rational for using the fish retina for modeling blinding diseases

The potential benefits of studying the fish retina, to gain insight about vision restoration, was recognized long ago (Lombardo, 1968). Due to continuous retinal growth

and the ability to regenerate retinal tissue following damage (Fernald, 1985; Johns and Easter, 1977), several studies were done to gain understanding about the teleost fish retina. In mature mammalian retina, there has been a lack of evidence showing a stem cell source, there appears to be no proliferation zone at the retinal margin, and there is limited evidence of regeneration capability (Reh and Levine, 1998). However, RPE cells and MCs of the mature mammalian retina have been shown to demonstrate some proliferation following damage such as FGF stimulated regeneration of the RPE cells in embryonic chick (Coulombre and Coulombre, 1965; Park and Hollenberg, 1989; Pittack et al., 1991) and even in mammalian retina (Ahmad et al., 2000; Tropepe et al., 2000). This limited regenerative capability of some birds and mammals is suggested to indicate a gradual loss of the proliferating CMZ over evolution (Lamba et al., 2008). However, if such evolutionary connections are possible, then understanding fish degeneration and regeneration may lend greater knowledge to the understanding and rescue of damaged retinal cells in mammals.

In the teleost fish, retinal degenerative diseases have been modeled and studied from many aspects by inducing the destruction of retinal neurons chemically (Braisted and Raymond, 1992), with light (Vihtelic and Hyde, 2000), and surgically (Cameron and Easter, 1995; Lombardo, 1968). A more recent approach is the use transgenic models. Zebrafish is the commonly used teleost model because they provide a cost efficient, rapidly developing, easily transducable organism, in which one can induce and identify specific gene mutations (Brockerhoff, 2011). Once the transgenic animals became a major model for genetic manipulations (Stuart et al., 1988), several other genetically engineered and mutant lines were developed, which demonstrated specific retinal defects

such as cone-specific or rod-specific degeneration (Brockerhoff, 2011; Collery et al., 2006). These transgenic models have provided a clearer understanding of the early stages of degeneration, but such models are inherently self-limiting due to their continuous degeneration of newly dividing cells once they reach the stage of cell specificity. In addition, unlike the well established transgenic mouse models for photoreceptor degeneration, which can feed and survive blind for months, survival is short for the genetically blind zebrafish (Fadool et al., 1997; Fadool and Dowling, 2008). Death is likely due to the reduced ability to feed. In addition, the cascade of mutant gene defects can be lethal to the animal (Brockerhoff, 2011). Thus, none of these transgenic fish models allow one to study the late stages of retinal degenerative diseases and regeneration.

In order to study the long-term consequences of photoreceptor loss and possibly regeneration afterwards, we needed an acute fish model that could survive long enough (months) for the chronic stages of degeneration to occur and to assess potential regeneration at those later periods.

To overcome the major shortcoming of existing transgenic fish models posed by the short lifespan, we speculated that the fish would require vision in one eye to eat and survive. Goldfish was chosen as our model of interest because of their appealing regenerative characteristics (persistent neurogensis), longer, hardier life-span (~ 15-20 years), similar photoreceptor ratio to humans (Morris et al., 2005), and desirable cell qualities for possible, future physiological studies (e.g. large BC terminals).

Based on the selective and complete photoreceptor degeneration induced experimentally by the toxic, carcinogenic drug MNU in other animal models, we chose

this drug to chemically-induce degeneration in goldfish retina (Herrold, 1967; Nagar et al., 2009; Nakajima et al., 1996; Taomoto et al., 1998; Tsubura, 1998). Both intraperitoneal (i.p.) and intravenous (i.v.) injections were ruled out as our preferred method of drug administration because both methods induced degeneration in the retinas of both eyes (Nagar et al., 2009; Nakajima et al., 1996; Taomoto et al., 1998).

Since there are limited physical connections between the opposite eyes of an animal, we decided to administer MNU via unilateral intraocular injection. Although the eyes are immunologically sequestered from systemic circulation (Xie et al., 2010), the fact that systemic MNU injections can cause photoreceptor degeneration indicates that MNU, or its toxic metabolites, pass through the ocular barriers and get into the retina. In our study, significant differences were seen in the ONL soma counts between the MNU-treated and sham-injected control eyes. Significant differences were also seen between the control and sham-injected eyes, which suggests that some MNU entered into the systemic circulation and reached the other eye. Together this data confirmed that most of the MNU remained in the injected eye and induced photoreceptor damage locally. The significant difference in ONL soma count between the MNU-treated and contralateral eyes of each fish and the survival of the MNU-treated goldfish at ~ 50 dpi, suggested that unilateral vision was preserved in the sham-injected eye. The long experiments (~ 50 dpi) performed here support the notion that carefully designed acute photoreceptor degeneration in fish might be a valuable model system for later stages of photoreceptor degeneration.

5.2. Intraocular MNU does not eliminate all photoreceptors in goldfish

We found that MNU, similar to what was found in mammals (Nagar et al., 2009; Nakajima et al., 1996; Ogino et al., 1993; Taomoto et al., 1998; Tsubura, 1998), selectively destroyed photoreceptors in fish. After intraocular delivery, the MNU-mediated destruction was uniformly distributed across the retina and remained primarily restricted to the treated eye. The MNU-triggered photoreceptor death was dose-dependent, but did not appear to be age-dependent based on our study. Similar to previously reported data in other species (Nakajima et al., 1996; Ogino et al., 1993; Taomoto et al., 1998; Tsubura, 1998; Yuge et al., 1996), degeneration was induced in the goldfish retina by 7 days post MNU injection. This was an advantage over other acute methods of retinal degeneration used in fish: some require long treatment times (e.g. phototoxicity) and most result in non-specific, non-uniform levels of retinal cell damage (Rapp et al., 1985; Vihtelic and Hyde, 2000).

The most prominent difference between the goldfish and the majority of tested mammalian retinas was in the efficacy of MNU at destroying photoreceptors. In past mammalian studies the investigators used relatively low MNU doses (15-90 mg/kg) to induce complete photoreceptor cell loss (Nakajima et al., 1996; Schaller et al., 1981; Taomoto et al., 1998). In our study, degeneration of the ONL, using 4µl of the most concentrated MNU stock solution (~ 40x that of the 60 mg/kg dose), never reached completion. Considering that the unilateral MNU injections caused retinal damage primarily in the injected eye, one would assume that most of the effective MNU would remain in the injected eye and that a little would enter the systemic circulation. However,

despite this high dose, the maximum photoreceptor loss was only 60% of photoreceptors compared the sham-injected control by 7 dpi.

In a recent mammalian study, a single i.p. injection of MNU into the *Arvicanthis ansorgei* (Sudanian grass rat) also reduced the number of photoreceptors by ~ 60% (Boudard et al., 2010). Similar to our results, elevated concentrations of MNU could not induce total photoreceptor degeneration. Bourdard and colleagues (2010) suggested that the incomplete degeneration might be related to the high cone content of the retina in their model. This speculation was based on the observation that during MNU-induced photoreceptor cell death, rod loss preceded the cone loss.

This phenomenon is not specific to MNU. In both genetic and non-genetic mammalian models of retinal degeneration, it has been noted that under the conditions, where photoreceptors are challenged, there appears to be a sequential loss of rods followed by cones (Cideciyan et al., 1998; Jimenez et al., 1996; Lewis, 2002). This correlates closely with most photoreceptor degenerative diseases in which mutations are generally found to be rod selective, yet cone degeneration still occurs (Mohand-Said et al., 2001). According to Mohand-Said and colleagues (2001) there are cell-cell interactions that help determine the fate of cells, patterning, and differentiation within retina. Thus, taking into account rod-cone interactions, the sequential loss of photoreceptors suggests that cone survival is dependant upon the presence of rods (Mohand-Said et al., 2001). Examples of this have been seen in goldfish and bovine retina, during the differentiation and functional development of the photoreceptors (DesJardin et al., 1993; Raymond et al., 1995). This pattern has also been seen in humans suffering from RP, where cone cell loss is thought to be dependent upon a specific

amount of rod cell damage (>75%) (Cideciyan et al., 1998). Similarly, in cone-rich zebrafish retina, extensive bright light exposure has been shown to cause simultaneous rod and cone degeneration, but the breakdown of rods was reported to be more complete (Vihtelic and Hyde, 2000).

In summary, rod photoreceptors appeared to be more sensitive to the MNU-induced insult. Thus, the relatively resistant and highly abundant cone photoreceptors of the goldfish retina may be a plausible reason for the incomplete degeneration seen in the current study.

5.3. MNU treatment has no chronic morphological consequences in the fish retina

In the human retina, photoreceptor cell death is followed by the second chronic stage of degeneration. This stage is characterized by the hypertrophy of MCs into the empty spaces of the ONL, left behind by dying photoreceptors, and entombment of the remaining neuronal retinal as it forms a seal (Marc and Jones, 2003). This process is commonly observed in transgenic photoreceptor degeneration models, such as the *rd* mice (Strettoi et al., 2002). In previous acute studies, in which mice received a single i.p. injection of MNU, a "glial seal" formation was produced secondary to the photoreceptor death, at about 28 dpi (Nagar et al., 2009; Tsubura et al., 2010).

In the current study, we used known MC markers, antibodies against the glial fibrillary acidic protein (GFAP) and vimentin (VIM) intermediate filaments, to qualitatively track the morphological changes of MCs in the MNU-damaged retina over the time course of degeneration. We hypothesized that if the hypertrophy of MCs and "glial seal" formation occurred, following photoreceptor loss, it would form a prominently labeled band lying in the empty space of the ONL adjacent to the RPE.

However, in our study similar levels of GFAP immunolabeling, unlike that found in mammals (Eng and Ghirnikar, 1994; Lewis and Fisher, 2003), was expressed at all times in the teleost retina. Furthermore, no extensive MC hypertrophy was seen spanning across the goldfish retina and even after repeated intraocular injections of MNU no "glial seal" formation was identified.

Based on the findings of previous degenerative models, the lack of a "glial seal" formation is likely due to the level of photoreceptor damage (Morris et al., 2007). As reported in transgenic zebrafish studies, the loss of a large number of rods or the loss of other retinal neurons in addition to rods was needed to activate the robust proliferation of MCs in which new neuronal progenitor migrate radially across the INL and ONL and differentiate into the missing neuronal cells (Montgomery et al., 2010). Similarly, in light-damaged zebrafish retinas, severe photoreceptor damage was needed to induce morphological changes in the MCs (Vihtelic et al., 2006b). This data suggests that massive rod loss or cone loss is needed to induce hypertrophy of MCs and to elicit a "glial seal" formation. In our experiments, we could not eliminate all of the photoreceptors. Therefore, the incomplete loss of photoreceptor and rapid response of the MCs to the damage may be responsible to the lack of "glial seal" formation in the MNU-treated goldfish retinas.

We also found no evidence of the third degenerative stage (remodeling) taking place. In order to determine whether remodeling was occurring within the INL following MNU-treatment, vertical cross-sections of retina from various time points were immunolabeled for cholinergic amacrine cells. This anti-ChAT antibody is known to label orthotopic and "displaced" cholinergic amacrine cells in the INL and GCL and to distinctly label two

straight bands across the IPL. Based on the qualitative labeling of the two straight bands observed over the ~ 50 dpi time course, no microneuroma formation was observed in the IPL of MNU-treated retinas. This evidence, taken together with the fact that we could not trigger "glial seal" formation in the goldfish retina with the MNU treatment, might suggest that the sequential nature of retinal remodeling events, as seen in mammalian circuitry (Marc and Jones, 2003), are applicable to fish. Thus, we concluded that we failed to trigger the concurrent stages required for remodeling to take place. Future experiments are necessary to test whether microneuroma formation can happen after "glial seal" formation in the goldfish retina.

5.4. Regeneration of MNU-treated goldfish retina

The MNU-induced photoreceptor loss in the goldfish retina was not permanent. Instead, photoreceptor soma counts began to increase between 21- 28 days post MNU injection and were not significantly different from the control counts by ~ 50 dpi, suggesting that regeneration occurred. This observation is consistent with the notion that in the teleost retina a rapid regeneration response accompanies most retinal injury or damage (Johns, 1977; Otteson and Hitchcock, 2003).

Previous studies have identified that stem cells (located in the CMZ) along with stem cell-like MCs capable of re-differentiating (located in the INL) are the source of regeneration in the teleost retina (Brockerhoff, 2011; Hitchcock et al., 2004; Montgomery et al., 2010). Antibodies against proliferating cell nuclear antigen (PCNA) have been commonly used to label these newly dividing cells. In previous degenerative studies the PCNA antibody has been shown to label unique clusters of cells that span the INL and ONL (Negishi et al., 1990). These PCNA+ cell clusters are considered to be positive

hallmarks of regeneration in the fish retina (Bernardos et al., 2007; Raymond et al., 1988; Vihtelic and Hyde, 2000). These rapid regenerative responses, starting with MC proliferation, have been seen in zebrafish, as early as 1 day post intravitreal injection of ouabain (Fimbel et al., 2007). According to previous studies, MCs respond to the retinal damage by reentering the cell cycle and generating new progenitor cells which follow the parallel tracks of the neighboring MCs into the ONL where they differentiate and replace the damaged retinal neurons (Fimbel et al., 2007; Thummel et al., 2008).

In order to confirm that regeneration was responsible for the increase in ONL soma numbers, observed in the current study, retinal cross-sections of control and MNU-treated retinas were immunolabeled for PCNA. In the control retinas PCNA+ round cells were located primarily in the CMZ. These results are consistent with the normal growth patterns that occur due to the stem cells population located in the CMZ of a growing fish retina (Otteson and Hitchcock, 2003). In the MNU-treated retinas, we observed PCNA+ neurons across the entire retina, suggesting that MCs had responded to the chemically-induced damage by generating new progenitor cells that migrate and differentiate to replace the damaged ONL. The time frame of regeneration in the current study (~ 50 dpi in goldfish) is similar to what was seen in ouabain-treated zebrafish retina (~ 60 dpi) (Fimbel et al., 2007). This data demonstrates that regeneration is most likely the reason for increased ONL soma counts at ~ 50 dpi.

The apparent retinal regeneration in MNU-treated goldfish raises questions about the "glial seal" formation. Such as: If a "glial seal" were to form, could the rapid regenerative response of proliferating MCs be responsible for preventing the formation of a solid, visibly encasing seal? If the seal were broken, would it be identifiable with the MC

marker (GFAP)? Furthermore, if the seal were broken, would retinal remodeling still take place? Future experiments are needed to address these possibilities.

5.5. Overall evaluation of MNU-treated goldfish retina as a degeneration model

The best studied genetic mouse model of photoreceptor degeneration is the *rd-1/rd-1* mouse, in which the rod and cone photoreceptors die in the first week after birth (Blanks et al., 1974). This model is important because degeneration in *rd-1/rd-1* mouse retina is known to follow the chronic morphological stages seen in humans (Marc et al., 2003). Recent studies using the *rd-1/rd-1* mouse to produce intrinsically light sensitive neurons have highlighted the limitations this transgenic model has for translational therapeutic research (Busskamp et al., 2010; Thyagarajan et al., 2010). Overall the results concluded that *rd-1/rd-1* mice do get some restoration of light sensitivity by targeting bacterial photosensitive proteins carried by viral vectors to surviving cone inner segments (Busskamp et al., 2010) or ganglion cells (GCs) (Busskamp et al., 2010; Thyagarajan et al., 2010) , but the neurons were much less sensitive to light than the normal retina. In the study reactivating the surviving cone inner segments, the *rd-1/rd-1* mouse model demonstrated a limited window of reactivation time due to the short lifespan of the cones (Busskamp et al., 2010). Since the GCs survive the initial stages of photoreceptor degeneration, studies targeting GCs for the production of intrinsically light sensitive neurons had a wider window (Busskamp et al., 2010; Thyagarajan et al., 2010). However, the cortical and behavioral visual performance of these animals showed minimal improvement after regaining some light sensitivity at the retinal level. The limited success of these models indicates why there is still a need for a more functionally applicable model for retinal degeneration.

Can our goldfish model system compete with the existing models? Based on the results of the current study the answer is no, not yet. The incompleteness of this model is paralleled by incomplete induction of acute MNU-mediated photoreceptor loss in the goldfish retina. It is unclear at this point whether the remaining photoreceptors and/or the re-differentiating MCs are responsible for preventing subsequent morphological changes associated with photoreceptor loss as seen in the mammalian retina. With these questions notwithstanding, our study has brought some promising results indicating that with modifications, an acute fish model could provide a competitive option for studying the later stages of photoreceptor degeneration especially if its regenerative nature is preserved.

The MNU-induced fish model demonstrated that unilateral photoreceptor degeneration would allow for one to study this model over a long period of time, making it theoretically possible to use fish as a platform for studying chronic morphological changes. In our study, MNU did not cause the extent of damage necessary to mimic the stages of degeneration, but it was promising to see that both the CMZ and the MC driven progenitor cells could outlive the carcinogenic toxin. The regenerative capabilities of the MNU-treated teleost retina remained strong enough to regenerate photoreceptor levels to their original state. Ultimately this study suggests that with appropriate methods used to eliminate all photoreceptors, one could model stem cell-based treatments. Nonetheless, it was concluded that MNU alone can be ruled out as an optimal way of causing complete photoreceptor degeneration in fish and mimicking the chronic stages seen in humans and rodents. However, if combined with another photoreceptor selective toxin or method, it may be useful. Future experiments will address other chemical agents and intense light as

possible factors to combine with MNU to cause complete photoreceptor degeneration in goldfish retina.

6. LITRATURE CITED

2007. AVMA Guidelines on Euthanasia. American Veterinary Medical Association Panel on Euthanasia. 15, 17, 20 p.

Ahmad I, Tang L, Pham H. 2000. Identification of neural progenitors in the adult mammalian eye. Biochem Biophys Res Commun 270(2):517-521.

Ahmadi MA, Lim JI. 2008. Pharmacotherapy of age-related macular degeneration. Expert Opinion on Pharmacotherapy 9(17):3045-3052.

Alkemade PP. 1968. Phenothiazine-retinopathy. Ophthalmologica 155(1):70-76.

Asher A, Segal WA, Baccus SA, Yaroslavsky LP, Palanker DV. 2007. Image processing for a high-resolution optoelectronic retinal prosthesis. IEEE Trans Biomed Eng 54(6 Pt 1):993-1004.

Bellhorn RW, Bellhorn M, Friedman AH, Henkind P. 1973. Urethan-induced retinopathy in pigmented rats. Invest Ophthalmol 12(1):65-76.

Bernardos RL, Barthel LK, Meyers JR, Raymond PA. 2007. Late-stage neuronal progenitors in the retina are radial Muller glia that function as retinal stem cells. J Neurosci 27(26):7028-7040.

Berson EL. 1993. Retinitis pigmentosa. The Friedenwald Lecture. Invest Ophthalmol Vis Sci 34(5):1659-1676.

Berson EL, Rosner B, Sandberg MA, Weigel-DiFranco C, Moser A, Brockhurst RJ, Hayes KC, Johnson CA, Anderson EJ, Gaudio AR, Willett WC, Schaefer EJ. 2004. Clinical trial of docosahexaenoic acid in patients with retinitis pigmentosa receiving vitamin A treatment. Arch Ophthalmol 122(9):1297-1305.

Bignami A. 1984. Glial fibrillary acidic (GFA) protein in Muller glia. Immunofluorescence study of the goldfish retina. Brain Res 300(1):175-178.

Binder S, Krebs I, Hilgers RD, Abri A, Stolba U, Assadoulina A, Kellner L, Stanzel BV, Jahn C, Feichtinger H. 2004. Outcome of transplantation of autologous retinal pigment epithelium in age-related macular degeneration: a prospective trial. Invest Ophthalmol Vis Sci 45(11):4151-4160.

Bink K, Walch A, Feuchtinger A, Eisenmann H, Hutzler P, Hofler H, Werner M. 2001. TO-PRO-3 is an optimal fluorescent dye for nuclear counterstaining in dual-colour FISH on paraffin sections. Histochemistry and Cell Biology 115(4):293-299.

Blanks JC, Adinolfi AM, Lolley RN. 1974. Photoreceptor degeneration and synaptogenesis in retinal-degenerative (rd) mice. J Comp Neurol 156(1):95-106.

Bohn W, Wiegers W, Beuttenmuller M, Traub P. 1992. Species-specific recognition patterns of monoclonal antibodies directed against vimentin. Exp Cell Res 201(1):1-7.

Bolte S, Cordelieres FP. 2006. A guided tour into subcellular colocalization analysis in light microscopy. J Microsc 224(Pt 3):213-232.

Boudard DL, Tanimoto N, Huber G, Beck SC, Seeliger MW, Hicks D. 2010. Cone Loss Is Delayed Relative to Rod Loss during Induced Retinal Degeneration in the Diurnal Cone-Rich Rodent Arvicanthis Ansorgei. Neuroscience 169(4):1815-1830.

Boycott BB, Wassle H. 1974. The morphological types of ganglion cells of the domestic cat's retina. J Physiol 240(2):397-419.

Braisted JE, Essman TF, Raymond PA. 1994. Selective regeneration of photoreceptors in goldfish retina. Development 120(9):2409-2419.

Braisted JE, Raymond PA. 1992. Regeneration of Dopaminergic-Neurons in Goldfish Retina. Development 114(4):913-919.

Braisted JE, Raymond PA. 1993. Continued search for the cellular signals that regulate regeneration of dopaminergic neurons in goldfish retina. Brain Res Dev Brain Res 76(2):221-232.

Bressler NM, Bressler SB, Fine SL. 1988. Age-related macular degeneration. Surv Ophthalmol 32(6):375-413.

Brindley GS, Lewin WS. 1968. The sensations produced by electrical stimulation of the visual cortex. J Physiol 196(2):479-493.

Bringmann A, Pannicke T, Grosche J, Francke M, Wiedemann P, Skatchkov SN, Osborne NN, Reichenbach A. 2006. Muller cells in the healthy and diseased retina. Progress in Retinal and Eye Research 25(4):397-424.

Brockerhoff SE, and James M. Fadool. 2011. Genetics of photoreceptor degeneration and regeneration in zebrafish. Cellular and Molecular Life Sciences 68:651-659.

Bruckner R. 1951. Spaltlampenmikroskopie und Ophthalmoskopie am Auge von Ratte und Maus. Doc Ophthalmol 5-6:452-454.

Bunker CH, Berson EL, Bromley WC, Hayes RP, Roderick TH. 1984. Prevalence of retinitis pigmentosa in Maine. Am J Ophthalmol 97(3):357-365.

Busskamp V, Duebel J, Balya D, Fradot M, Viney TJ, Siegert S, Groner AC, Cabuy E, Forster V, Seeliger M, Biel M, Humphries P, Paques M, Mohand-Said S, Trono D, Deisseroth K, Sahel JA, Picaud S, Roska B. 2010. Genetic reactivation of cone photoreceptors restores visual responses in retinitis pigmentosa. Science 329(5990):413-417.

Cajal SR. 1892. The Structure of the Retina. Spingfield, IL: Thomas.

Cameron DA, Easter SS. 1995. Cone Photoreceptor Regeneration in Adult Fish Retina - Phenotypic Determination and Mosaic Pattern-Formation. Journal of Neuroscience 15(3):2255-2271.

Cashman SM, Binkley EA, Kumar-Singh R. 2005. Towards mutation-independent silencing of genes involved in retinal degeneration by RNA interference. Gene Ther 12(15):1223-1228.

Chua J, Fletcher EL, Kalloniatis M. 2009. Functional remodeling of glutamate receptors by inner retinal neurons occurs from an early stage of retinal degeneration. J Comp Neurol 514(5):473-491.

Cid E, Santos-Ledo A, Parrilla-Monge M, Lillo C, Arevalo R, Lara JM, Aijon J, Velasco A. 2002. Prox1 expression in rod precursors and Muller cells. Exp Eye Res 90(2):267-276.

Cideciyan AV, Hood DC, Huang Y, Banin E, Li ZY, Stone EM, Milam AH, Jacobson SG. 1998. Disease sequence from mutant rhodopsin allele to rod and cone photoreceptor degeneration in man. Proc Natl Acad Sci U S A 95(12):7103-7108.

Collery RE, Cederlund ML, Smyth VA, Kennedy BN. 2006. Applying transgenic zebrafish technology to study the retina. Retinal Degenerative Diseases 572:201-207.

Costes SV, Daelemans D, Cho EH, Dobbin Z, Pavlakis G, Lockett S. 2004. Automatic and quantitative measurement of protein-protein colocalization in live cells. Biophys J 86(6):3993-4003.

Coulombre JL, Coulombre AJ. 1965. Regeneration of neural retina from the pigmented epithelium in the chick embryo. Dev Biol 12(1):79-92.

Craner SL, Radel JD, Jen LS, Lund RD. 1989. Light-evoked cortical activity produced by illumination of intracranial retinal transplants: experimental studies in rats. Exp Neurol 104(2):93-100.

De Monasterio FM, Gouras P. 1975. Functional properties of ganglion cells of the rhesus monkey retina. J Physiol 251(1):167-195.

Derrington AM, Krauskopf J, Lennie P. 1984. Chromatic mechanisms in lateral geniculate nucleus of macaque. J Physiol 357:241-265.

DesJardin LE, Timmers AM, Hauswirth WW. 1993. Transcription of photoreceptor genes during fetal retinal development. Evidence for positive and negative regulation. J Biol Chem 268(10):6953-6960.

Doubell TP, Stewart MG. 1993. Short-Term Changes in the Numerical Density of Synapses in the Intermediate and Medial Hyperstriatum-Ventrale Following One-Trial Passive-Avoidance Training in the Chick. Journal of Neuroscience 13(5):2230-2236.

Dowling J. 2009. Current and future prospects for optoelectronic retinal prostheses. Eye (Lond) 23(10):1999-2005.

Dowling JE. 1987. The Retina: An Approachable Part of the Brain. Cambridge, MA: Belknap Press.

Drager UC. 1983. Coexistence of Neurofilaments and Vimentin in a Neuron of Adult-Mouse Retina. Nature 303(5913):169-172.

Eichenbaum JW, Cinaroglu A, Eichenbaum KD, Sadler KC. 2009. A zebrafish retinal graded photochemical stress model. J Pharmacol Toxicol Methods 59(3):121-127.

Eng LF, Ghirnikar RS. 1994. GFAP and astrogliosis. Brain Pathol 4(3):229-237.

Fadool JM, Brockerhoff SE, Hyatt GA, Dowling JE. 1997. Mutations affecting eye morphology in the developing zebrafish (Danio rerio). Dev Genet 20(3):288-295.

Fadool JM, Dowling JE. 2008. Zebrafish: A model system for the study of eye genetics. Progress in Retinal and Eye Research 27(1):89-110.

Famiglietti EV, Jr., Kaneko A, Tachibana M. 1977. Neuronal architecture of on and off pathways to ganglion cells in carp retina. Science 198(4323):1267-1269.

Fernald RD. 1985. Growth of the Teleost Eye - Novel Solutions to Complex Constraints. Environmental Biology of Fishes 13(2):113-123.

Fimbel SM, Montgomery JE, Burket CT, Hyde DR. 2007. Regeneration of inner retinal neurons after intravitreal injection of ouabain in zebrafish. Journal of Neuroscience 27(7):1712-1724.

Gaillard F, Sauve Y. 2007. Cell-based therapy for retina degeneration: the promise of a cure. Vision Res 47(22):2815-2824.

Gallagher SK, Witkovsky P, Roux MJ, Low MJ, Otero-Corchon V, Hentges ST, Vigh J. 2010. beta-Endorphin Expression in the Mouse Retina. Journal of Comparative Neurology 518(15):3130-3148.

Gao WQ, Shinsky N, Armanini MP, Moran P, Zheng JL, Mendoza-Ramirez JL, Phillips HS, Winslow JW, Caras IW. 1998. Regulation of hippocampal synaptic plasticity by the tyrosine kinase receptor, REK7/EphA5, and its ligand, AL-1/Ephrin-A5. Molecular and Cellular Neuroscience 11(5-6):247-259.

Gehrs KM, Anderson DH, Johnson LV, Hageman GS. 2006. Age-related macular degeneration--emerging pathogenetic and therapeutic concepts. Ann Med 38(7):450-471.

Gonzalez RC, and Wintz, P. 1987. *Digital image processing*. Reading, MA: Addison-Wesley Publishing Co.

Gouras P, Flood MT, Kjedbye H, Bilek MK, Eggers H. 1985. Transplantation of cultured human retinal epithelium to Bruch's membrane of the owl monkey's eye. Curr Eye Res 4(3):253-265.

Hartong DT, Berson EL, Dryja TP. 2006. Retinitis pigmentosa. Lancet 368(9549):1795-1809.

Hattar S, Liao HW, Takao M, Berson DM, Yau KW. 2002. Melanopsin-containing retinal. ganglion cells: Architecture, projections, and intrinsic photosensitivity. Science 295(5557):1065-1070.

Haverkamp S, Wassle H. 2000. Immunocytochemical analysis of the mouse retina. J Comp Neurol 424(1):1-23.

Herrold KM. 1967. Pigmentary Degeneration of Retina Induced by N-Methyl-N-Nitrosourea - an Experimental Study in Syrian Hamsters. Archives of Ophthalmology 78(5):650-&.

Hitchcock P, Ochocinska M, Sieh A, Otteson D. 2004. Persistent and injury-induced neurogenesis in the vertebrate retina. Prog Retin Eye Res 23(2):183-194.

Hitchcock PF, Easter SS, Jr. 1986. Retinal ganglion cells in goldfish: a qualitative classification into four morphological types, and a quantitative study of the development of one of them. J Neurosci 6(4):1037-1050.

Hitchcock PF, Lindsey Myhr KJ, Easter SS, Jr., Mangione-Smith R, Jones DD. 1992. Local regeneration in the retina of the goldfish. J Neurobiol 23(2):187-203.

Hitchcock PF, Raymond PA. 1992. Retinal regeneration. Trends Neurosci 15(3):103-108.

Huang Y, Enzmann V, Ildstad ST. 2010. Stem Cell-Based Therapeutic Applications in Retinal Degenerative Diseases. Stem Cell Rev.

Ishida AT, Stell WK, Lightfoot DO. 1980. Rod and cone inputs to bipolar cells in goldfish retina. J Comp Neurol 191(3):315-335.

Jimenez AJ, Garcia-Fernandez JM, Gonzalez B, Foster RG. 1996. The spatio-temporal pattern of photoreceptor degeneration in the aged rd/rd mouse retina. Cell Tissue Res 284(2):193-202.

Johns PR. 1977. Growth of the adult goldfish eye. III. Source of the new retinal cells. J Comp Neurol 176(3):343-357.

Johns PR, Easter SS, Jr. 1977. Growth of the adult goldfish eye. II. Increase in retinal cell number. J Comp Neurol 176(3):331-341.

Jones BW, Marc RE. 2005. Retinal remodeling during retinal degeneration. Exp Eye Res 81(2):123-137.

Jones BW, Watt CB, Frederick JM, Baehr W, Chen CK, Levine EM, Milam AH, Lavail MM, Marc RE. 2003a. Retinal remodeling triggered by photoreceptor degenerations. J Comp Neurol 464(1):1-16.

Jones BW, Watt CB, Marc RE. 2005. Retinal remodelling. Clin Exp Optom 88(5):282-291.

Jones BW, Watt CB, Vaughan DK, Organisciak DT, Marc RE. 2003b. Retinal remodeling triggered by light damage in the albino rat. Investigative Ophthalmology & Visual Science 44:U715-U715.

Jones PS, Schechter N. 1987. Distribution of specific intermediate-filament proteins in the goldfish retina. J Comp Neurol 266(1):112-121.

Joselevitch C. 2005. The Twilight Zone: How Mixed-Input Bipolar Cells Process Rod and Cone Signals.1-176.

Kaneko A, Nishimura Y, Tachibana M, Tauchi M, Shimai K. 1981. Physiological and morphological studies of signal pathways in the carp retina. Vision Res 21(11):1519-1526.

Kaplan E, Shapley RM. 1986. The primate retina contains two types of ganglion cells, with high and low contrast sensitivity. Proc Natl Acad Sci U S A 83(8):2755-2757.

Keeler CE. 1924. The inheritance of a retinal abnormality in white mice. Proceedings of the National Academy of Sciences of the United States of America 10:329-333.

Kiuchi K, Yoshizawa K, Shikata N, Moriguchi K, Tsubura A. 2002. Morphologic characteristics of retinal degeneration induced by sodium iodate in mice. Curr Eye Res 25(6):373-379.

Kolb H, Gouras P. 1974. Electron microscopic observations of human retinitis pigmentosa, dominantly inherited. Invest Ophthalmol 13(7):487-498.

Koyama R, Yamada MK, Fujisawa S, Katoh-Semba R, Matsuki N, Ikegaya Y. 2004. Brain-derived neurotrophic factor induces hyperexcitable reentrant circuits in the dentate gyrus. Journal of Neuroscience 24(33):7215-7224.

Lamba D, Karl M, Reh T. 2008. Neural regeneration and cell replacement: a view from the eye. Cell Stem Cell 2(6):538-549.

Lee KP, Valentine R. 1990. Retinotoxicity of 1,4,-bis(4-aminophenoxy)-2-phenylbenzene (2-phenyl-APB-144) in albino and pigmented rats. Arch Toxicol 64(2):135-142.

Lewis GP, Charteris, D.G., Sethi, C.S., and Fisher, S.K. 2002. Animal models of retinal detachment and reattachment: identifying cellular events that may affect visual recovery. Eye 16:375-387.

Lewis GP, Fisher SK. 2003. Up-regulation of glial fibrillary acidic protein in response to retinal injury: its potential role in glial remodeling and a comparison to vimentin expression. Int Rev Cytol 230:263-290.

Liepe BA, Stone C, Koistinaho J, Copenhagen DR. 1994. Nitric oxide synthase in Muller cells and neurons of salamander and fish retina. J Neurosci 14(12):7641-7654.

Liu Y, Kintner DB, Begum G, Algharabli J, Cengiz P, Shull GE, Liu XJ, Sun D. 2010. Endoplasmic reticulum Ca2+ signaling and mitochondrial Cyt c release in astrocytes following oxygen and glucose deprivation. J Neurochem 114(5):1436-1446.

Lombardo F. 1968. Retinal Regeneration in Adult Teleostei. Atti Della Accademia Nazionale Dei Lincei Rendiconti-Classe Di Scienze Fisiche-Matematiche & Naturali 45(6):631-&.

Lu B, Kwan T, Kurimoto Y, Shatos M, Lund RD, Young MJ. 2002. Transplantation of EGF-responsive neurospheres from GFP transgenic mice into the eyes of rd mice. Brain Res 943(2):292-300.

Lyall AH. 1957. The Growth of the Trout Retina. Quarterly Journal of Microscopical Science 98(1):101-&.

Machida S, Kondo M, Jamison JA, Khan NW, Kononen LT, Sugawara T, Bush RA, Sieving PA. 2000. P23H rhodopsin transgenic rat: correlation of retinal function with histopathology. Invest Ophthalmol Vis Sci 41(10):3200-3209.

Mack AF. 2007. Evidence for a Columnar Organization of Cones, Muller Cells, and Neurons in the Retina of a Cichlid Fish. Neuroscience 144:1004-1014.

Mack AF, Germer A, Janke C, Reichenbach A. 1998. Muller (glial) cells in the teleost retina: Consequences of continuous growth. GLIA 22(3):306-313.

Manders EM, Stap J, Brakenhoff GJ, van Driel R, Aten JA. 1992. Dynamics of three-dimensional replication patterns during the S-phase, analysed by double labelling of DNA and confocal microscopy. J Cell Sci 103 (Pt 3):857-862.

Marc RE, Cameron D. 2001. A molecular phenotype atlas of the zebrafish retina. Journal of Neurocytology 30(7):593-654.

Marc RE, Jones BW. 2002. Molecular phenotyping of retinal ganglion cells. J Neurosci 22(2):413-427.

Marc RE, Jones BW. 2003. Retinal remodeling in inherited photoreceptor degenerations. Mol Neurobiol 28(2):139-147.

Marc RE, Jones BW, Watt CB, Strettoi E. 2003. Neural remodeling in retinal degeneration. Progress in Retinal and Eye Research 22(5):607-655.

Marc RE, Liu W. 2000. Fundamental GABAergic amacrine cell circuitries in the retina: nested feedback, concatenated inhibition, and axosomatic synapses. J Comp Neurol 425(4):560-582.

Marcus RC, Delaney CL, Easter SS. 1999. Neurogenesis in the visual system of embryonic and adult zebrafish (Danio rerio). Visual Neuroscience 16(3):417-424.

Margolis DJ, Detwiler PB. 2011. Cellular origin of spontaneous ganglion cell spike activity in animal models of retinitis pigmentosa. J Ophthalmol 2011.

Margolis DJ, Newkirk G, Euler T, Detwiler PB. 2008. Functional stability of retinal ganglion cells after degeneration-induced changes in synaptic input. J Neurosci 28(25):6526-6536.

Masland RH. 2001. The fundamental plan of the retina. Nature Neuroscience 4(9):877-886.

Masland RH, Mills JW. 1979. Autoradiographic identification of acetylcholine in the rabbit retina. J Cell Biol 83(1):159-178.

Matsumura M, Ohkuma M, Tsukahara I. 1986. Experimental chloroquine retinopathy. Ophthalmic Res 18(3):172-179.

Miller JW. 2010. Treatment of age-related macular degeneration: beyond VEGF. Jpn J Ophthalmol 54(6):523-528.

Mohand-Said S, Hicks D, Leveillard T, Picaud S, Porto F, Sahel JA. 2001. Rod-cone interactions: developmental and clinical significance. Prog Retin Eye Res 20(4):451-467.

Montgomery JE, Parsons MJ, Hyde DR. 2010. A Novel Model of Retinal Ablation Demonstrates That the Extent of Rod Cell Death Regulates the Origin of the Regenerated Zebrafish Rod Photoreceptors. Journal of Comparative Neurology 518(6):800-814.

Morris AC, Scholz TL, Brockerhoff SE, and James M. Fadool. 2007. Genetic Dissection Reveals Two Separate Pathways for Rod and Cone Regeneration in the Teleost Retina. Develomental Neurobiology:605-619.

Morris AC, Schroeter EH, Bilotta J, Wong RO, Fadool JM. 2005. Cone survival despite rod degeneration in XOPS-mCFP transgenic zebrafish. Invest Ophthalmol Vis Sci 46(12):4762-4771.

Nagar S, Krishnamoorthy V, Cherukuri P, Jain V, Dhingra NK. 2009. Early remodeling in an inducible animal model of retinal degeneration. Neuroscience 160(2):517-529.

Nakajima M, Yuge K, Senzaki H, Shikata N, Miki H, Uyama M, Tsubura A. 1996. Photoreceptor apoptosis induced by a single systemic administration of N-methyl-N-nitrosourea in the rat retina. Am J Pathol 148(2):631-641.

Nambu H, Yuge K, Nakajima M, Shikata N, Takahashi K, Miki H, Uyama M, Tsubura A. 1997. Morphologic characteristics of N-methyl-N-nitrosourea-induced retinal degeneration in C57BL mice. Pathol Int 47(6):377-383.

Negishi K, Shinagawa S. 1993. Fibroblast growth factor induces proliferating cell nuclear antigen-immunoreactive cells in goldfish retina. Neurosci Res 18(2):143-156.

Negishi K, Stell WK, Takasaki Y. 1990. Early histogenesis of the teleostean retina: studies using a novel immunochemical marker, proliferating cell nuclear antigen (PCNA/cyclin). Brain Res Dev Brain Res 55(1):121-125.

Newman E, Reichenbach A. 1996. The Muller cell: a functional element of the retina. Trends Neurosci 19(8):307-312.

Nikolic K, Grossman, N., Yan, H., Drakakis, E., Toumazou, C., and Degenaar, P. A non-invasive retinal prosthesis--testing the concept; 2007. p 6365-6368.

Noell WK, Walker VS, Kang BS, Berman S. 1966. Retinal damage by light in rats. Invest Ophthalmol 5(5):450-473.

Ogino H, Ito M, Matsumoto K, Yagyu S, Tsuda H, Hirono I, Wild CP, Montesano R. 1993. Retinal degeneration induced by N-methyl-N-nitrosourea and detection of 7-methyldeoxyguanosine in the rat retina. Toxicol Pathol 21(1):21-25.

Otteson DC, Hitchcock PF. 2003. Stem cells in the teleost retina: persistent neurogenesis and injury-induced regeneration. Vision Res 43(8):927-936.

Palanker D, Vankov A, Huie P, Baccus S. 2005. Design of a high-resolution optoelectronic retinal prosthesis. J Neural Eng 2(1):S105-120.

Parapuram SK, Cojocaru RI, Chang JR, Khanna R, Brooks M, Othman M, Zareparsi S, Khan NW, Gotoh N, Cogliati T, Swaroop A. 2010. Distinct signature of altered homeostasis in aging rod photoreceptors: implications for retinal diseases. PLoS One 5(11):e13885.

Park CM, Hollenberg MJ. 1989. Basic fibroblast growth factor induces retinal regeneration in vivo. Dev Biol 134(1):201-205.

Parysek LM, del Cerro M, Olmsted JB. 1985. Microtubule-associated protein 4 antibody: a new marker for astroglia and oligodendroglia. Neuroscience 15(3):869-875.

Pittack C, Jones M, Reh TA. 1991. Basic fibroblast growth factor induces retinal pigment epithelium to generate neural retina in vitro. Development 113(2):577-588.

Poher V, Grossman N, Kennedy GT, Nikolic K, Zhang HX, Gong Z, Drakakis EM, Gu E, Dawson MD, French PMW, Degenaar P, Neil MAA. 2008. Micro-LED arrays: a tool for two-dimensional neuron stimulation. Journal of Physics D-Applied Physics 41(9):-.

Pollard H, Khrestchatisky M, Moreau J, Benari Y, Represa A. 1994. Correlation between Reactive Sprouting and Microtubule Protein Expression in Epileptic Hippocampus (Vol 61, Pg 773, 1994). Neuroscience 63(2):627-627.

Polyak SL. 1941. The Retina. Chicago: University of Chicago Press.

Radtke ND, Aramant RB, Petry HM, Green PT, Pidwell DJ, Seiler MJ. 2008. Vision improvement in retinal degeneration patients by implantation of retina together with retinal pigment epithelium. Am J Ophthalmol 146(2):172-182.

Rapp LM, Jose JG, Pitts DG. 1985. DNA repair synthesis in the rat retina following in vivo exposure to 300-nm radiation. Invest Ophthalmol Vis Sci 26(3):384-388.

Raymond PA, Barthel LK, Curran GA. 1995. Developmental patterning of rod and cone photoreceptors in embryonic zebrafish. J Comp Neurol 359(4):537-550.

Raymond PA, Reifler MJ, Rivlin PK. 1988. Regeneration of goldfish retina: rod precursors are a likely source of regenerated cells. J Neurobiol 19(5):431-463.

Raymond PA, Rivlin PK. 1987. Germinal Cells in the Goldfish Retina That Produce Rod Photoreceptors. Developmental Biology 122(1):120-138.

Reh TA. 1987. Cell-specific regulation of neuronal production in the larval frog retina. J Neurosci 7(10):3317-3324.

Reh TA, Levine EM. 1998. Multipotential stem cells and progenitors in the vertebrate retina. J Neurobiol 36(2):206-220.

Represa A, Benari Y. 1992. Long-Term Potentiation and Sprouting of Mossy Fibers Produced by Brief Episodes of Hyperactivity. Epilepsy Research:261-269.

Rezai KA, Lappas A, Farrokh-siar L, Kohen L, Wiedemann P, Heimann K. 1997. Iris pigment epithelial cells of long evans rats demonstrate phagocytic activity. Exp Eye Res 65(1):23-29.

Riepe RE, and Norenberg, Michael D. 1978. Glutamine Synthetase in the Developing Rat Retina: An Immunohistochemical Study. Experimental Eye Research 27:435-444.

Rivolta C, Sharon D, DeAngelis MM, Dryja TP. 2002. Retinitis pigmentosa and allied diseases: numerous diseases, genes, and inheritance patterns. Human Molecular Genetics 11(10):1219-1227.

Royo PE, Quay WB. 1959. Retinal transplantation from fetal to maternal mammalian eye. Growth 23:313-336.

Saito T, Kujiraoka T, Yonaha T, Chino Y. 1985. Reexamination of photoreceptor-bipolar connectivity patterns in carp retina: HRP-EM and Golgi-EM studies. J Comp Neurol 236(2):141-160.

Santos F, MacDonald G, Rubel EW, Raible DW. 2006. Lateral line hair cell maturation is a determinant of aminoglycoside susceptibility in zebrafish (Danio rerio). Hearing Research 213(1-2):25-33.

Santos NC, Figueira-Coelho J, Martins-Silva J, Saldanha C. 2003. Multidisciplinary utilization of dimethyl sulfoxide: pharmacological, cellular, and molecular aspects. Biochem Pharmacol 65(7):1035-1041.

Sarthy V, and Harris Ripps. 2001. The Retinal Muller Cell: Structure and Function. Blakemore C, editor: Kluwer Academic/Plenum Publishers. 278 p.

Schaller JP, Wyman M, Weisbrode SE, Olsen RG. 1981. Induction of Retinal Degeneration in Cats by Methylnitrosourea and Ketamine-Hydrochloride. Veterinary Pathology 18(2):239-247.

Schiller PH. 2010. Parallel information processing channels created in the retina. Proc Natl Acad Sci U S A 107(40):17087-17094.

Scott PP, Greaves JP, Scott MG. 1964. Nutritional Blindness in the Cat. Exp Eye Res 3:357-364.

Seidehamel RJ, Dungan KW. 1974. Characteristics and pharmacologic utility of an intraocular pressure (IOP) model in unanesthetized rabbits. Invest Ophthalmol 13(4):319-322.

Serbedzija P, Madl JE, Ishii DN. 2009. Insulin and IGF-I prevent brain atrophy and DNA loss in diabetes. Brain Res 1303:179-194.

Silverman CA, and Yoshizumi, Marc O. . 1983. Ocular Toxicity of Experimental Intravitreal DMSO. Cutaneous and Ocular Toxicology 2:193-200.

Strauss O. 2005. The retinal pigment epithelium in visual function. Physiol Rev 85(3):845-881.

Strettoi E, Pignatelli V, Rossi C, Porciatti V, Falsini B. 2003. Remodeling of second-order neurons in the retina of rd/rd mutant mice. Vision Res 43(8):867-877.

Strettoi E, Porciatti V, Falsini B, Pignatelli V, Rossi C. 2002. Morphological and functional abnormalities in the inner retina of the rd/rd mouse. J Neurosci 22(13):5492-5504.

Stuart GW, McMurray JV, Westerfield M. 1988. Replication, integration and stable germ-line transmission of foreign sequences injected into early zebrafish embryos. Development 103(2):403-412.

Summerfelt RC, and Lynwood S. Smith 1990. Anesthesia, Surgery, and Related Techniques. In: Schreck CB, and Moyle, Peter B., editor. Methods For Fish Biology. Bethesda, MD: American Fisheries Society. p 217.

Sung CH, Chuang JZ. 2010. The cell biology of vision. J Cell Biol 190(6):953-963.

Suzuki S, Kaneko A. 1990. Identification of bipolar cell subtypes by protein kinase C-like immunoreactivity in the goldfish retina. Vis Neurosci 5(3):223-230.

Suzuki T, Fujikura K, Higashiyama T, Takata K. 1997. DNA staining for fluorescence and laser confocal microscopy. Journal of Histochemistry & Cytochemistry 45(1):49-53.

Swann PF. 1968. Rate of Breakdown of Methyl Methanesulphonate Dimethyl Sulphate and N-Methyl-N-Nitrosourea in Rat. Biochemical Journal 110(1):49-&.

Takahashi M, Palmer TD, Takahashi J, Gage FH. 1998. Widespread integration and survival of adult-derived neural progenitor cells in the developing optic retina. Mol Cell Neurosci 12(6):340-348.

Tansley K. 1946. The development of the rat eye in graft. J Exp Biol 22:221-224.

Taomoto M, Nambu H, Senzaki H, Shikata N, Oishi Y, Fujii T, Miki H, Uyama M, Tsubura A. 1998. Retinal degeneration induced by N-methyl-N-nitrosourea in Syrian golden hamsters. Graefes Arch Clin Exp Ophthalmol 236(9):688-695.

Thummel R, Kassen SC, Montgomery JE, Enright JM, Hyde DR. 2008. Inhibition of muller glial cell division blocks regeneration of the light-damaged zebrafish retina. Developmental Neurobiology 68(3):392-408.

Thyagarajan S, van Wyk M, Lehmann K, Lowel S, Feng G, Wassle H. 2010. Visual function in mice with photoreceptor degeneration and transgenic expression of channelrhodopsin 2 in ganglion cells. J Neurosci 30(26):8745-8758.

Tominaga Y, Tsuzuki T, Shiraishi A, Kawate H, Sekiguchi M. 1997. Alkylation-induced apoptosis of embryonic stem cells in which the gene for DNA-repair, methyltransferase, had been disrupted by gene targeting. Carcinogenesis 18(5):889-896.

Trenholm S, Baldridge WH. 2010. The effect of aminosulfonate buffers on the light responses and intracellular pH of goldfish retinal horizontal cells. J Neurochem 115(1):102-111.

Tropepe V, Coles BL, Chiasson BJ, Horsford DJ, Elia AJ, McInnes RR, van der Kooy D. 2000. Retinal stem cells in the adult mammalian eye. Science 287(5460):2032-2036.

Tsubura A, Yoshizawa K, Kiuchi K, Moriguchi K. 2003. N-methyl-N-nitrosourea-induced retinal degeneration in animals. Acta Histochemica Et Cytochemica 36(4):263-270.

Tsubura A, Yoshizawa K, Kuwata M, Uehara N. 2010. Animal models for retinitis pigmentosa induced by MNU; disease progression, mechanisms and therapeutic trials. Histol Histopathol 25(7):933-944.

Tsubura A, Yoshizawa, K., Miki, H., Oishi, Y., and T. Fugii. 1998. Phylogenetic and ontogenetic study of retinal lesions induced by N-methyl-N-nitrosourea in animals. Animal Eye Research 17:97-103.

Tumosa N, Eckenstein F, Stell WK. 1984. Immunocytochemical localization of putative cholinergic neurons in the goldfish retina. Neurosci Lett 48(3):255-259.

Vanderzee EA, Bolhuis JJ, Solomonia RO, Horn G, Luiten PGM. 1995. Differential Distribution of Protein-Kinase-C (Pkc-Alpha-Beta and Pkc-Gamma) Isoenzyme Immunoreactivity in the Chick Brain. Brain Research 676(1):41-52.

Vanreempts J, Dikova M, Werbrouck L, Clincke G, Borgers M. 1992. Synaptic Plasticity in Rat Hippocampus Associated with Learning. Behavioural Brain Research 51(2):179-183.

Vaquero CF, Velasco A, de la Villa P. 1997. Quantitative measurement of protein kinase C immunoreactivity in rod bipolar cells of the goldfish retina. Brain Res 773(1-2):208-212.

Vaughan DK, Lasater EM. 1990. Distribution of F-Actin in Bipolar and Horizontal Cells of Bass Retinas. American Journal of Physiology 259(2):C205-C214.

Vihtelic TS, Hyde DR. 2000. Light-induced rod and cone cell death and regeneration the adult albino zebrafish (Danio rerio) retina. Journal of Neurobiology 44(3):289-307.

Vihtelic TS, Soverly JE, Kassen SC, Hyde DR. 2006a. Retinal regional differences in photoreceptor cell death and regeneration in light-lesioned albino zebrafish. Experimental Eye Research 82(4):558-575.

Vihtelic TS, Soverly JE, Kassen SC, Hyde DR. 2006b. Retinal regional differences in photoreceptor cell death and regeneration in light-lesioned albino zebrafish. Exp Eye Res 82(4):558-575.

Voigt T. 1986. Cholinergic amacrine cells in the rat retina. J Comp Neurol 248(1):19-35.

Wan J, Zheng H, Hu BY, Xiao HL, She ZJ, Chen ZL, Zhou GM. 2006. Acute photoreceptor degeneration down-regulates melanopsin expression in adult rat retina. Neurosci Lett 400(1-2):48-52.

Wassle H. 2004. Parallel processing in the mammalian retina. Nat Rev Neurosci 5(10):747-757.

Wassle H, Boycott BB. 1991. Functional architecture of the mammalian retina. Physiol Rev 71(2):447-480.

Wassle H, Yamashita M, Greferath U, Grunert U, Muller F. 1991. The rod bipolar cell of the mammalian retina. Vis Neurosci 7(1-2):99-112.

Wiesel TN, Hubel DH. 1966. Spatial and chromatic interactions in the lateral geniculate body of the rhesus monkey. J Neurophysiol 29(6):1115-1156.

Wong IY, Koo SC, Chan CW. 2011. Prevention of age-related macular degeneration. Int Ophthalmol 31(1):73-82.

Xie J, Farage E, Sugimoto M, Anand-Apte B. 2010. A novel transgenic zebrafish model for blood-brain and blood-retinal barrier development. BMC Dev Biol 10:76.

Yazulla S, Studholme KM. 1997. Differential reinnervation of retinal bipolar cell dendrites and axon terminals by dopamine interplexiform cells following dopamine depletion with 6-OHDA. J Comp Neurol 382(4):535-545.

Yazulla S, Studholme KM. 1998. Differential distribution of Shaker-like and Shab-like K+-channel subunits in goldfish retina and retinal bipolar cells. J Comp Neurol 396(1):131-140.

Yoshizawa K, Nambu H, Yang J, Oishi Y, Senzaki H, Shikata N, Miki H, Tsubura A. 1999. Mechanisms of photoreceptor cell apoptosis induced by N-methyl-N-nitrosourea in Sprague-Dawley rats. Lab Invest 79(11):1359-1367.

Yuge K, Nambu H, Senzaki H, Nakao I, Miki H, Uyama M, Tsubura A. 1996. N-methyl-N-nitrosourea-induced photoreceptor apoptosis in the mouse retina. In Vivo 10(5):483-488.

Yurco P, Cameron DA. 2005. Responses of Muller glia to retinal injury in adult zebrafish. Vision Res 45(8):991-1002.

Zhang X, Fournier MV, Ware JL, Bissell MJ, Yacoub A, Zehner ZE. 2009. Inhibition of vimentin or beta1 integrin reverts morphology of prostate tumor cells grown in laminin-rich extracellular matrix gels and reduces tumor growth in vivo. Mol Cancer Ther 8(3):499-508.

Zrenner E. Restoring neuroretinal function by subretinal microphotodiode arrays. ; 2007; Fort Lauderdale, FL.

7. APPENDICES

APPENDIX 1

Two Way Analysis of Variance

Data source: CONTROL FISH: ONL SOMA COUNT

General Linear Model (No Interactions)

Dependent Variable: SOMA#

Normality Test (Shapiro-Wilk) Passed (P = 0.244)

Equal Variance Test: Passed (P = 1.000)

Source of Variation	DF	SS	MS	F	P
FISH	1	106.250	106.250	0.0782	0.782
POSITION	33	21455.191	650.157	0.478	0.981
Residual	33	44840.250	1358.795		
Total	67	66401.691	991.070		

The difference in the mean values among the different levels of FISH is not great enough to exclude the possibility that the difference is just due to random sampling variability after allowing for the effects of differences in POSITION. There is not a statistically significant difference (P = 0.782).

The difference in the mean values among the different levels of POSITION is not great enough to exclude the possibility that the difference is just due to random sampling variability after allowing for the effects of differences in FISH. There is not a statistically significant difference (P = 0.981).

Power of performed test with alpha = 0.0500: for FISH : 0.0500
Power of performed test with alpha = 0.0500: for POSITION : 0.0500

Least square means for FISH :

Group	Mean
1.000	240.471
2.000	242.971

Std Err of LS Mean = 6.322

Two Way Analysis of Variance

Data source: CONTROL FISH: ONL WIDTH

General Linear Model (No Interactions)

Dependent Variable: WIDTH#

Normality Test (Shapiro-Wilk) Passed (P = 0.936)

Equal Variance Test: Passed (P = 1.000)

Source of Variation	**DF**	**SS**	**MS**	**F**	**P**
FISH	1	38.335	38.335	2.603	0.116
POSITION	33	192.428	5.831	0.396	0.995
Residual	33	486.031	14.728		
Total	67	716.794	10.698		

The difference in the mean values among the different levels of FISH is not great enough to exclude the possibility that the difference is just due to random sampling variability after allowing for the effects of differences in POSITION. There is not a statistically significant difference (P = 0.116).

The difference in the mean values among the different levels of POSITION is not great enough to exclude the possibility that the difference is just due to random sampling variability after allowing for the effects of differences in FISH. There is not a statistically significant difference (P = 0.995).

Power of performed test with alpha = 0.0500: for FISH : 0.219
Power of performed test with alpha = 0.0500: for POSITION : 0.0500

Least square means for FISH :

Group	**Mean**
1.000	29.812
2.000	28.310

Std Err of LS Mean = 0.658

APPENDIX 2

Two Way Analysis of Variance

Data source: CONTROL VS. DMSO (CONTROL): ONL SOMA COUNT

General Linear Model

Dependent Variable: SOMA#

Normality Test (Shapiro-Wilk) Passed (P = 0.272)

Equal Variance Test: Failed (P < 0.050)

Source of Variation	DF	SS	MS	F	P
TREATMENT	1	10721.782	10721.782	7.567	0.007
POSITION	32	13731.733	429.117	0.303	1.000
TREATMENT x POSITION	32	28802.352	900.073	0.635	0.928
Residual	99	140274.667	1416.916		
Total	164	193945.176	1182.593		

The difference in the mean values among the different levels of TREATMENT is greater than would be expected by chance after allowing for effects of differences in POSITION. There is a statistically significant difference (P = 0.007). To isolate which group(s) differ from the others use a multiple comparison procedure.

The difference in the mean values among the different levels of POSITION is not great enough to exclude the possibility that the difference is just due to random sampling variability after allowing for the effects of differences in TREATMENT. There is not a statistically significant difference (P = 1.000).

The effect of different levels of TREATMENT does not depend on what level of POSITION is present. There is not a statistically significant interaction between TREATMENT and POSITION. (P = 0.928)

Power of performed test with alpha = 0.0500: for TREATMENT : 0.726
Power of performed test with alpha = 0.0500: for POSITION : 0.0500
Power of performed test with alpha = 0.0500: for TREATMENT x POSITION : 0.0500

Least square means for TREATMENT:

Group	Mean	SEM
CONTROL	242.394	4.633
DMSO	225.939	3.783

All Pairwise Multiple Comparison Procedures (Holm-Sidak method):
Overall significance level = 0.05

Comparisons for factor: **TREATMENT**

Comparison	Diff of Means	t	P	P<0.050
CONTROL vs. DMSO	16.455	2.751	0.007	Yes

Comparisons for factor: **TREATMENT within 1**

Comparison	Diff of Means	t	P	P<0.05
CONTROL vs. DMSO	37.667	1.096	0.276	No

Comparisons for factor: **TREATMENT within 2**

Comparison	**Diff of Means**	**t**	**P**	**P<0.05**
CONTROL vs. DMSO	56.333	1.639	0.104	No

Comparisons for factor: **TREATMENT within 3**

Comparison	**Diff of Means**	**t**	**P**	**P<0.05**
CONTROL vs. DMSO	72.333	2.105	0.038	Yes

Comparisons for factor: **TREATMENT within 4**

Comparison	**Diff of Means**	**t**	**P**	**P<0.05**
CONTROL vs. DMSO	42.000	1.222	0.225	No

Comparisons for factor: **TREATMENT within 5**

Comparison	**Diff of Means**	**t**	**P**	**P<0.05**
CONTROL vs. DMSO	20.500	0.597	0.552	No

Comparisons for factor: **TREATMENT within 6**

Comparison	**Diff of Means**	**t**	**P**	**P<0.05**
CONTROL vs. DMSO	34.333	0.999	0.320	No

Comparisons for factor: **TREATMENT within 7**

Comparison	**Diff of Means**	**t**	**P**	**P<0.05**
CONTROL vs. DMSO	30.167	0.878	0.382	No

Comparisons for factor: **TREATMENT within 8**

Comparison	**Diff of Means**	**t**	**P**	**P<0.05**
CONTROL vs. DMSO	30.833	0.897	0.372	No

Comparisons for factor: **TREATMENT within 9**

Comparison	**Diff of Means**	**t**	**P**	**P<0.05**
CONTROL vs. DMSO	23.667	0.689	0.493	No

Comparisons for factor: **TREATMENT within 10**

Comparison	**Diff of Means**	**t**	**P**	**P<0.05**
CONTROL vs. DMSO	36.833	1.072	0.286	No

Comparisons for factor: **TREATMENT within 11**

Comparison	**Diff of Means**	**t**	**P**	**P<0.05**
CONTROL vs. DMSO	14.333	0.417	0.677	No

Comparisons for factor: **TREATMENT within 12**

Comparison	**Diff of Means**	**t**	**P**	**P<0.05**
CONTROL vs. DMSO	37.000	1.077	0.284	No

Comparisons for factor: **TREATMENT within 13**

Comparison	**Diff of Means**	**t**	**P**	**P<0.05**
CONTROL vs. DMSO	20.833	0.606	0.546	No

Comparisons for factor: **TREATMENT within 14**

Comparison	**Diff of Means**	**t**	**P**	**P<0.05**
CONTROL vs. DMSO	32.667	0.951	0.344	No

Comparisons for factor: **TREATMENT within 15**

Comparison	**Diff of Means**	**t**	**P**	**P<0.05**
CONTROL vs. DMSO	48.500	1.411	0.161	No

Comparisons for factor: **TREATMENT within 16**

Comparison	**Diff of Means**	**t**	**P**	**P<0.05**
CONTROL vs. DMSO	35.333	1.028	0.306	No

Comparisons for factor: **TREATMENT within 17**

Comparison	**Diff of Means**	**t**	**P**	**P<0.05**
CONTROL vs. DMSO	38.500	1.120	0.265	No

Comparisons for factor: **TREATMENT within 18**

Comparison	**Diff of Means**	**t**	**P**	**P<0.05**
CONTROL vs. DMSO	16.667	0.485	0.629	No

Comparisons for factor: **TREATMENT within 19**

Comparison	**Diff of Means**	**t**	**P**	**P<0.05**
CONTROL vs. DMSO	7.167	0.209	0.835	No

Comparisons for factor: **TREATMENT within 20**

Comparison	**Diff of Means**	**t**	**P**	**P<0.05**
CONTROL vs. DMSO	20.500	0.597	0.552	No

Comparisons for factor: **TREATMENT within 21**

Comparison	**Diff of Means**	**t**	**P**	**P<0.05**
CONTROL vs. DMSO	21.000	0.611	0.543	No

Comparisons for factor: **TREATMENT within 22**

Comparison	**Diff of Means**	**t**	**P**	**P<0.05**
DMSO vs. CONTROL	23.500	0.684	0.496	No

Comparisons for factor: **TREATMENT within 23**

Comparison	**Diff of Means**	**t**	**P**	**P<0.05**
DMSO vs. CONTROL	38.333	1.116	0.267	No

Comparisons for factor: **TREATMENT within 24**

Comparison	**Diff of Means**	**t**	**P**	**P<0.05**
CONTROL vs. DMSO	3.167	0.0922	0.927	No

Comparisons for factor: **TREATMENT within 25**

Comparison	**Diff of Means**	**t**	**P**	**P<0.05**
CONTROL vs. DMSO	4.167	0.121	0.904	No

Comparisons for factor: **TREATMENT within 26**

Comparison	**Diff of Means**	**t**	**P**	**P<0.05**
DMSO vs. CONTROL	25.167	0.732	0.466	No

Comparisons for factor: **TREATMENT within 27**

Comparison	**Diff of Means**	**t**	**P**	**P<0.05**
DMSO vs. CONTROL	7.000	0.204	0.839	No

Comparisons for factor: **TREATMENT within 28**

Comparison	**Diff of Means**	**t**	**P**	**P<0.05**
DMSO vs. CONTROL	11.000	0.320	0.750	No

Comparisons for factor: **TREATMENT within 29**

Comparison	**Diff of Means**	**t**	**P**	**P<0.05**
CONTROL vs. DMSO	7.167	0.209	0.835	No

Comparisons for factor: **TREATMENT within 30**

Comparison	**Diff of Means**	**t**	**P**	**P<0.05**
DMSO vs. CONTROL	43.167	1.256	0.212	No

Comparisons for factor: **TREATMENT within 31**

Comparison	**Diff of Means**	**t**	**P**	**P<0.05**
CONTROL vs. DMSO	18.000	0.524	0.602	No

Comparisons for factor: **TREATMENT within 32**

Comparison	**Diff of Means**	**t**	**P**	**P<0.05**
CONTROL vs. DMSO	16.833	0.490	0.625	No

Comparisons for factor: **TREATMENT within 33**

Comparison	**Diff of Means**	**t**	**P**	**P<0.05**
DMSO vs. CONTROL	35.333	1.028	0.306	No

Two Way Analysis of Variance

Data source: CONTROL VS. DMSO (CONTROL): ONL WIDTH

General Linear Model

Dependent Variable: WIDTH#

Normality Test (Shapiro-Wilk) Failed (P < 0.050)

Equal Variance Test: Failed (P < 0.050)

Source of Variation	DF	SS	MS	F	P
TREATMENT	1	54.096	54.096	2.812	0.097
POSITION	32	302.693	9.459	0.492	0.988
TREATMENT x POSITION	32	373.266	11.665	0.606	0.946
Residual	99	1904.796	19.240		
Total	164	2720.607	16.589		

The difference in the mean values among the different levels of TREATMENT is not great enough to exclude the possibility that the difference is just due to random sampling variability after allowing for the effects of differences in POSITION. There is not a statistically significant difference (P = 0.097).

The difference in the mean values among the different levels of POSITION is not great enough to exclude the possibility that the difference is just due to random sampling variability after allowing for the effects of differences in TREATMENT. There is not a statistically significant difference (P = 0.988).

The effect of different levels of TREATMENT does not depend on what level of POSITION is present. There is not a statistically significant interaction between TREATMENT and POSITION. (P = 0.946)

Power of performed test with alpha = 0.0500: for TREATMENT : 0.250
Power of performed test with alpha = 0.0500: for POSITION : 0.0500
Power of performed test with alpha = 0.0500: for TREATMENT x POSITION : 0.0500

Least square means for TREATMENT :

Group	Mean	SEM
DMSO	30.337	0.441
CONTROL	29.169	0.540

APPENDIX 3

Two Way Analysis of Variance

Data source: DMSO (SHAM) VS. MNU: ONL SOMA COUNT

Balanced Design

Dependent Variable: SOMA#

Normality Test (Shapiro-Wilk) Passed (P = 0.076)

Equal Variance Test: Passed (P = 0.988)

Source of Variation	DF	SS	MS	F	P
TREATMENT	1	402095.006	402095.006	590.613	<0.001
POSITION	27	10307.208	381.748	0.561	0.958
TREATMENT x POSITION	27	6700.494	248.166	0.365	0.998
Residual	112	76250.667	680.810		
Total	167	495353.375	2966.188		

The difference in the mean values among the different levels of TREATMENT is greater than would be expected by chance after allowing for effects of differences in POSITION. There is a statistically significant difference (P = <0.001). To isolate which group(s) differ from the others use a multiple comparison procedure.

The difference in the mean values among the different levels of POSITION is not great enough to exclude the possibility that the difference is just due to random sampling variability after allowing for the effects of differences in TREATMENT. There is not a statistically significant difference (P = 0.958).

The effect of different levels of TREATMENT does not depend on what level of POSITION is present. There is not a statistically significant interaction between TREATMENT and POSITION. (P = 0.998)

Power of performed test with alpha = 0.0500: for TREATMENT : 1.000
Power of performed test with alpha = 0.0500: for POSITION : 0.0500
Power of performed test with alpha = 0.0500: for TREATMENT x POSITION : 0.0500

Least square means for TREATMENT :

Group	Mean
SHAM	184.548
MNU	86.702

Std Err of LS Mean = 2.847

All Pairwise Multiple Comparison Procedures (Holm-Sidak method):
Overall significance level = 0.05

Comparisons for factor: **TREATMENT**

Comparison	Diff of Means	t	P	P<0.050
SHAM vs. MNU	97.845	24.303	<0.001	Yes

Comparisons for factor: **TREATMENT within 1**

Comparison	Diff of Means	t	P	P<0.05
SHAM vs. MNU	107.333	5.038	<0.001	Yes

Comparisons for factor: **TREATMENT within 2**

Comparison	**Diff of Means**	**t**	**P**	**P<0.05**
SHAM vs. MNU	122.333	5.742	<0.001	Yes

Comparisons for factor: **TREATMENT within 3**

Comparison	**Diff of Means**	**t**	**P**	**P<0.05**
SHAM vs. MNU	120.333	5.648	<0.001	Yes

Comparisons for factor: **TREATMENT within 4**

Comparison	**Diff of Means**	**t**	**P**	**P<0.05**
SHAM vs. MNU	111.667	5.242	<0.001	Yes

Comparisons for factor: **TREATMENT within 5**

Comparison	**Diff of Means**	**t**	**P**	**P<0.05**
SHAM vs. MNU	96.667	4.537	<0.001	Yes

Comparisons for factor: **TREATMENT within 6**

Comparison	**Diff of Means**	**t**	**P**	**P<0.05**
SHAM vs. MNU	107.333	5.038	<0.001	Yes

Comparisons for factor: **TREATMENT within 7**

Comparison	**Diff of Means**	**t**	**P**	**P<0.05**
SHAM vs. MNU	100.000	4.694	<0.001	Yes

Comparisons for factor: **TREATMENT within 8**

Comparison	**Diff of Means**	**t**	**P**	**P<0.05**
SHAM vs. MNU	101.667	4.772	<0.001	Yes

Comparisons for factor: **TREATMENT within 9**

Comparison	**Diff of Means**	**t**	**P**	**P<0.05**
SHAM vs. MNU	106.000	4.976	<0.001	Yes

Comparisons for factor: **TREATMENT within 10**

Comparison	**Diff of Means**	**t**	**P**	**P<0.05**
SHAM vs. MNU	88.667	4.162	<0.001	Yes

Comparisons for factor: **TREATMENT within 11**

Comparison	**Diff of Means**	**t**	**P**	**P<0.05**
SHAM vs. MNU	101.000	4.741	<0.001	Yes

Comparisons for factor: **TREATMENT within 12**

Comparison	**Diff of Means**	**t**	**P**	**P<0.05**
SHAM vs. MNU	106.667	5.007	<0.001	Yes

Comparisons for factor: **TREATMENT within 13**

Comparison	**Diff of Means**	**t**	**P**	**P<0.05**
SHAM vs. MNU	102.667	4.819	<0.001	Yes

Comparisons for factor: **TREATMENT within 14**

Comparison	**Diff of Means**	**t**	**P**	**P<0.05**
SHAM vs. MNU	94.000	4.412	<0.001	Yes

Comparisons for factor: **TREATMENT within 15**

Comparison	**Diff of Means**	**t**	**P**	**P<0.05**
SHAM vs. MNU	100.333	4.710	<0.001	Yes

Comparisons for factor: **TREATMENT within 16**

Comparison	**Diff of Means**	**t**	**P**	**P<0.05**
SHAM vs. MNU	115.667	5.429	<0.001	Yes

Comparisons for factor: **TREATMENT within 17**

Comparison	**Diff of Means**	**t**	**P**	**P<0.05**
SHAM vs. MNU	106.333	4.991	<0.001	Yes

Comparisons for factor: **TREATMENT within 18**

Comparison	**Diff of Means**	**t**	**P**	**P<0.05**
SHAM vs. MNU	107.667	5.054	<0.001	Yes

Comparisons for factor: **TREATMENT within 19**

Comparison	**Diff of Means**	**t**	**P**	**P<0.05**
SHAM vs. MNU	85.667	4.021	<0.001	Yes

Comparisons for factor: **TREATMENT within 20**

Comparison	**Diff of Means**	**t**	**P**	**P<0.05**
SHAM vs. MNU	93.000	4.365	<0.001	Yes

Comparisons for factor: **TREATMENT within 21**

Comparison	**Diff of Means**	**t**	**P**	**P<0.05**
SHAM vs. MNU	92.333	4.334	<0.001	Yes

Comparisons for factor: **TREATMENT within 22**

Comparison	**Diff of Means**	**t**	**P**	**P<0.05**
SHAM vs. MNU	91.333	4.287	<0.001	Yes

Comparisons for factor: **TREATMENT within 23**

Comparison	**Diff of Means**	**t**	**P**	**P<0.05**
SHAM vs. MNU	85.667	4.021	<0.001	Yes

Comparisons for factor: **TREATMENT within 24**

Comparison	**Diff of Means**	**t**	**P**	**P<0.05**
SHAM vs. MNU	84.000	3.943	<0.001	Yes

Comparisons for factor: **TREATMENT within 25**

Comparison	**Diff of Means**	**t**	**P**	**P<0.05**
SHAM vs. MNU	75.000	3.520	<0.001	Yes

Comparisons for factor: **TREATMENT within 26**

Comparison	**Diff of Means**	**t**	**P**	**P<0.05**
SHAM vs. MNU	78.333	3.677	<0.001	Yes

Comparisons for factor: **TREATMENT within 27**

Comparison	**Diff of Means**	**t**	**P**	**P<0.05**
SHAM vs. MNU	77.667	3.646	<0.001	Yes

Comparisons for factor: **TREATMENT within 28**

Comparison	**Diff of Means**	**t**	**P**	**P<0.05**
SHAM vs. MNU	80.333	3.771	<0.001	Yes

Two Way Analysis of Variance

Data source: DMSO (SHAM) VS. MNU: ONL WIDTH

Balanced Design

Dependent Variable: WIDTH#

Normality Test (Shapiro-Wilk) Failed (P < 0.050)

Equal Variance Test: Passed (P = 0.834)

Source of Variation	DF	SS	MS	F	P
TREATMENT	1	3448.025	3448.025	373.947	<0.001
POSTION	27	91.237	3.379	0.366	0.998
TREATMENT x POSTION	27	114.701	4.248	0.461	0.989
Residual	112	1032.710	9.221		
Total	167	4686.673	28.064		

The difference in the mean values among the different levels of TREATMENT is greater than would be expected by chance after allowing for effects of differences in POSTION. There is a statistically significant difference (P = <0.001). To isolate which group(s) differ from the others use a multiple comparison procedure.

The difference in the mean values among the different levels of POSTION is not great enough to exclude the possibility that the difference is just due to random sampling variability after allowing for the effects of differences in TREATMENT. There is not a statistically significant difference (P = 0.998).

The effect of different levels of TREATMENT does not depend on what level of POSTION is present. There is not a statistically significant interaction between TREATMENT and POSTION. (P = 0.989)

Power of performed test with alpha = 0.0500: for TREATMENT : 1.000
Power of performed test with alpha = 0.0500: for POSTION : 0.0500
Power of performed test with alpha = 0.0500: for TREATMENT x POSTION : 0.0500

Least square means for TREATMENT :

Group	Mean
SHAM	21.541
MNU	12.480

Std Err of LS Mean = 0.331

All Pairwise Multiple Comparison Procedures (Holm-Sidak method):
Overall significance level = 0.05

Comparisons for factor: **TREATMENT**

Comparison	Diff of Means	t	P	P<0.050
SHAM vs. MNU	9.061	19.338	<0.001	Yes

Comparisons for factor: **TREATMENT within 1**

Comparison	Diff of Means	t	P	P<0.05
SHAM vs. MNU	11.303	4.559	<0.001	Yes

Comparisons for factor: **TREATMENT within 2**

Comparison	Diff of Means	t	P	P<0.05
SHAM vs. MNU	9.720	3.920	<0.001	Yes

Comparisons for factor: **TREATMENT within 3**

Comparison	**Diff of Means**	**t**	**P**	**P<0.05**
SHAM vs. MNU	11.367	4.585	<0.001	Yes

Comparisons for factor: **TREATMENT within 4**

Comparison	**Diff of Means**	**t**	**P**	**P<0.05**
SHAM vs. MNU	9.896	3.991	<0.001	Yes

Comparisons for factor: **TREATMENT within 5**

Comparison	**Diff of Means**	**t**	**P**	**P<0.05**
SHAM vs. MNU	9.098	3.669	<0.001	Yes

Comparisons for factor: **TREATMENT within 6**

Comparison	**Diff of Means**	**t**	**P**	**P<0.05**
SHAM vs. MNU	10.280	4.146	<0.001	Yes

Comparisons for factor: **TREATMENT within 7**

Comparison	**Diff of Means**	**t**	**P**	**P<0.05**
SHAM vs. MNU	9.197	3.709	<0.001	Yes

Comparisons for factor: **TREATMENT within 8**

Comparison	**Diff of Means**	**t**	**P**	**P<0.05**
SHAM vs. MNU	9.122	3.679	<0.001	Yes

Comparisons for factor: **TREATMENT within 9**

Comparison	**Diff of Means**	**t**	**P**	**P<0.05**
SHAM vs. MNU	10.366	4.181	<0.001	Yes

Comparisons for factor: **TREATMENT within 10**

Comparison	**Diff of Means**	**t**	**P**	**P<0.05**
SHAM vs. MNU	10.160	4.098	<0.001	Yes

Comparisons for factor: **TREATMENT within 11**

Comparison	**Diff of Means**	**t**	**P**	**P<0.05**
SHAM vs. MNU	9.788	3.948	<0.001	Yes

Comparisons for factor: **TREATMENT within 12**

Comparison	**Diff of Means**	**t**	**P**	**P<0.05**
SHAM vs. MNU	10.008	4.036	<0.001	Yes

Comparisons for factor: **TREATMENT within 13**

Comparison	**Diff of Means**	**t**	**P**	**P<0.05**
SHAM vs. MNU	10.224	4.124	<0.001	Yes

Comparisons for factor: **TREATMENT within 14**

Comparison	**Diff of Means**	**t**	**P**	**P<0.05**
SHAM vs. MNU	9.154	3.692	<0.001	Yes

Comparisons for factor: **TREATMENT within 15**

Comparison	**Diff of Means**	**t**	**P**	**P<0.05**
SHAM vs. MNU	9.174	3.700	<0.001	Yes

Comparisons for factor: **TREATMENT within 16**

Comparison	**Diff of Means**	**t**	**P**	**P<0.05**
SHAM vs. MNU	11.373	4.587	<0.001	Yes

Comparisons for factor: **TREATMENT within 17**

Comparison	**Diff of Means**	**t**	**P**	**P<0.05**
SHAM vs. MNU	10.236	4.128	<0.001	Yes

Comparisons for factor: **TREATMENT within 18**

Comparison	**Diff of Means**	**t**	**P**	**P<0.05**
SHAM vs. MNU	9.488	3.827	<0.001	Yes

Comparisons for factor: **TREATMENT within 19**

Comparison	**Diff of Means**	**t**	**P**	**P<0.05**
SHAM vs. MNU	8.942	3.607	<0.001	Yes

Comparisons for factor: **TREATMENT within 20**

Comparison	**Diff of Means**	**t**	**P**	**P<0.05**
SHAM vs. MNU	9.837	3.967	<0.001	Yes

Comparisons for factor: **TREATMENT within 21**

Comparison	**Diff of Means**	**t**	**P**	**P<0.05**
SHAM vs. MNU	7.353	2.966	0.004	Yes

Comparisons for factor: **TREATMENT within 22**

Comparison	**Diff of Means**	**t**	**P**	**P<0.05**
SHAM vs. MNU	8.478	3.419	<0.001	Yes

Comparisons for factor: **TREATMENT within 23**

Comparison	**Diff of Means**	**t**	**P**	**P<0.05**
SHAM vs. MNU	8.022	3.236	0.002	Yes

Comparisons for factor: **TREATMENT within 24**

Comparison	**Diff of Means**	**t**	**P**	**P<0.05**
SHAM vs. MNU	5.787	2.334	0.021	Yes

Comparisons for factor: **TREATMENT within 25**

Comparison	**Diff of Means**	**t**	**P**	**P<0.05**
SHAM vs. MNU	6.143	2.478	0.015	Yes

Comparisons for factor: **TREATMENT within 26**

Comparison	**Diff of Means**	**t**	**P**	**P<0.05**
SHAM vs. MNU	5.637	2.273	0.025	Yes

Comparisons for factor: **TREATMENT within 27**

Comparison	**Diff of Means**	**t**	**P**	**P<0.05**
SHAM vs. MNU	5.276	2.128	0.036	Yes

Comparisons for factor: **TREATMENT within 28**

Comparison	**Diff of Means**	**t**	**P**	**P<0.05**
SHAM vs. MNU	8.271	3.336	0.001	Yes

APPENDIX 4

Two Way Analysis of Variance

Data source: DMSO (CONTROL) VS. DMSO (SHAM): ONL SOMA COUNT

Balanced Design

Dependent Variable: SOMA#

Normality Test (Shapiro-Wilk) Passed (P = 0.067)

Equal Variance Test: Passed (P = 0.769)

Source of Variation	DF	SS	MS	F	P
TREATMENT	1	95676.021	95676.021	78.701	<0.001
POSITION	31	19435.979	626.967	0.516	0.983
TREATMENT x POSITION	31	10321.646	332.956	0.274	1.000
Residual	128	155608.667	1215.693		
Total	191	281042.313	1471.426		

The difference in the mean values among the different levels of TREATMENT is greater than would be expected by chance after allowing for effects of differences in POSITION. There is a statistically significant difference (P = <0.001). To isolate which group(s) differ from the others use a multiple comparison procedure.

The difference in the mean values among the different levels of POSITION is not great enough to exclude the possibility that the difference is just due to random sampling variability after allowing for the effects of differences in TREATMENT. There is not a statistically significant difference (P = 0.983).

The effect of different levels of TREATMENT does not depend on what level of POSITION is present. There is not a statistically significant interaction between TREATMENT and POSITION. (P = 1.000)

Power of performed test with alpha = 0.0500: for TREATMENT : 1.000
Power of performed test with alpha = 0.0500: for POSITION : 0.0500
Power of performed test with alpha = 0.0500: for TREATMENT x POSITION : 0.0500

Least square means for TREATMENT :

Group	Mean
CONTROL	227.229
DMSO	182.583

Std Err of LS Mean = 3.559

All Pairwise Multiple Comparison Procedures (Holm-Sidak method):
Overall significance level = 0.05

Comparisons for factor: **TREATMENT**

Comparison	Diff of Means	t	P	P<0.050
CONTROL vs. DMSO	44.646	8.871	<0.001	Yes

Comparisons for factor: **TREATMENT within 1**

Comparison	Diff of Means	t	P	P<0.05
CONTROL vs. DMSO	28.000	0.984	0.327	No

Comparisons for factor: **TREATMENT within 2**

Comparison	**Diff of Means**	**t**	**P**	**P<0.05**
CONTROL vs. DMSO	31.667	1.112	0.268	No

Comparisons for factor: **TREATMENT within 3**

Comparison	**Diff of Means**	**t**	**P**	**P<0.05**
CONTROL vs. DMSO	48.000	1.686	0.094	No

Comparisons for factor: **TREATMENT within 4**

Comparison	**Diff of Means**	**t**	**P**	**P<0.05**
CONTROL vs. DMSO	40.667	1.428	0.156	No

Comparisons for factor: **TREATMENT within 5**

Comparison	**Diff of Means**	**t**	**P**	**P<0.05**
CONTROL vs. DMSO	27.000	0.948	0.345	No

Comparisons for factor: **TREATMENT within 6**

Comparison	**Diff of Means**	**t**	**P**	**P<0.05**
CONTROL vs. DMSO	18.333	0.644	0.521	No

Comparisons for factor: **TREATMENT within 7**

Comparison	**Diff of Means**	**t**	**P**	**P<0.05**
CONTROL vs. DMSO	37.333	1.311	0.192	No

Comparisons for factor: **TREATMENT within 8**

Comparison	**Diff of Means**	**t**	**P**	**P<0.05**
CONTROL vs. DMSO	42.000	1.475	0.143	No

Comparisons for factor: **TREATMENT within 9**

Comparison	**Diff of Means**	**t**	**P**	**P<0.05**
CONTROL vs. DMSO	33.333	1.171	0.244	No

Comparisons for factor: **TREATMENT within 10**

Comparison	**Diff of Means**	**t**	**P**	**P<0.05**
CONTROL vs. DMSO	36.333	1.276	0.204	No

Comparisons for factor: **TREATMENT within 11**

Comparison	**Diff of Means**	**t**	**P**	**P<0.05**
CONTROL vs. DMSO	48.333	1.698	0.092	No

Comparisons for factor: **TREATMENT within 12**

Comparison	**Diff of Means**	**t**	**P**	**P<0.05**
CONTROL vs. DMSO	59.000	2.072	0.040	Yes

Comparisons for factor: **TREATMENT within 13**

Comparison	**Diff of Means**	**t**	**P**	**P<0.05**
CONTROL vs. DMSO	54.333	1.909	0.059	No

Comparisons for factor: **TREATMENT within 14**

Comparison	**Diff of Means**	**t**	**P**	**P<0.05**
CONTROL vs. DMSO	39.667	1.393	0.166	No

Comparisons for factor: **TREATMENT within 15**

Comparison	**Diff of Means**	**t**	**P**	**P<0.05**
CONTROL vs. DMSO	23.667	0.831	0.407	No

Comparisons for factor: **TREATMENT within 16**

Comparison	**Diff of Means**	**t**	**P**	**P<0.05**
CONTROL vs. DMSO	42.667	1.499	0.136	No

Comparisons for factor: **TREATMENT within 17**

Comparison	**Diff of Means**	**t**	**P**	**P<0.05**
CONTROL vs. DMSO	45.333	1.592	0.114	No

Comparisons for factor: **TREATMENT within 18**

Comparison	**Diff of Means**	**t**	**P**	**P<0.05**
CONTROL vs. DMSO	30.333	1.066	0.289	No

Comparisons for factor: **TREATMENT within 19**

Comparison	**Diff of Means**	**t**	**P**	**P<0.05**
CONTROL vs. DMSO	25.333	0.890	0.375	No

Comparisons for factor: **TREATMENT within 20**

Comparison	**Diff of Means**	**t**	**P**	**P<0.05**
CONTROL vs. DMSO	51.333	1.803	0.074	No

Comparisons for factor: **TREATMENT within 21**

Comparison	**Diff of Means**	**t**	**P**	**P<0.05**
CONTROL vs. DMSO	47.333	1.663	0.099	No

Comparisons for factor: **TREATMENT within 22**

Comparison	**Diff of Means**	**t**	**P**	**P<0.05**
CONTROL vs. DMSO	73.000	2.564	0.011	Yes

Comparisons for factor: **TREATMENT within 23**

Comparison	**Diff of Means**	**t**	**P**	**P<0.05**
CONTROL vs. DMSO	58.000	2.037	0.044	Yes

Comparisons for factor: **TREATMENT within 24**

Comparison	**Diff of Means**	**t**	**P**	**P<0.05**
CONTROL vs. DMSO	58.667	2.061	0.041	Yes

Comparisons for factor: **TREATMENT within 25**

Comparison	**Diff of Means**	**t**	**P**	**P<0.05**
CONTROL vs. DMSO	48.000	1.686	0.094	No

Comparisons for factor: **TREATMENT within 26**

Comparison	**Diff of Means**	**t**	**P**	**P<0.05**
CONTROL vs. DMSO	48.333	1.698	0.092	No

Comparisons for factor: **TREATMENT within 27**

Comparison	**Diff of Means**	**t**	**P**	**P<0.05**
CONTROL vs. DMSO	39.667	1.393	0.166	No

Comparisons for factor: **TREATMENT within 28**

Comparison	**Diff of Means**	**t**	**P**	**P<0.05**
CONTROL vs. DMSO	87.333	3.068	0.003	Yes

Comparisons for factor: **TREATMENT within 29**

Comparison	**Diff of Means**	**t**	**P**	**P<0.05**
CONTROL vs. DMSO	42.000	1.475	0.143	No

Comparisons for factor: **TREATMENT within 30**

Comparison	**Diff of Means**	**t**	**P**	**P<0.05**
CONTROL vs. DMSO	43.333	1.522	0.130	No

Comparisons for factor: **TREATMENT within 31**

Comparison	**Diff of Means**	**t**	**P**	**P<0.05**
CONTROL vs. DMSO	50.333	1.768	0.079	No

Comparisons for factor: **TREATMENT within 32**

Comparison	**Diff of Means**	**t**	**P**	**P<0.05**
CONTROL vs. DMSO	70.000	2.459	0.015	Yes

APPENDIX 5

Two Way Analysis of Variance

Data source: ONL SOMA COUNT: RIGHT VS. LEFT EYE

General Linear Model

Dependent Variable: SOMA#

Normality Test (Shapiro-Wilk) Failed (P < 0.050)

Equal Variance Test: Passed (P = 0.427)

Source of Variation	DF	SS	MS	F	P
TREATMENT	1	20309.402	20309.402	71.737	<0.001
EYE	1	34.615	34.615	0.122	0.730
TREATMENT x EYE	1	114.940	114.940	0.406	0.531
Residual	22	6228.444	283.111		
Total	25	31612.615	1264.505		

The difference in the mean values among the different levels of TREATMENT is greater than would be expected by chance after allowing for effects of differences in EYE. There is a statistically significant difference (P = <0.001). To isolate which group(s) differ from the others use a multiple comparison procedure.

The difference in the mean values among the different levels of EYE is not great enough to exclude the possibility that the difference is just due to random sampling variability after allowing for the effects of differences in TREATMENT. There is not a statistically significant difference (P = 0.730).

The effect of different levels of TREATMENT does not depend on what level of EYE is present. There is not a statistically significant interaction between TREATMENT and EYE. (P = 0.531)

Power of performed test with alpha = 0.0500: for TREATMENT : 1.000
Power of performed test with alpha = 0.0500: for EYE : 0.0500
Power of performed test with alpha = 0.0500: for TREATMENT x EYE : 0.0500

Least square means for TREATMENT :

Group	Mean
MNU	54.972
SHAM	115.528

Std Err of LS Mean = 5.056

Least square means for EYE :

Group	Mean	SEM
r	86.500	5.949
l	84.000	3.966

Least square means for TREATMENT x EYE :

Group	Mean	SEM
MNU x r	58.500	8.413
MNU x l	51.444	5.609
SHAM x r	114.500	8.413
SHAM x l	116.556	5.609

All Pairwise Multiple Comparison Procedures (Holm-Sidak method):
Overall significance level = 0.05

Comparisons for factor: **TREATMENT**

Comparison	**Diff of Means**	**t**	**P**	**P<0.050**
SHAM vs. MNU	60.556	8.470	<0.001	Yes

Comparisons for factor: **EYE**

Comparison	**Diff of Means**	**t**	**P**	**P<0.050**
r vs. l	2.500	0.350	0.730	No

Comparisons for factor: **EYE within MNU**

Comparison	**Diff of Means**	**t**	**P**	**P<0.05**
r vs. l	7.056	0.698	0.493	No

Comparisons for factor: **EYE within SHAM**

Comparison	**Diff of Means**	**t**	**P**	**P<0.05**
l vs. r	2.056	0.203	0.841	No

Comparisons for factor: **TREATMENT within r**

Comparison	**Diff of Means**	**t**	**P**	**P<0.05**
SHAM vs. MNU	56.000	4.707	<0.001	Yes

Comparisons for factor: **TREATMENT within l**

Comparison	**Diff of Means**	**t**	**P**	**P<0.05**
SHAM vs. MNU	65.111	8.209	<0.001	Yes

APPENDIX 6

Two Way Analysis of Variance

Data source: 14% VS 7% MNU DOSE: ONL SOMA COUNT

General Linear Model

Dependent Variable: SOMA#

Normality Test (Shapiro-Wilk) Failed (P < 0.050)

Equal Variance Test: Passed (P = 0.473)

Source of Variation	DF	SS	MS	F	P
TREATMENT	1	16888.706	16888.706	39.732	<0.001
DOSE	1	2649.150	2649.150	6.232	0.020
TREATMENT x DOSE	1	1234.134	1234.134	2.903	0.101
Residual	24	10201.644	425.069		
Total	27	35425.250	1312.046		

The difference in the mean values among the different levels of TREATMENT is greater than would be expected by chance after allowing for effects of differences in DOSE. There is a statistically significant difference (P = <0.001). To isolate which group(s) differ from the others use a multiple comparison procedure.

The difference in the mean values among the different levels of DOSE is greater than would be expected by chance after allowing for effects of differences in TREATMENT. There is a statistically significant difference (P = 0.020). To isolate which group(s) differ from the others use a multiple comparison procedure.

The effect of different levels of TREATMENT does not depend on what level of DOSE is present. There is not a statistically significant interaction between TREATMENT and DOSE. (P = 0.101)

Power of performed test with alpha = 0.0500: for TREATMENT : 1.000
Power of performed test with alpha = 0.0500: for DOSE : 0.590
Power of performed test with alpha = 0.0500: for TREATMENT x DOSE : 0.249

Least square means for TREATMENT :

Group	Mean
SHAM	119.778
MNU	68.522

Std Err of LS Mean = 5.750

Least square means for DOSE :

Group	Mean	SEM
14.000	84.000	4.860
7.000	104.300	6.520

Least square means for TREATMENT x DOSE :

Group	Mean	SEM
SHAM x 14.000	116.556	6.872
SHAM x 7.000	123.000	9.220
MNU x 14.000	51.444	6.872
MNU x 7.000	85.600	9.220

All Pairwise Multiple Comparison Procedures (Holm-Sidak method):
Overall significance level = 0.05

Comparisons for factor: **TREATMENT**

Comparison	**Diff of Means**	**t**	**P**	**P<0.050**
SHAM vs. MNU	51.256	6.303	<0.001	Yes

Comparisons for factor: **DOSE**

Comparison	**Diff of Means**	**t**	**P**	**P<0.050**
7.000 vs. 14.000	20.300	2.496	0.020	Yes

Comparisons for factor: **DOSE within SHAM**

Comparison	**Diff of Means**	**t**	**P**	**P<0.05**
7.000 vs. 14.000	6.444	0.560	0.580	No

Comparisons for factor: **DOSE within MNU**

Comparison	**Diff of Means**	**t**	**P**	**P<0.05**
7.000 vs. 14.000	34.156	2.970	0.007	Yes

Comparisons for factor: **TREATMENT within 14**

Comparison	**Diff of Means**	**t**	**P**	**P<0.05**
SHAM vs. MNU	65.111	6.699	<0.001	Yes

Comparisons for factor: **TREATMENT within 7**

Comparison	**Diff of Means**	**t**	**P**	**P<0.05**
SHAM vs. MNU	37.400	2.868	0.008	Yes

APPENDIX 7

Two Way Analysis of Variance

Data source: TIME COURSE (SINGLE INJECTION) ONL SOMA COUNT

General Linear Model

Dependent Variable: Soma#

Normality Test (Shapiro-Wilk) Passed (P = 0.478)

Equal Variance Test: Failed (P < 0.050)

Source of Variation	DF	SS	MS	F	P
Treatment	1	36746.218	36746.218	103.755	<0.001
Day	10	19212.679	1921.268	5.425	<0.001
Treatment x Day	10	25848.533	2584.853	7.298	<0.001
Residual	106	37541.475	354.165		
Total	127	124580.219	980.947		

Main effects cannot be properly interpreted if significant interaction is determined. This is because the size of a factor's effect depends upon the level of the other factor.

The effect of different levels of Treatment depends on what level of Day is present. There is a statistically significant interaction between Treatment and Day. (P = <0.001)

Power of performed test with alpha = 0.0500: for Treatment : 1.000
Power of performed test with alpha = 0.0500: for Day : 0.999
Power of performed test with alpha = 0.0500: for Treatment x Day : 1.000

Least square means for Treatment :

Group	Mean
SHAM	110.998
MNU	76.402

Std Err of LS Mean = 2.402

All Pairwise Multiple Comparison Procedures (Holm-Sidak method):
Overall significance level = 0.05

Comparisons for factor: **Treatment**

Comparison	Diff of Means	t	P	P<0.050
SHAM vs. MNU	34.596	10.186	<0.001	Yes

Comparisons for factor: **Treatment within 1**

Comparison	Diff of Means	t	P	P<0.05
MNU vs. SHAM	13.600	1.143	0.256	No

Comparisons for factor: **Treatment within 3**

Comparison	Diff of Means	t	P	P<0.05
MNU vs. SHAM	11.833	1.089	0.279	No

Comparisons for factor: **Treatment within 5**

Comparison	Diff of Means	t	P	P<0.05
SHAM vs. MNU	36.333	3.344	0.001	Yes

Comparisons for factor: **Treatment within 7**

Comparison	**Diff of Means**	**t**	**P**	**P<0.05**
SHAM vs. MNU	65.111	7.339	<0.001	Yes

Comparisons for factor: **Treatment within 10**

Comparison	**Diff of Means**	**t**	**P**	**P<0.05**
SHAM vs. MNU	61.400	5.159	<0.001	Yes

Comparisons for factor: **Treatment within 14**

Comparison	**Diff of Means**	**t**	**P**	**P<0.05**
SHAM vs. MNU	59.167	5.445	<0.001	Yes

Comparisons for factor: **Treatment within 21**

Comparison	**Diff of Means**	**t**	**P**	**P<0.05**
SHAM vs. MNU	77.800	6.537	<0.001	Yes

Comparisons for factor: **Treatment within 28**

Comparison	**Diff of Means**	**t**	**P**	**P<0.05**
SHAM vs. MNU	37.000	3.678	<0.001	Yes

Comparisons for factor: **Treatment within 35**

Comparison	**Diff of Means**	**t**	**P**	**P<0.05**
SHAM vs. MNU	18.833	1.733	0.086	No

Comparisons for factor: **Treatment within 42**

Comparison	**Diff of Means**	**t**	**P**	**P<0.05**
SHAM vs. MNU	28.600	2.403	0.018	Yes

Comparisons for factor: **Treatment within 49**

Comparison	**Diff of Means**	**t**	**P**	**P<0.05**
SHAM vs. MNU	21.750	1.634	0.105	No

Two Way Analysis of Variance

Data source: TIME COURSE (SINGLE INJECTION) INL SOMA COUNT

General Linear Model

Dependent Variable: SOMA#

Normality Test (Shapiro-Wilk) Passed (P = 0.839)

Equal Variance Test: Passed (P = 0.094)

Source of Variation	DF	SS	MS	F	P
TREATMENT	1	430.368	430.368	2.158	0.145
DAY	10	2996.758	299.676	1.503	0.148
TREATMENT x DAY	10	1790.778	179.078	0.898	0.538
Residual	106	21137.948	199.415		
Total	127	26371.742	207.652		

The difference in the mean values among the different levels of TREATMENT is not great enough to exclude the possibility that the difference is just due to random sampling variability after allowing for the effects of differences in DAY. There is not a statistically significant difference (P = 0.145).

The difference in the mean values among the different levels of DAY is not great enough to exclude the possibility that the difference is just due to random sampling variability after allowing for the effects of differences in TREATMENT. There is not a statistically significant difference (P = 0.148).

The effect of different levels of TREATMENT does not depend on what level of DAY is present. There is not a statistically significant interaction between TREATMENT and DAY. (P = 0.538)

Power of performed test with alpha = 0.0500: for TREATMENT : 0.174
Power of performed test with alpha = 0.0500: for DAY : 0.245
Power of performed test with alpha = 0.0500: for TREATMENT x DAY : 0.0500

Least square means for TREATMENT :

Group	Mean
SHAM	50.553
MNU	54.297

Std Err of LS Mean = 1.802

APPENDIX 8

Two Way Analysis of Variance

Data source: TIME COURSE (DOUBLE INJECTION) ONL SOMA COUNT

General Linear Model

Dependent Variable: SOMA#

Normality Test (Shapiro-Wilk) Passed (P = 0.414)

Equal Variance Test: Failed (P < 0.050)

Source of Variation	DF	SS	MS	F	P
TREATMENT	1	11693.231	11693.231	37.103	<0.001
DAY	2	23.612	11.806	0.0375	0.963
TREATMENT x DAY	2	1453.837	726.919	2.307	0.126
Residual	20	6303.167	315.158		
Total	25	23534.462	941.378		

The difference in the mean values among the different levels of TREATMENT is greater than would be expected by chance after allowing for effects of differences in DAY. There is a statistically significant difference (P = <0.001). To isolate which group(s) differ from the others use a multiple comparison procedure.

The difference in the mean values among the different levels of DAY is not great enough to exclude the possibility that the difference is just due to random sampling variability after allowing for the effects of differences in TREATMENT. There is not a statistically significant difference (P = 0.963).

The effect of different levels of TREATMENT does not depend on what level of DAY is present. There is not a statistically significant interaction between TREATMENT and DAY. (P = 0.126)

Power of performed test with alpha = 0.0500: for TREATMENT : 1.000
Power of performed test with alpha = 0.0500: for DAY : 0.0500
Power of performed test with alpha = 0.0500: for TREATMENT x DAY : 0.241

Least square means for TREATMENT :

Group	Mean
SHAM	101.044
MNU	53.589

Std Err of LS Mean = 5.509

Least square means for DAY :

Group	Mean	SEM
21.000	78.700	5.614
28.000	77.000	5.125
35.000	76.250	8.876

Least square means for TREATMENT x DAY :

Group	Mean	SEM
SHAM x 21.000	94.800	7.939
SHAM x 28.000	109.333	7.248
SHAM x 35.000	99.000	12.553
MNU x 21.000	62.600	7.939

MNU x 28.000	44.667	7.248
MNU x 35.000	53.500	12.553

All Pairwise Multiple Comparison Procedures (Holm-Sidak method):
Overall significance level = 0.05

Comparisons for factor: **TREATMENT**

Comparison	**Diff of Means**	**t**	**P**	**P<0.050**
SHAM vs. MNU	47.456	6.091	<0.001	Yes

Comparisons for factor: **DAY**

Comparison	**Diff of Means**	**t**	**P**	**P<0.050**
21.000 vs. 35.000	2.450	0.233	0.994	No
21.000 vs. 28.000	1.700	0.224	0.969	No
28.000 vs. 35.000	0.750	0.0732	0.942	No

Comparisons for factor: **DAY within SHAM**

Comparison	**Diff of Means**	**t**	**P**	**P<0.05**
28.000 vs. 21.000	14.533	1.352	0.471	No
28.000 vs. 35.000	10.333	0.713	0.734	No
35.000 vs. 21.000	4.200	0.283	0.780	No

Comparisons for factor: **DAY within MNU**

Comparison	**Diff of Means**	**t**	**P**	**P<0.05**
21.000 vs. 28.000	17.933	1.668	0.297	No
21.000 vs. 35.000	9.100	0.613	0.795	No
35.000 vs. 28.000	8.833	0.609	0.549	No

Comparisons for factor: **TREATMENT within 21**

Comparison	**Diff of Means**	**t**	**P**	**P<0.05**
SHAM vs. MNU	32.200	2.868	0.010	Yes

Comparisons for factor: **TREATMENT within 28**

Comparison	**Diff of Means**	**t**	**P**	**P<0.05**
SHAM vs. MNU	64.667	6.309	<0.001	Yes

Comparisons for factor: **TREATMENT within 35**

Comparison	**Diff of Means**	**t**	**P**	**P<0.05**
SHAM vs. MNU	45.500	2.563	0.019	Yes

APPENDIX 9

Image A: 042111dv Fish 87L15a GFAP 1to1000 VIM 1to500 Slice 10of15 Split Resize Rotate Crop Change Adjust.tif (red)
Image B: 042111dv Fish 87L15a GFAP 1to1000 VIM 1to500 Slice 10of15 Split Resize Rotate Crop Change Adjust.tif (green)

Pearson's Coefficient:
r=0.572

Overlap Coefficient:
r=0.622

r^2=k1xk2:
k1=0.246
k2=1.569

Using thresholds (thrA=84 and thrB=72)

Overlap Coefficient:
r=0.94

r^2=k1xk2:
k1=0.567
k2=1.559

Manders' Coefficients (original):
M1=0.991 (fraction of A overlapping B)
M2=0.933 (fraction of B overlapping A)

Manders' Coefficients (using threshold value of 84 for imgA and 72 for imgB):
M1=0.198 (fraction of A overlapping B)
M2=0.97 (fraction of B overlapping A)

Costes' automatic threshold set to 56 for imgA & 16 for imgB
Pearson's Coefficient:
r=0.526 (0.0 below thresholds)
M1=0.592 & M2=0.362

Van Steensel's Cross-correlation Coefficient between 042111dv Fish 87L15a GFAP 1to1000 VIM 1to500 Slice 10of15 Split Resize Rotate Crop Change Adjust.tif (red) and 042111dv Fish 87L15a GFAP 1to1000 VIM 1to500 Slice 10of15 Split Resize Rotate Crop Change Adjust.tif (green):
CCF min.: 0.059 (obtained for dx=20) CCF max.: 0.572 (obtained for dx=0)

Results for fitting CCF on a Gaussian (CCF=a+(b-a)exp(-(xshift-c)^2/(2d^2))):
Formula: y = a + (b-a)*exp(-(x-c)*(x-c)/(2*d*d))
Time: 0ms
Number of iterations: 525 (8000)
Number of restarts: 2 (2)
Sum of residuals squared: 0.0015
Standard deviation: 0.0060
R^2: 0.9988

Parameters:
  a = 0.0181
  b = 0.5756
  c = -0.8771
  d = 9.1990
FWHM=21.662 pixels

Cytofluorogram's parameters:
a: 0.208
b: 4.427
Correlation coefficient: 0.572

Li's Intensity correlation coefficient:
ICQ: 0.17119890737900667

Costes' randomization based colocalization:
Parameters: Nb of randomization rounds: 1000, Resolution (bin width): 0.0010
r (original)=0.572
r (randomized)=0.0±0.0010 (calculated from the fitted data)
P-value=100.0% (calculated from the fitted data)

Results for fitting the probability density function on a Gaussian (Probability=a+(b-a)exp(-(R-c)^2/(2d^2))):
Formula: y = a + (b-a)*exp(-(x-c)*(x-c)/(2*d*d))
Time: 0ms
Number of iterations: 468 (8000)
Number of restarts: 2 (2)
Sum of residuals squared: 0.0013
Standard deviation: 0.0096
R^2: 0.9839
Parameters:
  a = 0.0011
  b = 0.2071
  c = 0.0000
  d = 0.0019
FWHM=0.0040

Colocalization based on distance between centres of mass
Threshold for Image A=84; Image B=72
Particles size between 0 & 1048488
Image A: 1 centre(s) colocalizing out of 39
Image B: 1 centre(s) colocalizing out of 41

Colocalization based on centres of mass-particles coincidence
Threshold for Image A=84; Image B=72
Particles size between 0 & 1048488
Image A: 4 centre(s) colocalizing out of 39
Image B: 4 centre(s) colocalizing out of 41